IMPROVEMENT OF CRACKING AND CHLORIDE PENETRATION RESISTANCE OF SLAG CONCRETE BY UTILIZING HIGH ALITE CEMENT

(高エーライトセメントの活用によるスラグコンクリートのひび割れ抵抗性と塩分浸透抵抗性の改善)

by
HUYNH PHUONG NAM

A Dissertation Submitted to
Yokohama National University

In Partial Fulfillment of the Requirements
for the Degree of
Doctor of Engineering

Supervisor
Associate Professor AKIRA HOSODA

Graduate School of Urban Innovation
Yokohama National University
Yokohama, Japan

September 2014

ACKNOWLEDGEMENTS

First and foremost, I have to thank my research supervisor, Associate Professor Akira HOSODA. Without his assistance and dedicated involvement in every step throughout the process, the dissertation would have never been accomplished. I would like to thank you very much for your tireless support, encouragement, and understanding over these past three years.

Great gratitude goes to Professor Tatsuya TSUBAKI, Concrete Laboratory at Yokohama National University for his support, advice and helpful suggestions. His advice has served me well and I owe him my heartfelt appreciation.

Special thanks are devoted to Dr. Kazuhiko HAYASHI and Dr. Satoshi KOMATSU for their patient instruction and support in experimental works. Members of Concrete Laboratory also deserve my sincerest thanks, their friendship, collaboration, and disinterested assistance has meant more to me than I could ever express.

Sincere appreciation goes to Dr. Naoya KASAI at Yokohama National University for his kind and professional advices regarding the application of the acoustic emission technique.

Grateful acknowledgement is given to the Ministry of Education, Culture, Sports, Science and Technology of Japan for the allocation of financial support. The research would not have been possible without this generous grant.

Most importantly, none of this could have happened without my family. My wife and daughter, who offered their continuous encouragement, are always beside me. Every time I was ready to quit, you did not let me and I am forever grateful. To my parents and my sister– it would be an understatement to say that, as a family, we have experienced some ups and downs in the past three years. This dissertation stands as a testament to your unconditional love and encouragement.

ABSTRACT

The durability of concrete is one of the most concerns of researchers and engineers. Early ages are the time concrete suffers from many factors those induce cracking in the concrete. Microcracking in concrete adversely affects macroscopic tensile strength of concrete that will leads to the severe cracking in later ages. Especially with the addition of mineral additives such as ground granulated blast furnace slag or fly ash, concrete is susceptible to microcracking particularly under temperature variation. These microcracks must be one of the causes of severe macrocracks observed in real structures using slag concrete.

Not only microcracking, chloride attack is one of the main factors lowering the durability of concrete structures, particularly for the structures in very cold region, where deicing agent is frequently used in winter. Deicing agent can cause severe deterioration of concrete structures such as scaling, corrosion of steels, and ASR.

This study deals with improvement of cracking and chloride penetration resistance of slag and fly ash concrete by using a new type of cement named high alite cement (HAC). HAC is newly developed Portland cement with very high alite ($3CaO.SiO_2$) content and almost no belite ($2CaO.SiO_2$).

Due to its sensitivity and the rich information it yields from collected parameters, the acoustic emission (AE) technique has been widely used to detect cracking in hardened concrete. Nevertheless, AE measurement at a very early age is difficult because AE sensors cannot be directly attached on the surface of unhardened concrete. Therefore, a waveguide embedded inside concrete has been employed. Unfortunately, attenuation of acoustic waves in high moisture content ambient led to the diminished effectiveness of the waveguide in detecting AE signals in concrete with high water to binder ratio (W/B).

One part of the research is to solve the problem of attenuation. An addition of two perpendicular bars on main rod of the waveguide was proposed. Due to these wings, the distance from cracking points in concrete to waveguide was significantly reduced. It was proved that the redesigned waveguide worked more effectively than the previous one, especially in concrete with high W/B.

By using this redesigned waveguide, microcracking was intensively investigated in slag concrete with W/B of 0.3 and 0.5 subjected to temperature history simulating steam curing. In all types of concrete, the replacement ratio of slag for cement was 50%. Because the coefficient of thermal expansion (CTE) of materials is one of the important parameters affecting microcracking in concrete, two types of coarse aggregate with the same maximum particle size of 19 mm but remarkably different CTEs, namely limestone and andesite were used in the study.

The test results showed that net shrinkage of HAC mortar with W/B of 0.3 was much larger than that of OPC mortar because of its larger autogenous shrinkage. Normally, larger shrinkage of mortar results in more extensive cracking in concrete. However, the number and the degree of microcracks in HAC slag concrete with W/B of 0.3 were smaller than those in OPC slag concrete. This means that HAC slag concrete with W/B of 0.3 obviously achieved larger resistance against microcrack than OPC slag concrete. On the other hand, net shrinkage of HAC mortar with W/B of 0.5 was a bit smaller than that of OPC mortar due to its smaller thermal contraction. Therefore, microcracking in HAC slag concrete with W/B of 0.5 was also smaller than that in OPC slag concrete.

The interesting characteristic of HAC explored in the research is that it could improve resistance against microcracking in slag concrete. AE data revealed HAC concretes could disperse tensile stress, leading to the formation of many small cracks rather than concentrating tensile stress to create a severe crack. Evenly distributed calcium hydroxide (CH) crystals acting as a kind of buffer that prevents the propagation of microcracks in HAC slag concrete might be one of the reasons. Another reason for the high cracking resistance of HAC slag concrete was the strong bond between mortar and coarse aggregate. This high bond strength was more clearly observed in concrete with low W/B than in concrete with high W/B. The high bond strength of HAC slag concrete was verified through tensile strength test, AE test, visual observation, and scanning electron microscope images. The strong bond in HAC slag concretes might be due to the formation of secondary CSH gel from the reaction of CH and active SiO_2 in slag at pores near the interface transition zone.

The effects of fly ash on the microcracking resistance of concrete subjected to temperature variation at very young ages were also investigated by AE, physical and

mechanical tests. Fly ash was used as a cementitious material as well as fine aggregate. In addition, a combination of fly ash and HAC, which was effective in improving resistance against microcracking in slag concrete, was studied.

Concrete containing fly ash was not so weak against elevated temperature. Nevertheless, fly ash reduced tensile strength of concrete remarkably. The reason is that fly ash is not so active in early ages even under steam curing.

It is found that HAC can significantly improve tensile strength of concrete containing fly ash due to high hydration rate of HAC. However, high bond strength in HAC fly ash concrete was not observed from the direct tensile test as in HAC slag concrete. Further research is necessary to clarify the cracking resistance of fly ash concrete.

Another important part of the research is to show the effectiveness of HAC to improve the resistance against chloride ingress of concrete containing additives by using HAC. The effectiveness was analyzed by Surface Water Absorption Test (SWAT) and water/chloride penetration depth test. Four types of binder were used: OPC, HAC, slag, and fly ash. Concrete with OPC only was the control mix. In other mixes, the cements were replaced by slag or fly ash with the replacement ratios of 40% or 15% by mass, respectively. Coarse aggregate of andesite with maximum particle size of 19 mm was used. Air content of concrete was controlled at 6 ± 0.5% to prevent concrete from scaling under freeze/thaw cycles. In order to obtain a wide range of concrete quality, three W/B of 0.4, 0.5, and 0.6 and five curing conditions covering from very good to very poor condition were applied. Three-binder concretes containing slag and fly ash with W/B of 0.4 were also prepared. To investigate the effect of bond on mass transfer in concrete, some concretes made with limestone were added in the cases of concrete with W/B of 0.4 and 0.5.

Experimental results presented that there were good correlations between water absorption rate at 10 minutes (p_{600}) and penetration depth of water and chloride ions in all kinds of concrete. It means that SWAT can be applied to evaluate the resistance against mass transfer into concrete. The same linear relationship was observed between the water penetration depth and p_{600} regardless of the type of binder. It means that p_{600} is related to a kind of governing characteristic regarding the microstructure of concrete, which should be

studied further. The effects of curing conditions were fully reflected in SWAT results. If linear lines expressing the correlations between SWAT index and parameters related to durability of concrete such as penetration depth of water or chloride ion, carbonation depth, etc. are established, SWAT index can be used as an indicator of durability of concrete structures. This is very significant because SWAT is a simple, automatic, and rapid method and it is easy to be applied for concrete structures in actual sites.

It is found that slag or fly ash could improve the resistance against chloride ingress of concrete remarkably due to the chloride binding ability of C_3A component existing in slag and fly ash. However, OPC concretes containing additives were much more sensitive to curing conditions than concretes with OPC only.

Owing to the high hydration rate of C_3S, HAC slag/fly ash concrete was less sensitive to curing conditions than OPC slag/fly ash. Thus, HAC should be utilized with slag or fly ash in concrete structures subjected to severe conditions.

TABLE OF CONTENTS

LIST OF FIGURES

LIST OF TABLES

Chapter 1 Introduction

1.1 Backgrounds

1.1.1 Cracking in slag concrete

The durability of concrete is one of the most important concerns of researchers and engineers. Early ages are the time concrete suffers from many factors those induce cracking in the concrete. At early ages, microcracking is derived from the volume change of the ingredients of the concrete. Microcracking in concrete adversely affects macroscopic tensile strength of concrete that will leads to the severe cracking in the later ages.

In recent years, because of its advantages, such as better workability, high compressive strength, environmental conservation and high durability [1.1], concrete using ground granulated blast furnace slag (GGBFS) is being widely used all over the world, especially in Japan. The usage of GGBFS is also a good approach for protecting environment. Unfortunately, it has been found that concrete containing GGBFS is susceptible to microcracking, particularly under temperature variation, due to the large autogenous shrinkage and thermal deformation of matrix [1.2]. These microcracks must be one of the causes of severe macrocracks observed in real structures (**Fig. 1.1**). Overcoming this problem is a big challenge.

Fig. 1.1 Severe thermal cracks in concrete with slag cement type B and limestone.

According to the previous research [1.2], to use small-size coarse aggregate, light weight fine aggregate, or coarse aggregate with small different coefficient thermal expansion compared with the mortar proved to be effective measures to mitigate microcracking in slag concrete. As those measures cannot be adopted in all construction sites, practical solutions to mitigate microcracking should be proposed.

In the previous research [1.2], microcracking in concrete at early ages was analyzed by acoustic emission (AE) technique owing a wave guide embedded inside concrete. However, the researcher faced to the problem of attenuation of acoustic wave in concrete with high water to binder ratio, that is a high moisture content ambient. Improvement of the wave guide is necessary to precisely investigate microcracking mechanism. This will be discussed in detail in chapter 3.

1.1.2 Durability of concrete in severe condition

Chloride attack is one of the main factors lowering the serviceability of concrete structures in Japan due to its long coast line. More seriously, in cold regions in winter, deicing agent is frequently used for roads which can cause severe deterioration of concrete structures such as scaling, corrosion of steels (**Fig. 1.2**), and ASR.

Fig. 1.2 Severe reinforcing bars corrosion.

In order to improve the resistance of concrete against severe deterioration (scaling, ASR, corrosion), to utilize GGBFS or fly ash will be effective if microcracking in concrete is well controlled.

The durability of concrete structures cannot be measured directly. Nevertheless, it can be evaluated by the resistance of covercrete against the ingress of harmful substances. To evaluate the quality of covercrete, Surface Water Absorption Test (SWAT) has been developed by Hayashi and Hosoda [1.3]. SWAT is a fully nondestructive and automatic method using liquid water under natural pressure. Absorbed water is measured by the reduction of water head with the initial head of 300 mm. Fundamental researches on SWAT [1.3-1.5] have showed that several indices from SWAT measurement may have good correlation with concrete properties related to durability. Iwamoto [1.5] also found that the ultimate penetration depth of water in ordinary Portland cement (OPC) concrete had a good correlation with SWAT index. SWAT may be utilized in actual structures with GGBFS or fly ash to evaluate the durability of the structures after construction.

1.1.3 High alite cement (HAC)

HAC is a cement with high alite ($3CaO.SiO_2$ – C_3S) content and almost no belite ($2CaO.SiO_2$ – C_2S). In Japan, it has been recently developed by Prof. Sakai and D.C. Corporation [1.6]. The only difference between HAC and OPC is mineral composition; therefore it can easily become one of the universal cements. Because of high alite content, HAC produces more $Ca(OH)_2$ (CH) than OPC, which plays an important role in early strength development. The reaction between CH and GGBFS or fly ash will bring continuous strength development. HAC was developed to be used with GGBFS or fly ash, in order to achieve initial and long-term high performance of concrete.

In the past research [1.7], HAC showed a high compressive strength in early ages as well as continuous strength development when it combined with slag at the replacement ratio of slag of around 50% by mass. Therefore, HAC slag or HAC fly ash concrete may have high tensile strength, which improves the cracking resistance of concrete structures. It is also expected that HAC concrete containing mineral additives can improve the durability of concrete structures.

1.2 Objectives

The first objective of this research is to investigate the effectiveness of HAC in mitigating microcracking and increasing tensile strength in slag and fly ash concrete subjected to elevated temperature in early ages by combining AE technique using a redesigned waveguide with physical and mechanical tests and SEM observation.

The second objective of the study is to clarify the effectiveness of HAC in improving the resistance of covercrete containing mineral additives against water and chloride penetration. The effectiveness of HAC will be clarified by SWAT and water/chloride penetration depth test. Based on the investigation results in this research, a method to utilize SWAT to evaluate the durability of actual structures will be proposed.

1.3 Significances of the research

Cracking of slag concrete structures is a severe practical problem; therefore to clarify the effectiveness of HAC in improving the cracking resistance of slag concrete will strongly promote utilizing GGBFS with HAC. One of the disadvantages of fly ash concrete is slow strength development, but fly ash with HAC will overcome this problem. HAC concrete with GGBFS or fly ash showed high performance in resisting against water/chloride penetration. Hopefully, HAC concrete with GGBFS or fly ash will be utilized in cold regions to achieve durable structures.

A new wave guide for AE developed in this research with less effect of attenuation will be utilized for analyzing the characteristics of very young age concrete.

According to this research, SWAT can be fully utilized as an effective technique to evaluate the quality of covercrete in real structures. This is very significant because SWAT is a simple, rapid, and nondestructive method.

1.4 Outline of the thesis

Some fundamental knowledge relating to this research is reviewed in chapter 2, “Literature Reviews”. Characteristics of ground granulated blast furnace slag and fly ash, operating principles and application of acoustic emission, high alite cement, chloride penetration, and surface water absorption test are the specific topics of the chapter.

Chapter 3, “Improvement of Resistance against Microcracking of Slag Concrete by Using High Alite Cement”, is devoted to analyze the mechanism of HAC in improving cracking resistance of slag concrete in early ages. In this chapter, a combination of AE technique using a new-shaped wave-guide with physical and mechanical tests and SEM observation were applied to investigate the effectiveness of HAC in slag concrete subjected to temperature regime simulating steam curing in early ages to mitigate microcracking. Better bond property between HAC mortar and coarse aggregate leading to higher cracking resistance will be intensively investigated.

Chapter 4, “Effects of fly ash in concrete subjected to elevated temperature in early ages”, deals with the effectiveness of fly ash, a by product of coal power generation, in concrete in term of resistance microcracking. The influence of fly ash content, the effect of HAC in fly ash concrete and the use of fly ash as a part of fine aggregate are the topics of the chapter.

Combination of HAC and slag or fly ash to improve chloride resistance of concrete is the content of chapter 5, “Improvement of chloride penetration resistance of concretes containing mineral admixtures”. Surface Water Absorption Test (SWAT) and penetration depth test were employed to evaluate water and chloride immigration into concrete. The effects of additives, curing condition, and type of cement on water and chloride resistance of concrete are investigated in this chapter.

The thesis ends with chapter 6, Conclusions and Recommendations, which summarizes the significant outcomes and conclusions. Important recommendations for future works are also proposed in the chapter.

References

[1.1] ACI committee 233, “Ground Granulated Blast-Furnace Slag as a Cementitious Constituent in Concrete”, *American Concrete Institute (ACI)*, 1995.

[1.2] Son, H. N., and Hosoda, A., “Detection of Microcracking in Concrete Subjected to Elevated Temperature at Very Early Age by Acoustic Emission,” *Journal of Advanced Concrete Technology*, Vol. 8, pp.201–211, 2010.

[1.3] Hayashi, K. and Hosoda, A., “Developement of Water Absorption Test Method Applicable to Actual Concrete Structures”, *Proceeding of the JCI*, Vol. 33, No.1, pp.

1769-1774, 2011. (in Japanese)
[1.4] Usman, K., PhD thesis submitted to Yokohama National University (Concrete Laboratory), 2012.
[1.5] Iwamoto, Y., Master thesis submitted to Yokohama National University (Concrete Laboratory), 2014. (in Japanese)
[1.6] Siribudhaiwan, N., *et al*., "Influence of alite content on the hydration of blended cement", *The 1st International Conference on Concrete Sustainability (ICCS13)*, pp. 447-452, 2013.
[1.7] Hashimoto, A., *et al*., "Properties of high alite cement", *Proceeding of the JCA*, Vol. 66, pp. 32-33, 2012. (in Japanese)

Chapter 2 Literature Reviews

2.1 Introduction

This research relied on fundamental knowledge from many familiar studies in the past. Therefore, a brief view of ground granulated blast furnace slag, fly ash, acoustic emission, crack resistance of concrete, chloride penetration in concrete and surface water absorption test is the content of this chapter.

2.2 Ground Granulated Blast Furnace Slag

2.2.1 Introduction

Blast furnace slag is a waste product in the manufacture of pig iron, about 300 kg of slag being produced for each ton of pig iron. Chemically, slag is a mixture of lime, silica, and alumina – the same oxides contained in Portland cement but not the same proportions [2.1]. Granulated blast furnace slag (GBFS) is the glassy granular material created by rapidly chilling molten blast furnace slag in the water. Ground granulated blast furnace slag (GGBFS) is blast furnace slag which is ground until suitable fineness and is a hydraulic material [2.2].

The use of separate GGBFS and Portland cement has two advantages: the optimum fineness of each material can be reached and the mix proportion can be adjusted depend on each specific requirement.

The principal hydration product of GGBFS is essentially the same as that is formed when Portland cement hydrates, i.e., calcium-silicate hydrate (CSH). In the hydration of slag, the slag reacts with alkali and calcium hydroxide to produce additional CSH. In general, hydration of GGBFS in combination with Portland cement at normal temperature is a two-stage reaction. Initially and during the early hydration, the predominant reaction is with alkali hydroxide, but subsequent reaction is predominantly with calcium hydroxide.

2.2.2 Effects of GGBFS on properties concrete

GGBFS can improve many characteristics fresh concrete as well as hardened concrete. Wood (1981) reported that workability and placeability of concrete containing GGBFS improve when compared with concrete without GGBFS [2.3]. Slag concrete is found to respond very well under elevated temperature curing conditions in accordance to the Arrhenius Law reported by Roy and Idorn (1982) [2.4]. Conversely, when cured at normal or low temperature, strength of slag concrete is expected to reduce in early ages. Nevertheless, in later ages, compressive strength of slag concrete is higher than that of OPC concrete (**Fig. 2.1**) [2.2]. Slag concrete also has high resistance against sulfate attack, alkali-silica reaction (ASR), freezing and thawing, and deicing chemicals. However, creep and shrinkage are greater in concrete containing GGBFS (**Fig. 2.2**) [2.2**]**.

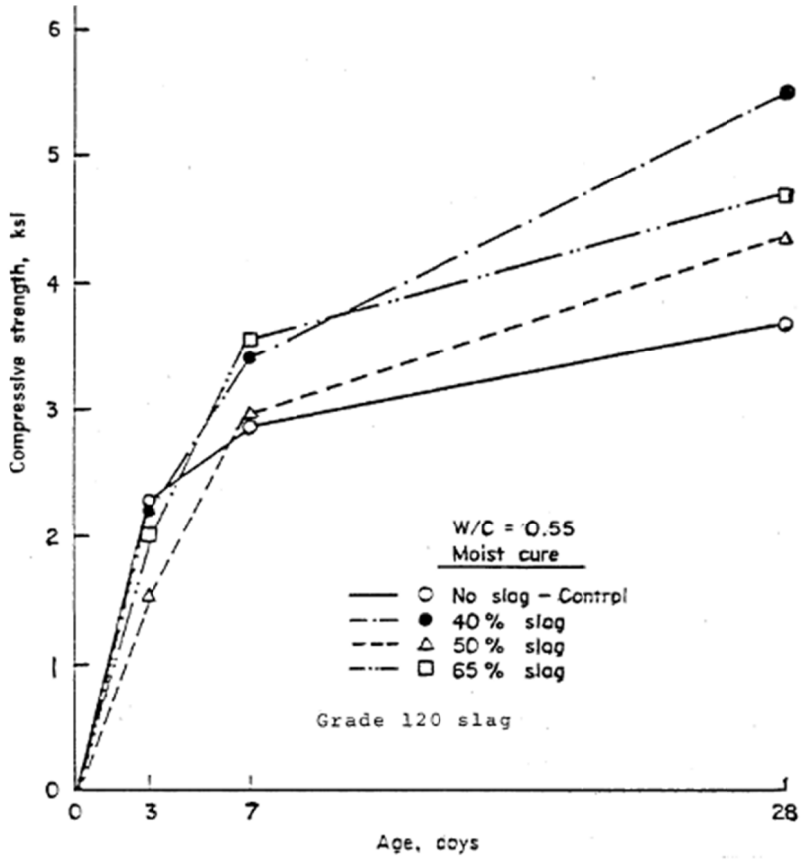

Fig. 2.1 Compressive strength of concrete containing various blends of GGBF slag, compared to concrete using only Portland cement as cementitious material (Hogan and Meusel 1981) (1 ksi = 6.89 MPa) [2.2].

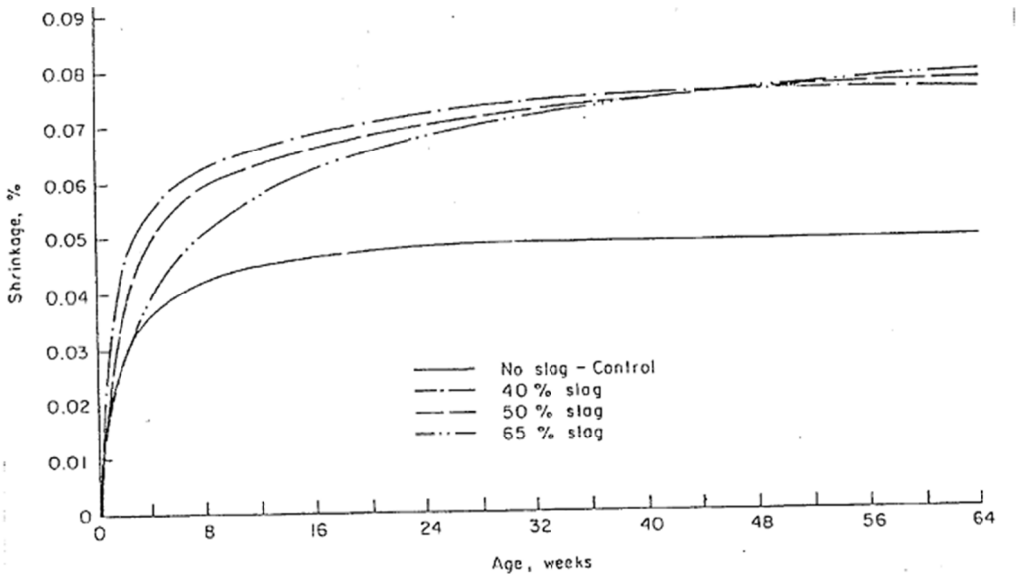

Fig. 2.2 Drying shrinkage of non-air-entrained concrete for various slag replacements (w/c = 0.55) [2.2].

2.2.3 Thermal microcracking of slag concrete

(1) Mechanisms of thermal microcracking in concrete

It is apparent that thermal microcracking just generates in concrete subjected to temperature variation when there exists a restraint that restricts the deformation of concrete. Restraint in concrete is classified into two types: mesoscopic restraint and macroscopic restraint [2.5]. Because mortar deforms much larger than coarse aggregate due to thermal and autogenous shrinkage, mesoscopic restraint is defined as the restraint of coarse aggregate against deformation of mortar. In case of concrete as a whole is subjected to an external restriction, it is classified as macroscopic restraint. For instant in massive concrete structure when the current lift is placed, its deformation will be restrained by the hardened previous lifts. The restriction of hardened lifts is called macroscopic restraint.

A theoretical model for composite in mesoscopic level is shown in **Fig. 2.3**. Under temperature variation, stresses induced in mortar are as follows [2.5]:

$$\sigma_r = P(R/r)^3 \tag{2.1}$$

$$\sigma_t = -P(R/r)^3 \tag{2.2}$$

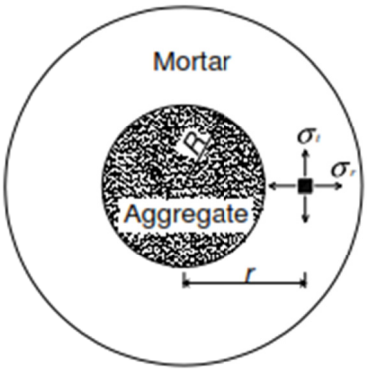

Fig. 2.3 Model for concrete composite in mesoscopic level [2.5].

$$P = \frac{\Delta D_t + S_m}{\frac{1+\upsilon_m}{E_m} + \frac{1-2\upsilon_a}{E_a}} \tag{2.3}$$

where,

σ_r, σ_t : radial and tangential stresses in mortar, respectively,

R : nominal radius of coarse aggregate,

r : distance from the center of aggregate particle

P : pressure act on inner face of the matrix due to both thermal deformation and shrinkage

ΔT : temperature gap

α_m, α_a : coefficient of thermal expansion (CTE) of mortar and aggregate

S_m : shrinkage of mortar

υ_m, υ_a : Poisson's ratio of mortar and aggregate

E_m, E_a : Young's modulus of mortar and aggregate

From equations 2.1 to 2.3, it can be pointed out that mesoscopic tensile stress in concrete is directly proportional to the difference of CTE between mortar and aggregate, shrinkage of mortar, size of aggregate. The larger these factors, the bigger the tensile tress.

(2) Thermal microcracking in slag concrete

Son and Hosoda [2.6] (2010) found that slag concrete is easily subjected to microcracking in early ages under accelerated temperature (**Fig. 2.4**) due to higher autogenous shrinkage and high CTE of mortar with GGBFS. Cracking in slag concrete was characterized by a large number of small microcracks. Microcracking in concrete with

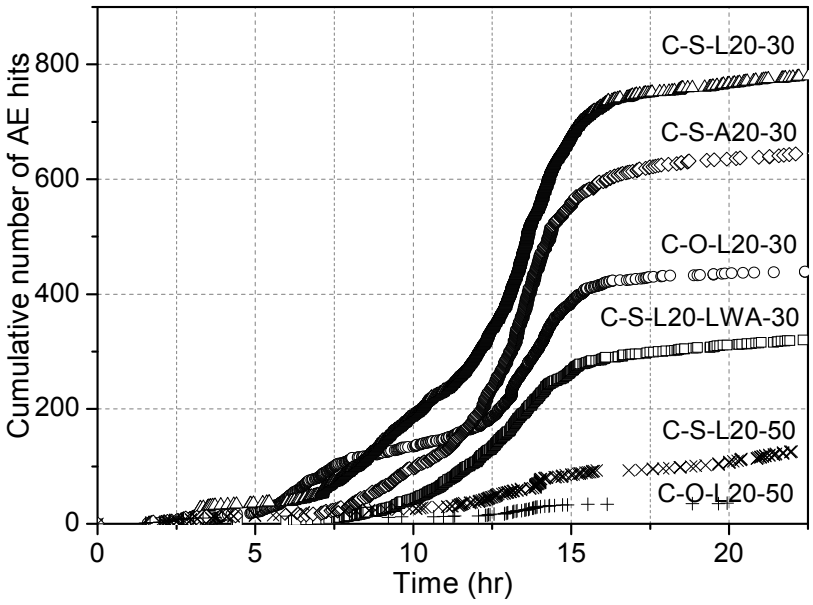

Fig. 2.4 Development of AE hits in slag concretes and OPC concretes [2.6].

GGBFS tended to release lower energy, which implied that microcracks might appear at a lower stress, as compared with that in OPC concrete. Brittleness might be the reason for lower cracking resistance of slag concrete.

(3) Improvement the resistance against cracking in slag concrete

In the research of Son [2.5], he pointed out that the use of saturated fine light weight aggregate (LWA) could decrease autogenous shrinkage and thus, mitigate microcracking in slag concrete with low W/B ratio. Using small-size coarse aggregate also reduce microcracking in concrete owing to the decrease of tensile stress.

One of the ways to prevent concrete from cracking is improvement of the strength of the interface transition zone (ITZ), which is more porous than the hydrated cement paste further away from the coarse aggregate [2.7]. The strength of the ITZ can improve with time due to the secondary reaction of $Ca(OH)_2$ (CH), a product of cement hydration, and pozzolana [2.8]. Therefore, if the amount of CH during hydration of cement raises, the strength of the ITZ will increase.

2.3 Fly ash

Fly ash is a by-product during the coal power generation and consists mainly of SiO_2, Al_2O_3, Fe_2O_3 and CaO. The fly ash particles are spherical (which is advantageous

from the water requirement point of view) and have a very high fineness: the vast majority of particles have a diameter between less than 1 μm and 100 μm, and the specific surface of fly ash is usually between 250 and 260 m^2/kg (**Fig. 2.5**). The high specific surface of the fly ash means that the material is readily available for reaction with calcium hydroxide [2.9]. Fly ash has been used in concrete as a cementitious material as well as fine aggregate.

2.3.1 Classification

Fly ashes have been generally classified into two classes prescribed to ASTM C618-94a, which is based on the type of coal from which the ash originates. Class F fly ash deriving from bituminous coal is mainly siliceous and is the most common fly ash. It contains more than 70% of SiO_2, Al_2O_3, and Fe_2O_3 and exhibits the pozzolanic characteristics. The other is Class C fly ash collected from sub-bituminous coal and lignite. It is high-lime ash with the total content of SiO_2, Al_2O_3, and Fe_2O_3 between 50 and 70% and the lime content as high as 24%. Class C fly ash has some cementitious properties of its own but, because its lime will combine with the silica and alumina portions of the ash, there will be less of these compounds to react with lime liberated by the hydration of cement [2.9].

The variability of fly ash arises from the fact that fly ash is not the specially manufactured product and cannot, therefore, be governed by strict requirements of a standard. The main influences are the nature of the coal and the manner of its pulverization, the operation of the furnace, the process of precipitation of ash from the combustion gages, and especially the extent of classification of the particles in the exhaust system [2.9].

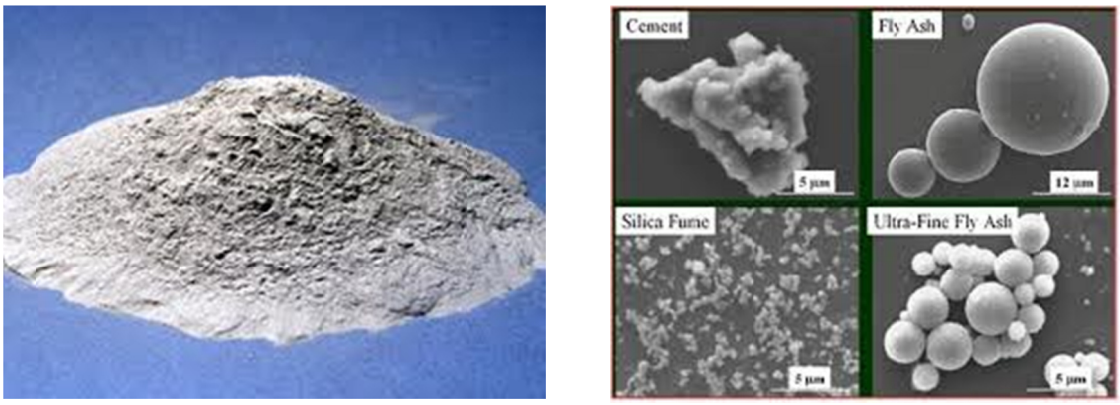

Fig. 2.5 Dimension of fly ash grain.
Source: http://www.us-concrete.com, accessed on March 26, 2014

2.3.2 Hydration process

The products of fly ash reaction closely resemble calcium silicate hydrate (CSH) produced by hydration of OPC. However, the reaction does not start until 7 days after mixing [2.10]. In the case of Class F fly ash, this can be as long as one week or even more. These products diffuse away and precipitate within the capillary pore system; this result in a reduction in the capillary porosity and, consequently, a finer pore structure. Because the reactions of fly ash in concrete take a long time, prolonged wet curing is essential. High temperature, between 20 and 80^{o}C accelerates the reactions of fly ash to a greater extent than is the case with OPC alone [2.9].

Incorporating fly ash in cement paste would affect the hydration rate of fly ash and consumption of calcium hydroxide. Due to its pozzolanic reaction fly ash concrete shows less calcium hydroxide than OPC concrete. Reaction rate of fly ash depends on curing temperature, curing age and fly ash replacement ratio. The pozzolanic reaction of fly ash may continue after the fully hydration of cement, and consequently, microcracks can be filled by hydrated products of fly ash resulting in higher resistance to carbonation test. Fly ash also presents a self-healing capacity [2.11].

The reaction ratio of fly ash depended on the glass content. Fly ash with high glass content had a larger reaction ratio than that with a low one during the period from 28 to 270 days. This tendency was evident when the replacement ratio of fly ash is low. However, the reaction ratio of fly ash at 360 days was regardless of glass content (**Fig. 2.6**) [2.10].

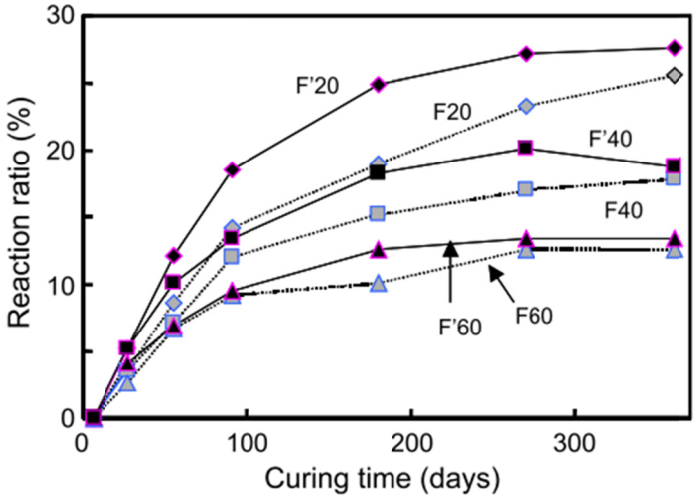

Fig. 2.6 Reaction ratio of fly ash wit high (F') and low (F) glass content [2.10].

Fly ash also affected the hydration of cement clinker minerals in the fly ash cement. The long-term hydration of alite was accelerated, while on the other hand, that of belite and C_4AF was retarded [2.10].

2.3.3 Characteristics of concrete containing fly ash

(1) Fresh concrete

The main influence of fly ash on properties of fresh concrete is that on water demand and on workability. For a constant workability, the reduction in water demand of concrete due to fly ash is usually between 5 and 15% by comparison with an OPC-only mix having the same cementitious material content; the reduction is larger at higher w/c [2.9]. This was also confirmed by Berndt (2009) [2.12].

A concrete mix containing fly ash is cohesive and has a reduced bleeding capacity. The influence of fly ash on the properties of fresh concrete is linked to the shape of the fly ash particles. One consequence of high carbon content in fly ash is that it adversely affects workability. Fly ash in the mix has a retarding effect, typically of about 1 hour, probably caused by the release of SO_3^{--} present at the surface of fly ash particles [2.9].

Li and Guo (2010) [2.13] reported that fly ash can also reduce the autogenous shrinkage because it reduces cement hydration.

(2) Hardened concrete

Due to the slow rate of hydration of fly ash, the concrete with high volume fly ash showed lower compressive strength and lower durability performance than OPC concrete at early ages [2.14,2.15]. Berndt (2009) [2.12] also stated that partial replacement of cement with 50% fly ash results in decreased strength of concrete using recycled concrete aggregate, particularly at 7 day. It cannot be assumed that all sources fly ash will necessarily improve the properties of concrete at high replacement levels and that detailed testing of specific materials and mix proportions is recommended before use in construction projects.

After a slowing of the early rate of strength contribution by OPC, the continued pozzolanic activity of fly ash contributes to increased strength gains at greater ages if the concrete is kept moist. Fraay et al [2.16] explained this phenomenon, stating that the glass

material in fly ash is broken down only when pH value of the pore water is at least 13.2, and the increase in the alkalinity of the pore water requires that a certain amount of hydration of Portland cement in the mix has taken place.

Thus, concrete with fly ash showed the better compressive (after 7 days) and flexural strength but the lower splitting tensile strength compared with no-fly ash concrete (**Fig. 2.7**). At early ages, the no-fly ash mixture showed higher modulus of elasticity than the fly ash mixtures. The difference between the mixtures became significantly small as curing was extended beyond 7 days [2.17].

Shi and Shao (2002) [2.18] concluded that fly ash concrete is more sensitive to elevated temperature curing than OPC concrete due to the higher activation energy for pozoolanic reaction. Elevated temperature curing increased the strength development rate, but decreased the ultimate strength of concrete. Grinding can also increase the reactivity of fly ash to some extend. However, the use of chemical activator(s) was the most efficient and inexpensive technique for enhancing reactivity of fly ashes compared with these above ones. Na_2SO_4 was more affective at early ages and $CaCl_2.2H_2O$ at later ages. The same conclusion was also derived by Jueshi et al (2001) [2.19].

Li and Zhao (2003) [2.20] indicated that when Class F fly ash was used with GGBFS as cementitious materials, it can improve both short- and long-term characteristics of concrete while fly ash-only concrete required a relatively longer time to get its beneficial effect.

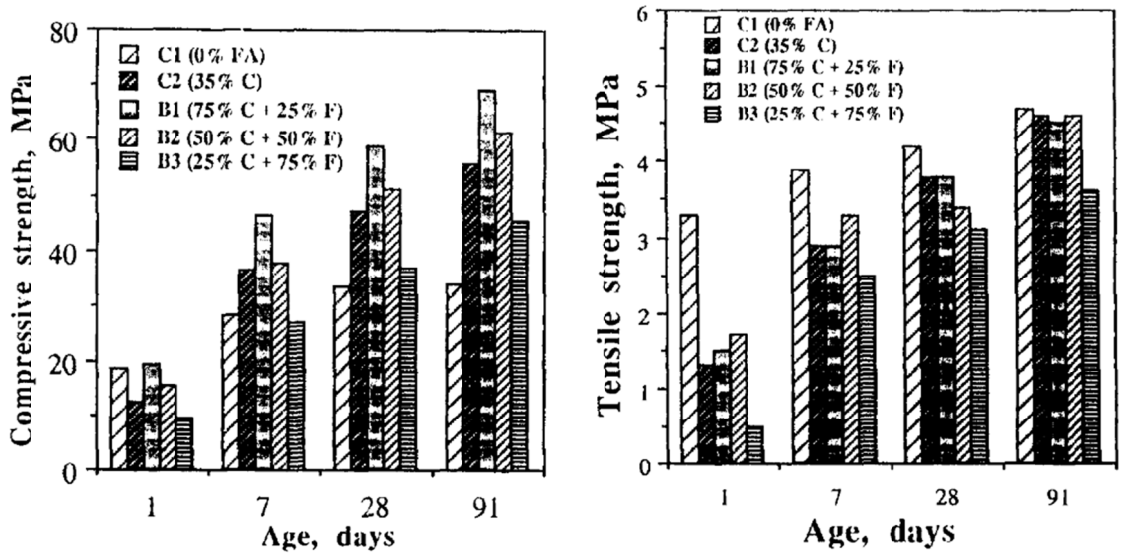

Fig. 2.7 Compressive (left) and tensile (right) strength of concrete containing FA [2.17].

As well as GGBFS concrete, fly ash concrete has good resistance to chloride ions due to these reasons as showed below [2.21]:

- Fly ash may improve the distribution of pore size and pore shape of concrete.

- More CSH gel may be formed when fly ash and slag concrete hydrate, which may absorb more chloride ions and block diffusing path.

- Fly ash has more C_3A which can absorb more chloride ions.

The similar results were observed by Uysal and Akyuncu (2012) [2.10]

Moreover, influence of fly ash on properties of concrete depends on the type of fly ash. The use of Class C fly ash instead of Class F fly ash with the same cement dosage and fly ash percentage generally caused to higher compressive strength. The chloride ion permeability of the concretes containing Class C and Class F fly ashes decreased when the fly ash content regardless of fly ash type was increased. Sorptivity of the concretes containing Class C and Class F fly ashes decreased with the increase in the fly ash content for each series. Incorporation of Class C and Class F fly ashes substantially improved durability performance of the concretes [2.22].

(3) Fly ash as fine aggregate

Some researchers have also investigated fly ash not as cementitious material but as a part of fine aggregate. Siddique (2003) [2.23] carried out experimental investigation to evaluate the mechanical properties of concrete in which fine aggregate was partial replaced with 10%, 20%, 30%, 40%, and 50% of Class F fly ash by weight. The results showed that compressive, splitting tensile, flexural strength and modulus of elasticity of fine aggregate replaced fly ash concrete specimens were higher than the plain concrete specimens at all the ages (**Fig. 2.8**). The maximum values of above chemical characteristics were gained when the replacement ratio of fine aggregate by fly ash was 50%. He also found that the abrasion resistance of concrete increased with the increase in percentage fine aggregate replacement with fly ash [2.24].

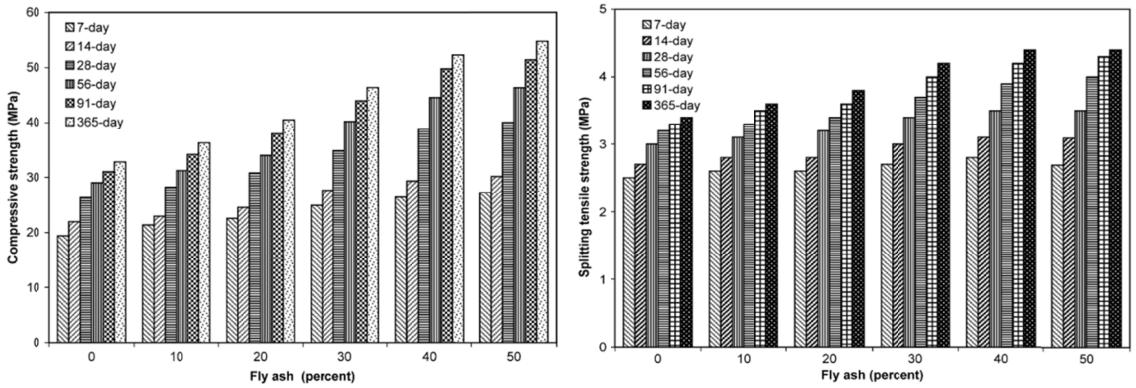

Fig. 2.8 Compressive (left) and splitting tensile (right) strength versus FA content [2.23].

As well, Varughese and Chaturvedi (2002) [2.25] opined that fine aggregates in combination with fly ash and river sand showed synergism in strength behavior and resistance to water absorption of polyester based polymer concrete up to the level of 75% by weight of fly ash.

Fly ash as fine aggregate was also studied in term of combination with blast furnace slag in the research of Singha Roy (2011) [2.26]. Experiments about properties of concrete with partial replacement of sand by fly ash and blast furnace slag as coarse aggregate were conducted. The result showed that up to 40% replacement of sand by fly ash, concretes presented superior compressive and flexural strength but comparable splitting tensile strength, higher modulus of elasticity, smaller porosity and hence, better water absorption resistance. He concluded that 40 per cent was the suitable fraction for the replacement of sand by fly ash.

2.4 High Alite Cement (HAC)

2.4.1 What is HAC?

HAC is special cement with high alite ($3CaO.SiO_2 – C_3S$) content and almost no belite ($2CaO.SiO_2 – C_2S$). In Japan, it has been recently developed by Prof. Sakai and D.C. Corporation [2.1]. Because of high alite content, HAC produces more $Ca(OH)_2$ (CH) than OPC, which plays an important role in strength development, durability of hardened concrete, and reactivity with blending materials such as slag or fly ash.

2.4.2 Properties of HAC concrete

(1) Hydration rate

It is found that heat liberation in blended cement when using HAC is higher compared with OPC blended. Alite phase is also reacted faster when blending materials is added due to the finer particle's size of additives [2.27]. The faster rate of hydration of alite phase may improve tensile strength of HAC concrete at early ages that enhances the ability in resisting against microcracking of concrete subjected to elevated curing temperature.

(2) Compressive strength of HAC concrete

The comparison of compressive strength development between concrete with OPC, slag cement type B (BB), HAC, and HAC with slag with some replacement ratios is shown in **Fig. 2.9** [2.28]. Concrete with HAC only presented the highest strength in early ages but lowest long-term strength compared with the other concretes. HAC concretes with slag showed high early strength as well as good strength development. It can be said that HAC should be utilized additive, for instance slag, because of its good long-term behavior. The most suitable replacement ratio of slag in HAC concrete might be 50%.

However, the effect of HAC on tensile strength of concrete, the important factor influencing cracking resistance, has been not found in literature.

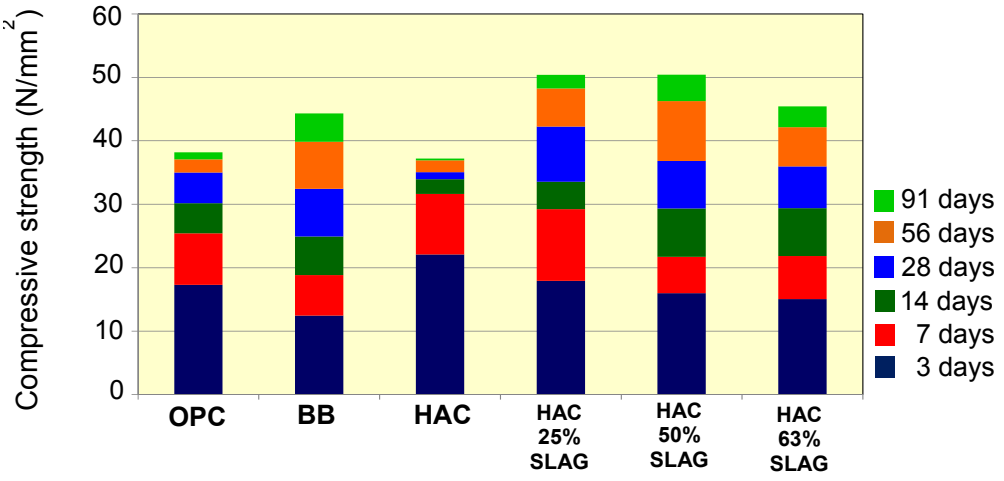

Fig. 2.9 Compressive strength development of concretes [2.28].

2.5 Acoustic Emission

2.5.1 Introduction

Acoustic emission testing (AET) has become a recognized nondestructive test (NDT) method commonly used to detect and locate faults in mechanically loaded structures and components. AE can provide comprehensive information on the origination of a discontinuity (flaw) in a stressed component and also provides information pertaining to the development of this flaw as the component is subjected to continuous or repetitive stress.

Discontinuities in components release energy as the component is subjected to mechanical loading or stress. This energy travels in the form of high-frequency stress waves. These waves or oscillations are received with the use of sensors (transducers) that in turn convert the energy into a voltage. This voltage is electronically amplified and with the use of timing circuits is further processed as AE signal data. Analysis of the collected data comprises the characterization of the received voltage (signals) according to their source location, voltage intensity and frequency content.

Acoustic emission is a passive technique in detecting cracking in materials. The major difference between the AE method of NDT and the other NDT methods is that this method is passive, whereas the others, in a sense, are for the most part active. With ultrasonic, radiographic or the other NDT methods, the source of information is derived by creating some effect in or on the material by external application of energy or compounds. AE relies on energy that is initiated within the component or material under test. When cracks generate inside material, they will emit sound depicted as acoustic waves. These acoustic waves will be transmitted through continuous medium to the surface and are recorded by acoustic sensors (**Fig. 2.10**). By analyzing the parameters of acoustic waves, the properties of crack can be observed. The sources causing fracture in materials are abundant. They can be an application of external loading or an internal stimulus such as the incompatible deformation of each component in a composite material.

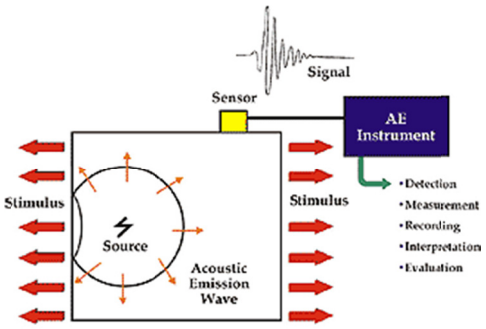

Fig. 2.10 Schematic of AE event generation and recording.

Source: http://www.pacndt.com, accessed on March 12, 2014

AET is a completely nondestructive testing method. Not similar as the other methods those can only measure fracture in material at a definite time, AET can detect and analyze the whole progress of cracking, i.e. from generation to propagation of cracking. The range of materials can be applied AET is wide; include metal, wood, polymers, concrete and other materials. Because of its high sensitivity, AET can recognize a defect in material at very early period.

2.5.2 Terminologies and definition

A typical AE system is showed in **Fig. 2.11**. Terminologies and their definition were collected from Physical Acoustic Corporation [2.29]. The key definitions for an AE signal feature can be observed in **Fig. 2.12** [2.30].

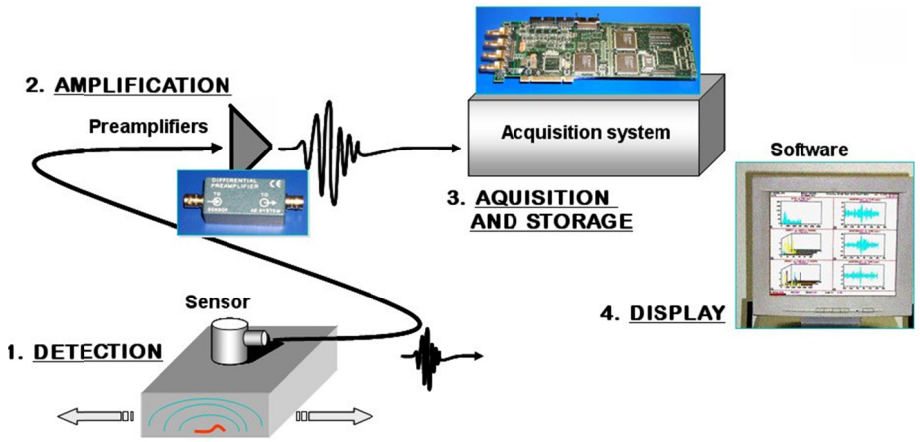

Fig. 2.11 A typical AE system.

Source: http://www.epandt.com, accessed on March 12, 2014

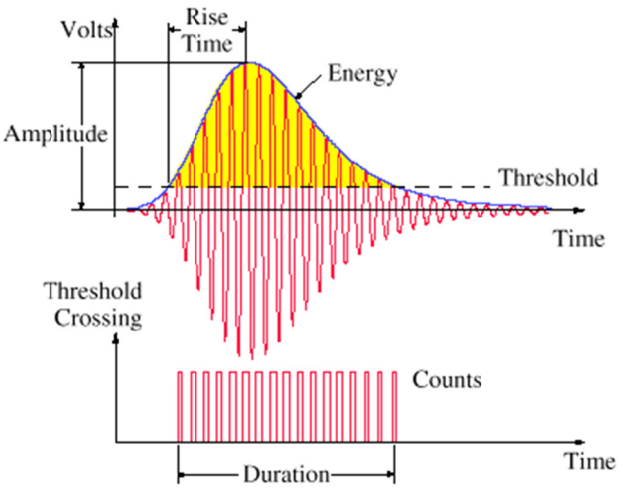

Fig. 2.12 The definitions of an AE signal [2.2].

1. **Activation**: the onset of AE due to the application of a stimulus such as force, pressure, heat, etc.
2. **Activity**: a measure of emission quantity, usually the cumulative energy count, event count, ring down count, or other rates of change of these quantities.
3. **Amplitude**: the largest voltage peak in the AE signal waveform; customarily expressed in decibels relative to 1 microvolt at the preamplifier input (dB) assuming a 40 dB preamp. For this case, 0 dB corresponds to a 100-μvolt peak at the output of the 40 dB preamplifier and 100 dB would correspond to a 10-volt peak signal at the output of the preamplifier.
4. **Amplitude distribution**: a digital display of the number of AE signals at (or greater than) a particular amplitude, plotted as a function of amplitude.
5. **Attenuation**: loss of amplitude with distance as the wave travels through the test structure.
6. **Channel**: a single AE sensor and the related equipment components for transmitting, conditioning, detecting and measuring the signals that comes from it.
7. **Count**: the number of times the AE signal crosses the detection threshold. Also known as “ring down count”, “threshold crossing count”.
8. **Decibel (dB)**: a unit of measurement for AE signal amplitude A, defined by $A(\text{dB})=20\log V_p$ where V_p is the peak signal voltage in microvolts referred to the preamplifier input.
9. **Detection**: recognition of the presence of a signal.

10. **Event**: a local material change giving rise to acoustic emission.
11. **Event data set**: the set of numbers used to describe an event, pursuant to data processing that recognizes that a single event can produce more than one hit.
12. **Event energy**: the total elastic energy (in the wave) released by an AE event. (Definitions of energies are different in AE system suppliers, but it is generally defined as a measured area under the rectified signal envelope.)
13. **Felicity effect**: (the reverse of the Kaiser effect) the presence of AE at stress levels below the maximum previously experienced.
14. **Frequency**: for an oscillating signal or process, the number of cycles occurring in unit time.
15. **Hit**: the detection and measurement of an AE signal on a channel.
16. **Hit data set**: The set of numbers representing signal features and other information, stored as a result of a hit.
17. **Intensity**: a measure of the size of the emission signals detected, such as the average amplitude, average AE energy.
18. **Kaiser effect**: the absence of detectable acoustic emission at a fixed sensitivity level, until previously applied stress levels are exceeded.
19. **Noise**: non-relevant indications; signals produced by causes other than AE, or by AE sources that are not relevant to the purpose of test.
20. **RA value**: a calculated feature derived from rise time divided by peak amplitude [2.26]
21. **Rise time**: the time from an AE signal's first threshold crossing to its peak.
22. **Sensor**: a device containing a transducing element that turns AE wave motion into an electronic voltage.
23. **Signal**: the electrical signal coming from the transducing element and passing through the subsequent signal conditioning equipment (amplifiers, frequency filters).
24. **Signal description**: the result of hit process: a digital (numerical) description of an AE signal and/or its environmental context.
25. **Signal features**: measurable characteristics of AE signal, such as amplitude, AE energy, duration, counts, rise time, that can be stored as a part of the AE signal description.
26. **Signal strength**: the strength of the absolute value of a detected AE signal. Also known as "relative energy", "MARSE", and "signal strength".

27. **Source**: the physical origin of one or more AE events.

2.5.3 Analysis of AE signal

Two approaches to analyze AE signals include *parameter-based* and *signal-based* [2.31]. Both approaches are currently applied with success for different applications. The main advantages of parameter-based technique are the high recording and data storing speeds that facilitate fast visualization of the data. This makes the technique very economical. However, decreasing a complex signal to only a few parameters can be a remarked limitation and sometimes be downright misunderstanding. On the other hand, even though significant technical advances have been made in recent years, it is still not possible to use signal-based techniques to monitor large structures. In addition, the relatively high financial costs and the time required to apply modern signal-based techniques are reasons why parameter-based techniques are still popular.

In this research, only parameter-based analysis is utilized. Some conventional parameters were employed such as hit, count, rise time, duration, energy, frequency. This is a statistical method and can not give a clear picture about the fracture of material or structure but it is useful when compared with the controlled specimen. The relationship between cumulative hit, count, energy and collapsed time also reveals the appearance, propagation and level of cracking.

2.5.4 Application of AE technique

Due to the demand of the development of advanced inspection method for concrete structures, modern AE research in concrete was started in 1970s. This technique has been applied to study not only hardened but also young age concretes. However, the number of researches concerning about the latter has been much smaller than that about the former.

(1) AE for young age concrete

AE technique can be applied for fresh from mixing to assess some its properties. By directly attaching AE sensor to the outer surface of a concrete mixer, Ohtsu et al (1995) could estimate quickly the consistency of fresh concrete during mixing due to the observed AE energy [2.32]. The result in **Fig. 2.13** showed that there was a relationship between the

transition point in cumulative AE energy line and VC value, which represents for the consistency of concrete.

AE measurement was also utilized to simply estimate the level of compaction by Kunisue et al (2002) [2.32]. By coupling AE sensor to the outer surface of mold during dynamic compaction, they stated that full compaction can be achieved at the time AE count rate and energy shift from the active state to steady state.

Son and Hosoda (2010) are the first authors that investigate micocracking in concrete during hydration under elevated temperature [2.6]. Not as similar as the aforementioned experiments, they use a wave-guide embedded in concrete to collect AE signals emitting from microcracks because in very early ages AE sensor can not be directly attached to the surface of concrete. AE sensor can not be also coupled to the outer surface of mold because during hydration process, concrete will shrink and detach from the inner surface of mold leading to discontinuous ambient for AE wave transition. This method will be described in detail in the next chapter.

(2) AE for hardened concrete

So far majority of AE measurement has been applied for hardened concrete. AE source of hardened concrete is normally cracking due to itself deterioration (shrinkage, creep), temperature variation, or external loading.

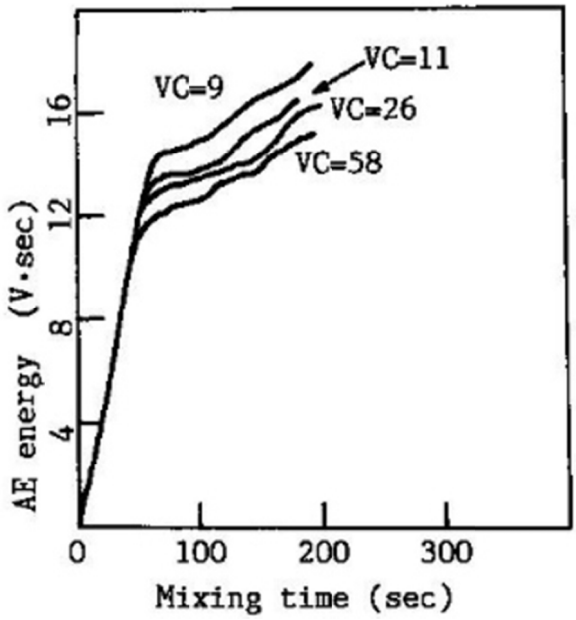

Fig. 2.13 Cumulative AE energy during mixing [2.32].

Soulioti et al (2009) [2.33] utilized AE to characterize of the failure process of steel fiber reinforced concrete beam under four-point bending. Analysis revealed that particular AE parameters change monotonically with the progress of damage.

Due to the distinct in arrival time of acoustic waves, AE can be applied to locate the crack in concrete structures in one dimension (Heam and Shield, 1997), two dimensions, or three dimensions (Ohtsu, 1995). The located AE source in reinforced concrete beam in the experiment of Ohtsu (1995) is shown in **Fig. 2.14 [**2.32].

AE measurement has been successful in quantitative damage evaluation of concrete. Ohtsu and Watanabe (2001) [2.34] applied AE technique to investigate damage in laboratory concrete sample as well as concrete-core samples taken from a real structure. The results suggest that the damage of concrete at the current state could be readily estimated from AE rate process analysis without knowing the original state of the concrete at construction. Kim and Weiss (2003) [2.35] used AE to quantify damage in restrained fiber-reinforced cement mortars due to the fact that as the concrete neared the age of visible cracking, the acoustic waves generated in the restrained specimens had a greater amplitude and duration. Measurement of AE energy may provide a better indication of the time of cracking, while the rate of AE energy release may provide information as to the development and propagation of a localized crack.

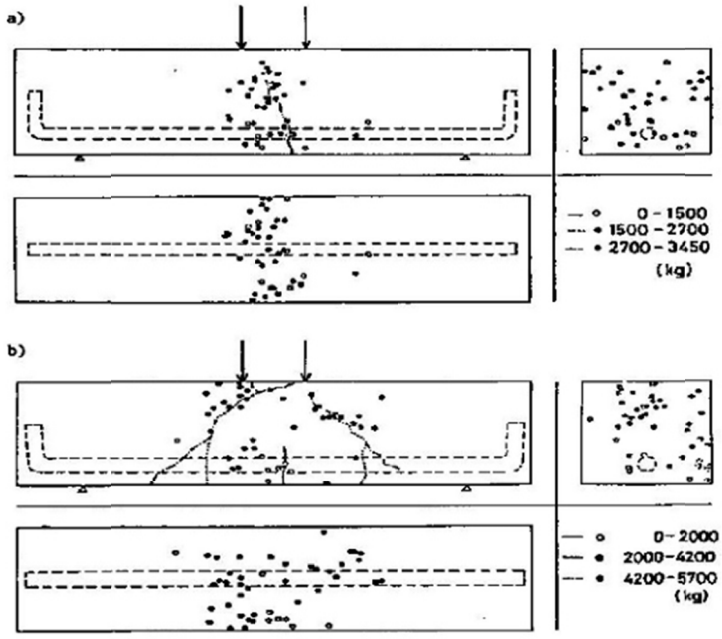

Fig. 2.14 Located AE source in reinforced concrete beams of **(a)** bending-mode failure and **(b)** shear-mode failure [2.32].

2.5.5 Attenuation of AE wave

When an acoustic wave transits through material, its amplitude reduces. This phenomenon is known as attenuation and is illustrated (in case of steel plate) in **Fig. 2.15** [2.36]. The longer the distance from AE source is, the smaller the signal amplitude is.

Attenuation is due to several factors. In most structures, the key factors are geometric spreading, scatter at the structural boundaries and geometrical discontinuities, and absorption. The first factor is fundamental to wave propagation, the second one makes a part of wave energy be reflected, and the last one will convert absorbed elastic and kinetic energies in the wave into heat.

Aggelis at el (2005) [2.37] reported an increase in attenuation of AE wave with an increase of frequency. Landis (2008) [2.38] noted that moisture content has an influence on attenuation. Therefore, it is expected that attenuation in concrete with higher W/B is higher. This was confirmed in experiments of Son and Hosoda (2010) [2.6] where there was almost no AE hit recorded in very early ages (up to 5 hours from mixing) because in this state moisture content in concrete was very high due to remained water not consumed in hydration.

It can be said that, reducing the effect of attenuation of acoustic wave is a big challenge in application of AE technique to investigate microcracking in concrete in early ages, especially in concrete with high W/B.

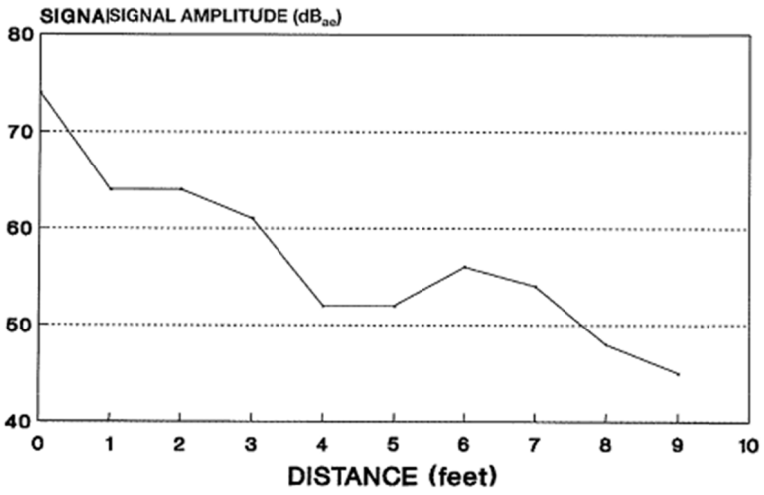

Fig. 2.15 Attenuation amplitude decreases with distance [2.36].

2.6 Chloride penetration in concrete

2.6.1 Introduction

The deterioration of concrete is due either to external impacts or internal factors within the concrete itself. The various actions can be mechanical, physical and chemical. Chemical attack includes alkali-silica and alkali-carbonate reaction, carbonation induced corrosion of reinforcement, and chloride induced corrosion of reinforcing bar [2.39].

Degradation of concrete due to chloride attack is more popular in the region near ocean, where chloride in sea water is moved by wind to the surface of concrete structure. More seriously, in very cold region, in the winter deicing salt is used to thaw ice layer on the surface of road. This agent will penetrate to concrete structure and cause severe deterioration.

2.6.2 Mechanisms and factors affecting chloride penetration

There are three mechanisms relating to penetration of chloride ion: capillary absorption, permeation and diffusion. The difference of these mechanisms is due to driving force for the transfer of chloride.

The principal mechanism of chloride ingress is diffusion, the transportation of chloride ion under a differential in concentration. Conditions for diffusion are that the concrete must have a continuous liquid phase and there must be a chloride ion concentration gradient.

The second mechanism for chloride penetration is permeation due to an absolute pressure gradient. If there is an applied water head on one face of the concrete and chlorides are present, they may permeate into the concrete.

A more common method is absorption, the capillary movement in the pores in concrete which are open to the environment. As a concrete surface is exposed to the ambient medium, it will undergo wetting and drying cycles. When water (possibly containing chlorides) encounters a dry surface, it will be drawn into the pore structure though capillary suction. Driving force of absorption is moisture gradients.

There are two main factors that affect the ingress of chloride ion in concrete:

chemistry (chloride binding and pore solution pH) and its microstructure (tortuosity, permeation) as shown in **Fig. 2.16** [2.40]. If concrete is more porous or the pathway of permeation is more tortuous, chloride diffusion coefficient will decrease. Pore structure in term is affected by the water to cement ratio, the appearance of additives and the degree of hydration of the concrete.

The rate of chloride ingress into concrete is also influenced by the chloride binding ability of the concrete. If the matrix can react with chloride ions to form chemical or physical bound, chloride diffusion rate will be reduced. The chloride binding capacity is controlled by the cementitous materials in the concrete. Chemically, chloride ions can be bound by C_3A to form calcium chloroaluminate, $3CaO.Al_2O_3.CaCl_2.10H_2O$, sometimes related as Friedel's salt [2.41]. It means that cement with high C_3A content has high resistance against chloride ingress [2.42].

2.6.3 Methods for evaluating chloride penetration

Chloride penetration can be evaluated by several methods. AASHTO T295 [2.43] (salt ponding test) is the test that evaluate one-dimensional chloride penetration into concrete in long-term of 90 days after curing and conditioning (**Fig. 2.17**). Bulk diffusion test (Nordtest NTBuild 443) is also a long-term test that is more advanced than salt ponding test [2.44].

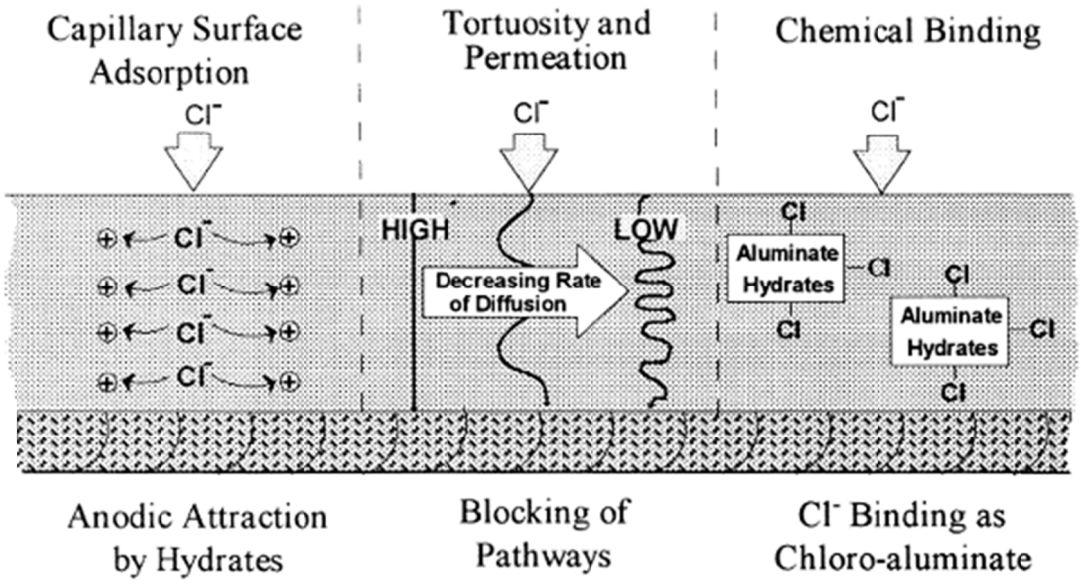

Fig. 2.16 Mechanisms controlling chloride ingress in concrete [2.40].

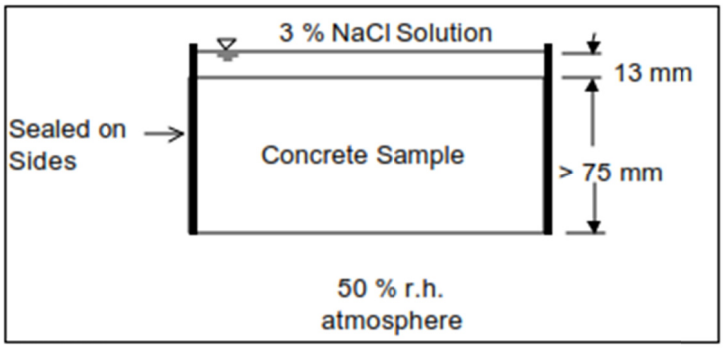

Fig. 2.17 AASHTO T259 test setup [2.43].

Because these test procedures take so much time, some short-term tests of chloride ingress has been developed. AASHTO T277 [2.45] (rapid chloride permeability test – RCPT), whose originally proposed by Whiting, evaluates chloride ion penetrability according to total charge passed through concrete within 6 hours (**Fig. 2.18**). The rapid migration test (CTH test) developed by Tang and Nilsson (1992) [2.46] spends 8 hours to obtain the result.

Indirect measurement of chloride penetration has also been developed. Armaghani and Bloomquist [2.47] have accessed the correlation between water permeability and chloride ion permeability (RCPT results). Unfortunately, there has been no relationship between the results of the field permeability test and the RCPT, although field permeability test has been correlated to the laboratory permeability results [2.48].

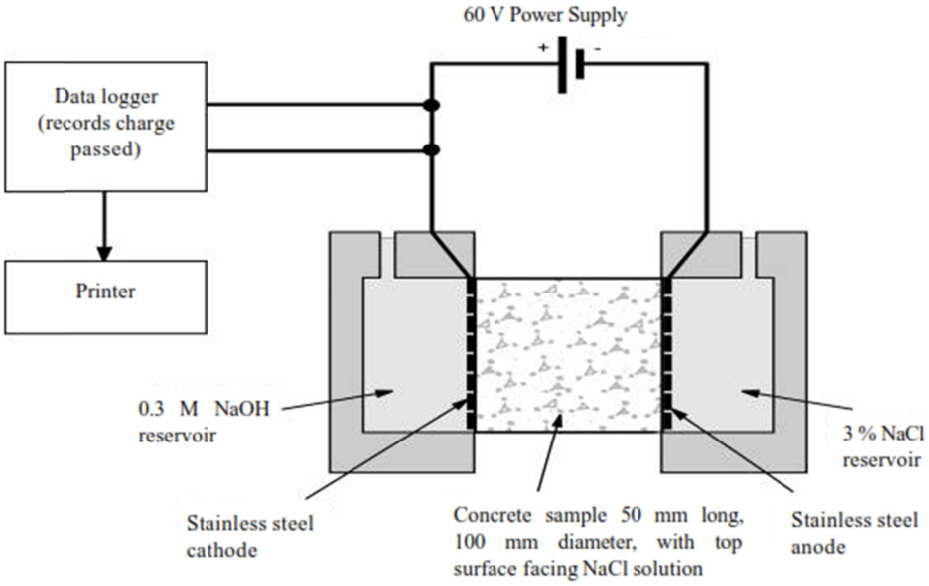

Fig. 2.18 AASHTO T277 test setup [2.45].

Another substance, which can diffuse into concrete, has been used to examine diffusion of chlorides in concrete. Feldman has used the diffusion measurement of propan-2-ol into a saturated cement paste [2.49] while Sharif, et al. has applied gas for their experiment [2.50]. Then, the results have been related to achieve diffusion of chloride ions.

It can be said that the movement of chloride ions into concrete is a complex, multi mechanistic phenomenon. Each aforementioned test has its own advantages as well as disadvantages. So far as there has been no method which is rapid, precise and flexible to evaluate penetration of chloride ions at both laboratory and real site.

2.7 Surface Water Absorption Test (SWAT)

2.7.1 Introduction

Surface Water Absorption Test (SWAT) is a fully non-destructive method to evaluate the quality of covercrete. This method has been developed by Hayashi and Hosoda [2.51]. It even does not require any destructive setup arrangement. Unlike other tests that utilize only one index, SWAT system gives three indices that all have their significance and represents particular physical meaning. SWAT can be easily applied in both laboratory and actual site. Especially, the data of SWAT is automatically recorded, i.e. the test can obtain highly precise data.

2.7.2 SWAT apparatus and mechanism of water absorption

The surface water absorption test apparatus consists of a water cup and a graduated tube as shown in **Fig. 2.19**. The setup for SWAT automatic measurement is presented in **Fig. 2.20**.

The inside diameter of the water cup is 80 mm. The height of the tube from the center of the cup is 300 mm with an inside diameter of 8 mm. It is approved that the water head of arrange from 100 mm to 500 mm has insignificant effect on the SWAT value. Thus, 300 mm head is appropriate for SWAT system. A special rubber gasket with 5 mm thickness, which does not absorb water, is attached on the circular edge of the cup to avoid leaking of water. Water can be fulfilled in less than 10 seconds.

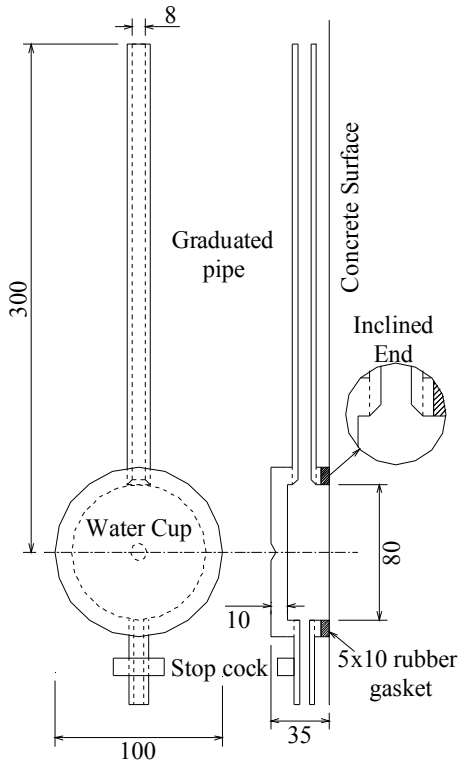

Fig. 2.19 SWAT apparatus [2.52].

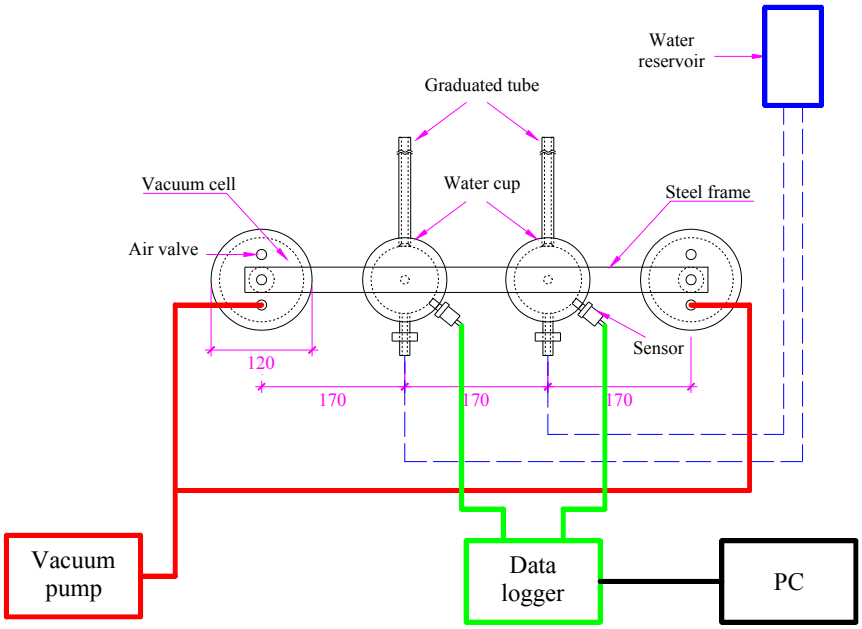

Fig. 2.20 Auto measure SWAT system [2.52].

Once water goes up to the top of the tube, the stop cock is closed and the record of dropped water level for 10 minutes from the filling up time of 10 seconds is conducted. From the collected data the Water Absorption Factor (WAF) is calculated. WAF is defined

as "*the rate of water absorption in* ml/m^2/s" [2.53].

The mechanism of water absorption is capillary suction under the application of the water head and the governing equation proposed by Levitt for Initial Surface Absorption Test [2.54] is also applicable in this test.

$$p = at^{-n} \tag{2.1}$$

where

p = instantaneous rate of water absorption at each time in ml/m^2/s

t = time in seconds

n = coefficient regarding the reduction of rate of water absorption with passage of time

a = initial water absorption rate (water absorption rate at 1 second)

The values of *"a"* and *"n"* in equation (2.1) are showed in **Fig. 2.21** where "*n"* is the incline of the line. The value of index *"a"* is strongly affected by the quality of the skin of concrete. When the surface of covercrete has microcrack, *"a"* value becomes large. On the other hand, in concretes without surface micorcacking *"a"* value is small. The value of index "*n"* depends on the microstructure in depth direction and moisture content of covercrete. Generally, it varies from 0.3 to 0.7 [2.54].

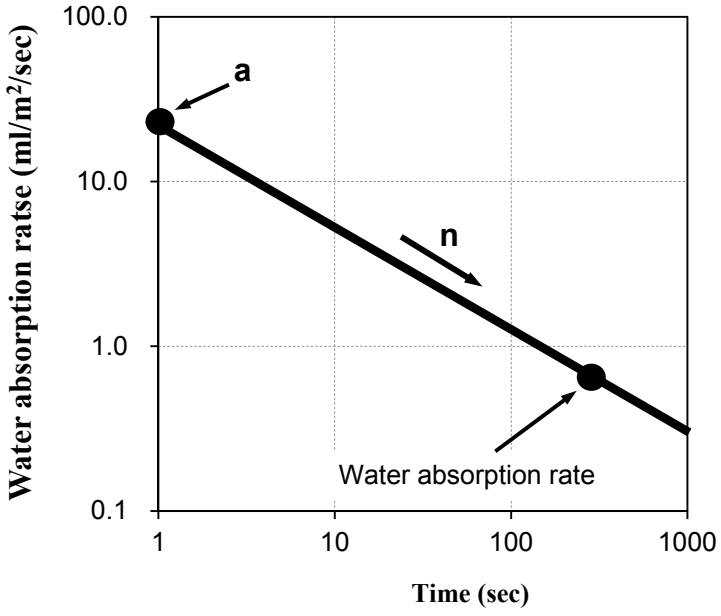

Fig. 2.21 Surface water absorption rate vs time in log scale.

It has been found that the 10 minutes SWAT test could evaluate the quality of covercrete up to 10 to 30 mm. Moreover, 10 minutes SWAT results have good relationship with that of long term absorption test results. Therefore, 10 minutes SWAT result is enough for inspection of covercrete quality.

2.7.3 Correlation between SWAT and penetration depth of water and chloride ion

After applying SWAT for OPC concrete specimens, Iwamoto [2.55] conducted penetration test by immersing the specimens in salt water and found that there was a good correlation between water absorption factors at 2 minutes and ultimate depths of water and chloride ion (**Fig. 2.22**).

It can be seen in **Fig. 2.22** that the SWAT index distributes in a wide range according to the quality of concrete. It is well known the quality of concrete is sensitive with curing condition. Concrete with high W/B subjected good curing even shows higher quality than concrete with low W/B subjected to poor curing. The widely variation of SWAT index implies SWAT can be applied to detect quality of curing of real structures.

Moreover, the good correlation between SWAT index and penetration depth maybe also allow the application of SWAT in inspection chloride attack. However, this correlation needs to be confirmed in other types of concrete.

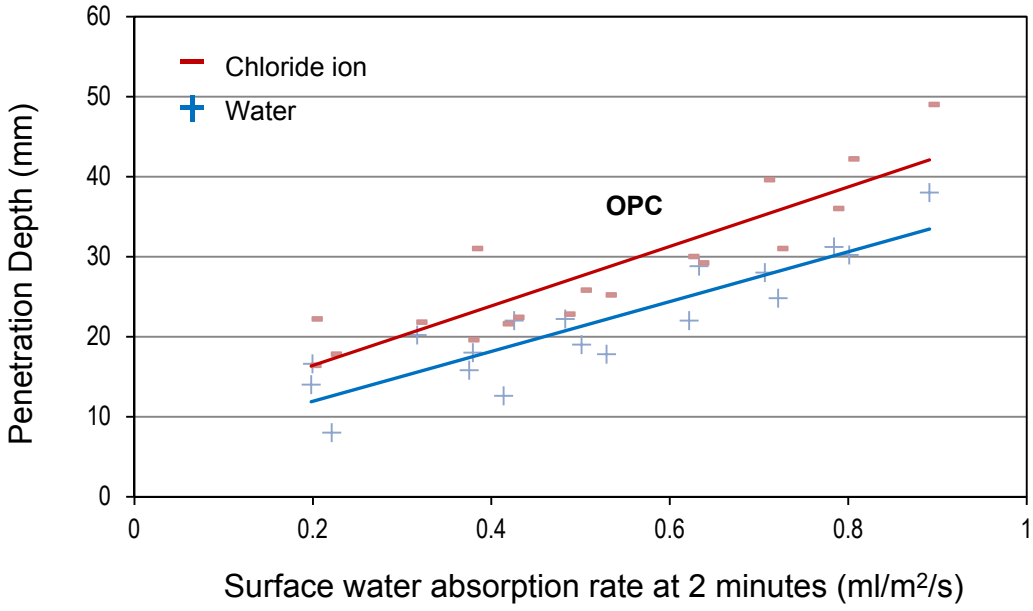

Fig. 2.22 Correlation between penetration depth and SWAT index [2.55].

In OPC concrete penetration of chloride ions (identified by $AgNO_3$) was deeper than that of water (identified by colored change agent), i.e. when water stopped penetrating chloride ions continued diffusing into concrete (**Fig. 2.22**). Nonetheless, in concrete containing slag the trend may be converse due to the capacity of slag in binding chloride ions [2.56]. Additionally, the combination of HAC and slag or fly ash maybe enhances the resistance against liquid transfer into concrete.

References

[2.1] Neville, A. M., "Properties of Concrete," John Wiley & Sons, pp.79-83, 1996.

[2.2] ACI, "Ground Granulated Blast-Furnace Slag as a Cementitious Constituent in Concrete", *ACI committee 233*, 1995.

[2.3] Wood, K., "Twenty years of experience with slag cement", *Symposium on Slag Cement*, University of Alabama, Birmingham, 1981.

[2.4] Roy, D. M., and Idorn, G. M., "Hydration, structure, and properties of blast furnace slag cements, mortars, and concretes," Proceeding, ACI Journal, Vol. 79, No.6, pp. 445-457, 1993

[2.5] Son, H. N., PhD thesis submitted to Yokohama National University (Concrete Laboratory), 2010.

[2.6] Son, H. N., and Hosoda, A., "Detection of Microcracking in Concrete Subjected to Elevated Temperature at Very Early Age by Acoustic Emission," *Journal of Advanced Concrete Technology*, Vol. 8, pp.201–211, 2010

[2.7] Scrivener, K. L. and Gariner, E. M., "Microstructural gradients in cement paste around aggregate particles", *Proceeding of the Materials Research Symposium*, Vol. 114, pp. 77-85, 1988.

[2.8] Neville, A. M., "Properties of Concrete", John Wiley & Sons, pp.300-302, 1996.

[2.9] Neville, A. M., "Properties of Concrete", John Wiley & Sons, pp. 84-85, 653-656, 1996.

[2.10] Sakai, E., Miyahara, S., Ohsawa, S., Lee, S. H., and Daimon, M., "Hydration of fly ash cement", *Cement and Concrete Research*, Vol. 35, No. 6, pp. 1135-1140, 2005.

[2.11] Na, S. H., Hama, Y., Taniguchi, M., Sagawa, T., and Zakaria, M., "Experimental investigation on reaction rate and self-healing ability in fly ash blended cement mixtures", *Journal of Advanced Concrete Technology*, Vol. 10, No. 7, pp. 240-253, 2012.

[2.12] Berndt, M. L., "Properties of sustainable concrete containing fly ash, slag and

recycled concrete aggregate", *Construction and Building Materials*, Vol. 23, No. 7, pp. 2606-2613, 2009.

[2.13] Li, Y., Bao, J., and Guo, Y., "The relationship between autogenous shrinkage and pore structure of cement paste with mineral admixtures", *Construction and Building Materials*, Vol. 24, No. 10, pp. 1855-1860, 2010.

[2.14] Malhotra, V. M, Zhang, M. H., Read, P. H., and Ryell, J., "Long-term mechanical properties and durability characteristics of high-strength/high-performance concrete incorporating supplementary cementing materials under outdoor exposure conditions", *ACI Materials Journal*, Vol. 97, No. 5, pp. 518-525, 2000.

[2.15] Langley, W., Carette, G. G., and Malhotra, V. M., "Strength development and temperature rise in large concrete blocks containing high volumes of low-calcium (ASTM Class F) fly ash", *ACI Materials Journal*, Vol. 89, No. 4, pp. 362-368, 1992.

[2.16] Fraay, A. L. A., Bijen, J. M., and De Haan, Y. M., "The reaction of fly ash in concrete a critical examination", *Cement and Concrete Research*, Vol. 19, No. 2, pp. 235-246, 1989.

[2.17] Naik, T. R., Singh, S. S., and Hossain, M. M., "Enhancement in mechanical properties of concrete due to blended ash", *Cement and Concrete Research*, Vol. 26, No. 1, pp. 49-54, 1996.

[2.18] Shi, C., and Shao, Y., "What is the most efficient way to activate the reactivity of fly ashes ash?", *2nd Materials Specialty Conference of the Canadian Society for Civil Engineering*, Montré, Qué bec, Canada, June 5-8, 2002, pp. 1-10, 2002.

[2.19] Jueshi, Q., Caijun, S., and Zhi, W., "Activation of blended cements containing fly ash", *Cement and Concrete Research*, Vol. 31, No. 8, pp. 1121-1127, 2001.

[2.20] Li, G., and Zhao, X., "Properties of concrete incorporating fly ash and ground granulated blast-furnace slag", *Cement & Concrete Composites*, Vol. 25, No. 3, pp. 293-299, 2003.

[2.21] Leng, F., Feng, N., and Lu, X., "An experimental study on the properties of resistance to diffusion of chloride ions of fly ash and blast furnace slag concrete", *Cement and Concrete Research*, Vol. 30, No. 6, pp. 989-992, 2000.

[2.22] Uysal, M., and Akyuncu, V., "Durability performance of concrete incorporating Class F and Class C fly ashes", *Construction and Building Materials*, Vol. 34, pp. 170-178, 2012.

[2.23] Siddique, R., "Effect of fine aggregate replacement with Class F fly ash on the

mechanical properties of concrete", *Cement and Concrete Research*, Vol. 33, No. 4, pp. 539-547, 2003.

[2.24] Siddique, R., "Effect of fine aggregate replacement with Class F fly ash on the abrasion resistance of concrete", *Cement and Concrete Research*, Vol. 33, No. 11, pp. 1877-1881, 2003.

[2.25] Varughese, K. T., and Chaturvedi, B. K., "Fly ash as fine aggregate in polyester based polymer concrete", Cement & Concrete Composites, Vol. 18, No. 2, pp. 105-108, 1996.

[2.26] Singha Roy, D. K., "Performance of blast furnace slag concrete with partial replacement of sand by fly ash", *International Journal of Earth Sciences and Engineering*, Vol. 4, No. 6, pp. 949-952, 2011.

[2.27] Siribudhaiwan, N., *et al*., "Influence of alite content on the hydration of blended cement", *The 1st International Conference on Concrete Sustainability (ICCS13)*, pp. 447-452, 2013.

[2.28] Hashimoto, A., *et al*., "Properties of high alite cement", *Proceeding of the JCA*, Vol. 66, pp. 32-33, 2012. (in Japanese)

[2.29] Physical Acoustics Corporation, User's manual, 2003.

[2.30] Huang, M., et al., "Using Acoustic Emission in Fatigue and Fracture Materials Research," JOM, Vol. 50, pp. 1-12, 1998.

[2.31] Grosse, C.U. and Linzer, L.M., "Signal-based AE analysis" in Grosses, C.U. and Otsu, M., *Acoustic emission testing*, Springer-Verlag, pp. 53-99, 2008.

[2.32] Otsu, M., "Concrete" in Grosses, C.U. and Otsu, M., *Acoustic emission testing*, Springer-Verlag, pp. 211-237, 2008.

[2.33] Soulioti, D., Barkoula, N. M., Paipetis, A., Matikas, T. E., Shiotani, T. and Aggelis, D. G., "Acoustic emission behavior of steel fibre reinforced concrete under bending", *Construction and Building Materials*, Vol. 23, No. 12, pp. 3532–3536, 2009.

[2.34] Ohtsu, M. and Watanabe, H., "Quantitative damage estimation of concrete by acoustic emission", *Construction and Building Materials*, Vol. 15, pp. 217–224, 2001.

[2.35] Kim, B. and Weiss, W. J., "Using acoustic emission to quantify damage in restrained fiber-reinforced cement mortars", *Cement and Concrete Research*, Vol. 33, No. 2, pp. 207-214, 2003.

[2.36] Hellier, C. J., *Handbook of Nondestructive Evaluation*, McGraw Hill, 2nd edition, pp. 10.1-10.39, 2001.

[2.37] Aggelis, D. G., Polyzos, D., and Philippidis, T. P., “Wave dispersion and attenuation in fresh mortar: theoretical predictions vs. experimental results”, *Journal of the Mechanics and Physics of Solids*, Vol. 53, No. 4, pp. 857-883, 2005.

[2.38] Landis, E. N., “Acoustic Emission in Wood” in Grosses, C.U. and Otsu, M., *Acoustic emission testing*, Springer-Verlag, pp. 311-322, 2008.

[2.39] Neville, A. M., "Properties of Concrete," John Wiley & Sons, pp.482-483, 1996.

[2.40] Dhir, R. K. and Jones, M. R., “Development of chloride-resisting concrete using fly ash ", *Fuel*, Vol. 78, pp. 137-142, 1999.

[2.41] Neville, A. M., “Chloride attack of reinforced concrete: an overview”, *Materials and Structures*, Vol. 28, pp. 63-70, 1995.

[2.42] Hansson, C. M., and Sorenson, B., “The Threshold Concentration of Chloride in Concrete for the Initiation of Corrosion”, *Corrosion Rates of Steel in Concrete,* ASTM SP 1065(99), pp. 3-16, 1990.

[2.43] “Standard Method of Test for Resistance of Concrete to Chloride Ion Penetration”, (T259-80), American Association of State Highway and Transportation Officials, Washington, D.C., U.S.A., 1980.

[2.44] *Nordtest Method: Accelerated Chloride Penetration into Hardened Concrete*, Nordtest, Espoo, Finland, Proj. 1154-94, 1995.

[2.45] ”Electrical Indication of Concrete’s Ability to Resist Chloride”, (T277-93), American Association of State Highway and Transportation Officials, Washington, D.C., U.S.A., 1983

[2.46] Tang, L. and Nilsson, L.-O., ”Chloride Diffusivity in High Strength Concrete", *Nordic Concrete Research*, Vol. 11, pp. 162-170, 1992.

[2.47] Armaghani, J. M., and Bloomquist, D. G., “Durability Specification and Rating For Concrete”, *Concrete 2000*: *Economic and Durable Construction Through Excellence*, (eds. R.K. Dhir and M.R. Jones), Vol. 2, E & FN Spon, Cambridge, pp. 1639-1652, 1993.

[2.48] Meletiou, C. A., Tia, M., and Bloomquist, D. G., “Development of a Field Permeability Test Apparatus and Method for Concrete”, *ACI Materials Journal*, Vol. 89, No. 1, pp. 83-89, 1992.

[2.49] Feldman, R.F., “Diffusion Measurements in Cement paste By Water Replacement Using Propan-2-ol”, *Cement and Concrete Research*, Vol. 17, pp. 602-612, 1987.

[2.50] Sharif, A., Loughlin, K. F., Azad, A.K., and Navaz, C. M., “Determination of the Effective Chloride Diffusion Coefficient in Concrete via a Gas Diffusion Technique”, *ACI Materials Journal*, Vol. 94, No. 3, pp. 227-233, 1997.

[2.51] Hayshi, K. and Hosoda, A., “Developement of Water Absorption Test Method Applicable to Actual Concrete Structures”, *Pro Proceeding of the JCI*, Vol. 33, No.1, pp.

1769-1774, 2011. (in Japanese)

[2.52] Usman, K., PhD thesis submitted to Yokohama National University (Concrete Laboratory), 2012.

[2.53] Usman, K., Hosoda, A., Hayashi, K., and Motoshige, N., "Inspection of cover concrete of an actual structure by Surface Water Absorption Test", *Proceedings of the 9th International Symposium on High Performance Concrete-Design*, *Verification and Utilization,* Rotorua, New Zealand, C9-1 U, 2011.

[2.54] Levitt, M., "Non-destructive Testing of Concrete by the initial surface absorption method", *Proceedings of a Symposium on Non-Destructive Testing of Concrete and Timber*, London, pp. 23-26, 1969.

[2.55] Iwamoto, Y., Master thesis submitted to Yokohama National University (Concrete Laboratory), 2014. (in Japanese)

[2.56] Hansson, C. M., and Sorenson, B., "The Threshold Concentration of Chloride in Concrete for the Initiation of Corrosion", *Corrosion Rates of Steel in Concrete,* ASTM SP 1065(99), pp. 3-16, 1990.

Chapter 3 Improvement of resistance against microcracking of slag concrete by using High Alite Cement

3.1 Introduction

In the early age of concreting, the hydration process of cement produces a large amount of heat, leading to deformation of the main constituents of concrete such as aggregate and cement paste. Most aggregates have a smaller coefficient of thermal expansion (CTE) than the matrix, resulting in smaller thermal deformation. Moreover, due to the superposition of autogenous shrinkage, the matrix shrinks to a much larger extent than aggregate. Because of the incompatible deformation of concrete components, microscopic stress occurs. If it exceeds the tensile strength of concrete, microcracks will be generated inside the concrete even without the application of external load. Microscopic thermal stress appears remarkably in the case of massive concrete and heat curing because of large temperature variation.

A number of approaches are used to investigate microcracking in concrete. Due to its sensitivity and the rich information it yields from collected parameters, the AE technique has been widely used to detect cracking in hardened concrete. It was applied to estimate quantitative damage of structural concrete without the original data of the concrete at construction (Ohtsu and Watanabe, 2001) [3.1]. Verstrynge *et al*. (2009) studied unstable damage in masonry specimens during short-term and long-term creep tests by using this technique [3.2]. AE was also employed in bending test to characterize the fracture process in plain concrete (Sagar, 2009) [3.3] or in fiber reinforced concrete beam (Aggelis *et al*., 2011) [3.4]. In all aforementioned studies, AE sensors were coupled on the concrete surface. Nevertheless, few researchers have used AE to record defects in concrete at very early ages. AE measurement at a very early age is difficult because AE sensors cannot be directly attached on the surface of unhardened concrete.

Nowadays, because of its advantages, which include better workability, high compressive strength, environmental conservation and high durability [3.5], concrete using ground granulated blast furnace slag (GGBFS) is being widely used all over the world,

especially in Japan. However, Son and Hosoda (2010) [3.6] found that slag concrete is also easily subjected to more severe nonstructural microcracks than OPC concrete under temperature variation at early ages. It has also been recognized that slag concrete has lower resistance against carbonation. To solve the disadvantages of slag concrete, a new type of cement named high alite cement (HAC) was proposed. In the research of Hashimoto *et al*. (2012) [3.7] about compressive strength development of HAC, HAC slag concrete showed good performance in terms of long-term continuous strength development as well as early age strength.

In this chapter, the combination of the AE technique using a redesigned waveguide with physical and mechanical tests and SEM observation was applied to investigate the effectiveness of HAC in mitigating microcracking and increasing tensile strength in slag concrete subjected to a temperature regime simulating steam curing in early ages, with particular focus on the contribution of bond properties between HAC mortar and coarse aggregate to higher cracking resistance.

3.2 Experimental program

3.2.1 Materials and mix proportions

In this research, three types of binders were used: Ordinary Portland Cement (OPC), HAC, and GGBFS. HAC is newly developed special cement with very high content of alite ($3CaO.SiO_2$) and almost no belite ($2CaO.SiO_2$) [3.8]. The chemical composition and physical properties of the binders are presented in **Table 3.1**. The mineral compositions of OPC and HAC are calculated from the chemical composition by Bogue's equations and main compounds of cements are listed in **Table 3.2**. Because the CTE of

Table 3.1 Chemical composition and physical properties of binders.

Binder	Chemical composition (%)								Density (g/cm^3)	Specific area (cm^2/g)
	SiO_2	Al_2O_3	Fe_2O_3	CaO	MgO	SO_3	Na_2O	K_2O		
OPC	20.36	5.33	3.04	64.09	1.50	2.13	0.28	0.36	3.16	3310
HAC	18.76	5.18	2.85	64.16	1.88	3.97	0.42	0.38	3.11	5480
GGBFS	32.30	14.20	0.31	43.40	5.70	1.93	0.26	0.27	2.90	4030

Table 3.2 Main compounds of cements.

Cement	Compound composition (%)			
	C_3S	C_2S	C_3A	C_4AF
OPC	59.88	13.52	8.99	9.24
HAC	68.36	2.57	8.91	8.66

materials is one of the important parameters affecting microcracking in concrete (Son and Hosoda, 2010) [3.6], two types of coarse aggregates with the same maximum particle size of 19 mm but remarkably different CTEs, namely limestone and andesite, were used in this research. However, it should be noted here that the chemical reaction between limestone and slag mortar also affects the mechanical properties of concrete [3.9]. Fine aggregate used in this research was pit sand. All the materials were placed in a curing room with temperature of around 20^{o}C before mixing.

The mix proportions of the mortars and concretes are given in **Table 3.3**. As mentioned above, in terms of compressive strength, HAC showed the best results when it was combined with GGBFS with slag replacement ratio of around 50 percent. Thus, in this study, the proportion of cement and GGBFS was set at 50-50. The mix proportions of the respective mortars for each kind of concrete were determined by just removing the coarse aggregate from the concrete while retaining the other proportions.

3.2.2 Acoustic emission system

The experimental system of AE tests is described in **Fig. 3.1**. A two-channel AE system and general-purpose sensors with 150 kHz resonance frequency (R15-α) were used. In each test, two sensors were coupled on a sensor seat located at the top of a stainless steel waveguide, whose design is explained in detail in section 3.2.3. The waveguide was embedded in the specimen and the assembly was placed in a temperature-controlled chamber.

Table 3.3 Mix proportions.

Mixture	Water (kg/m^3)	OPC (kg/m^3)	HAC (kg/m^3)	GGBFS (kg/m^3)	Pit-sand (kg/m^3)	Limestone (kg/m^3)	Andesite (kg/m^3)	SP (kg/m^3)	W/B
M-O-30	251	418	-	418	1229	-	-	4.2	0.3
M-H-30	250	-	417	417	1225	-	-	5.8	0.3
M-O-50	265	265	-	265	1454	-	-	-	0.5
M-H-50	277	-	277	277	1397	-	-	-	0.5
C-O-L-30	165	275	-	275	810	838	-	2.8	0.3
C-O-A-30	165	275	-	275	810	-	816	2.8	0.3
C-H-L-30	165	-	275	275	808	836	-	3.9	0.3
C-H-A-30	165	-	275	275	808	-	814	3.9	0.3
C-O-L-50	165	165	-	165	904	936	-	-	0.5
C-O-A-50	165	165	-	165	904	-	911	-	0.5
C-H-L-50	175	-	175	175	882	912	-	-	0.5
C-H-A-50	175	-	175	175	882	-	888	-	0.5

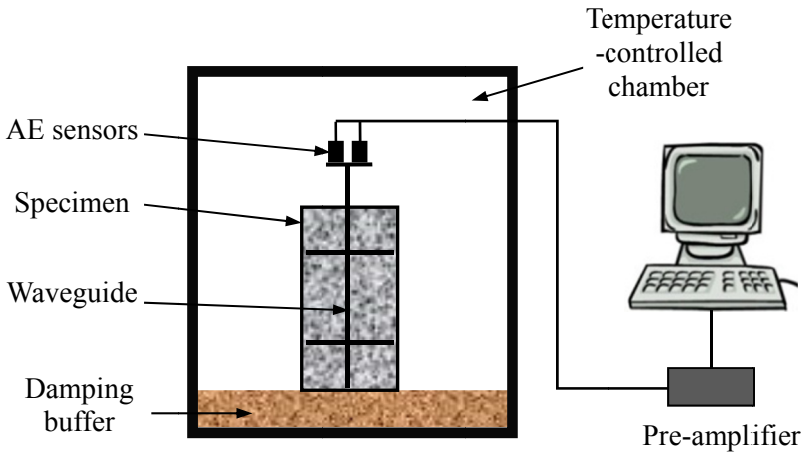

Fig. 3.1 AE testing system.

Noise deriving from the dynamic parts of the temperature-controlled chamber and the operation of other surrounding machines is a big problem. Son and Hosoda [3.6] were successful in using damping buffer to isolate the unwanted noises. By setting a threshold value of 40 dB, sound from the outside ambient transmitting through air was rejected. During tests, changes in the electric pulses from electrical facilities can interfere with AE signal detection. The waveform of event induced by electric potential change is characterized by very short rise time and duration (nearly equal zero) and few counts (**Fig. 3.2**). That waveform is significantly different from waveform of event created from cracking in concrete which is identified by longer rise time or duration and much larger number of counts (**Fig. 3.3**). To avoid such interference, all sensors, pre-amplifiers, and connectors were wrapped by alumina sheets (**Fig. 3.4**).

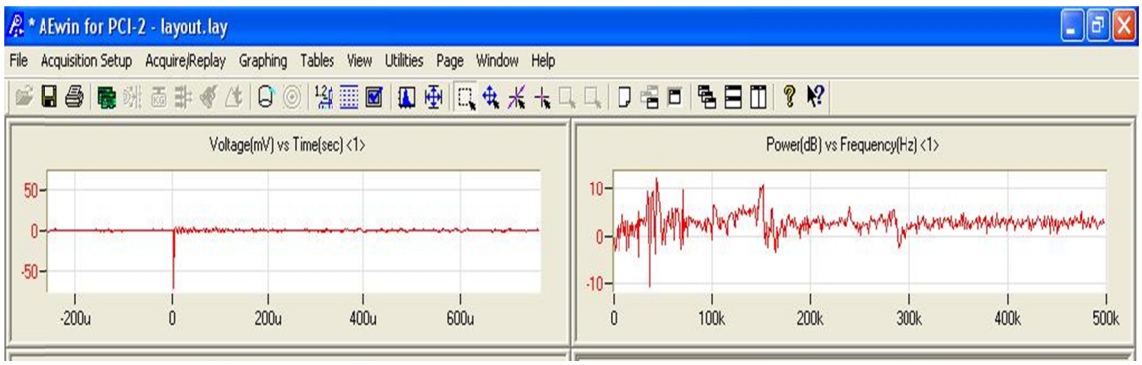

Fig. 3.2 Waveform of event deriving from electric potential change.

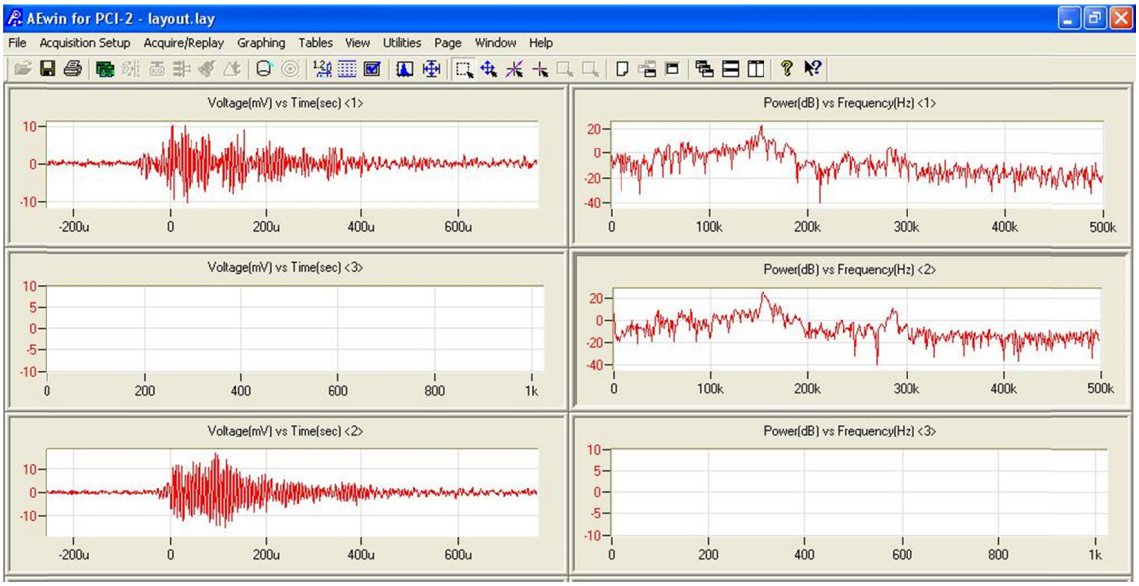

Fig. 3.3 Waveform of event deriving from cracking in concrete.

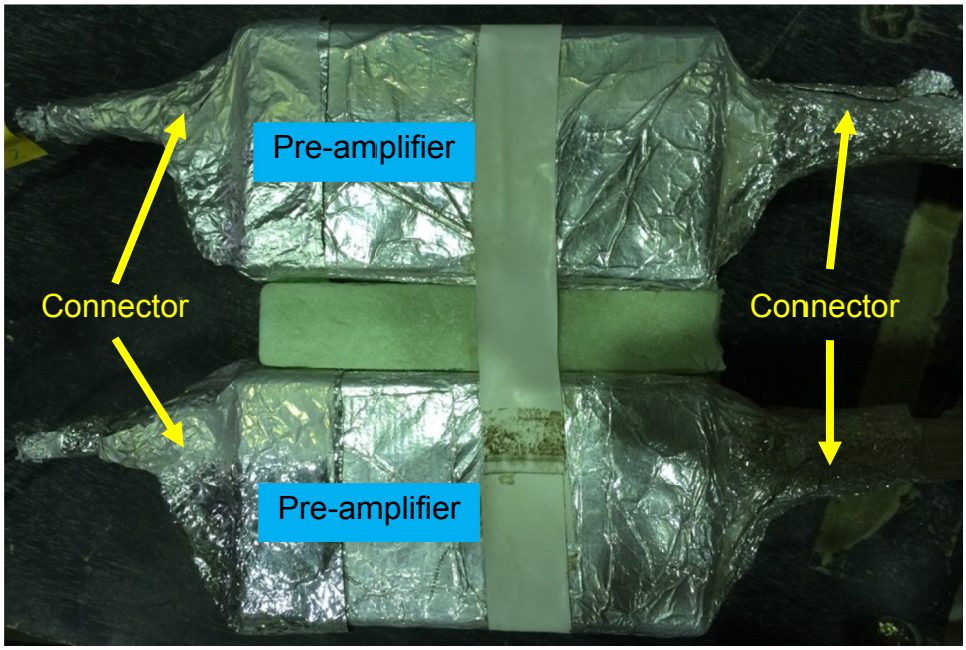

Fig. 3.4 Pre-amplifiers and connectors were wrapped by alumina sheet.

Cylindrical tin molds of 100 mm diameter and 200 mm height were used for all tests. To eliminate noise induced by the friction between concrete and molds due to their different deformations under temperature variation, the inside face of each mold was covered with a 0.5 mm thick Teflon sheet (**Fig. 3.5a**).

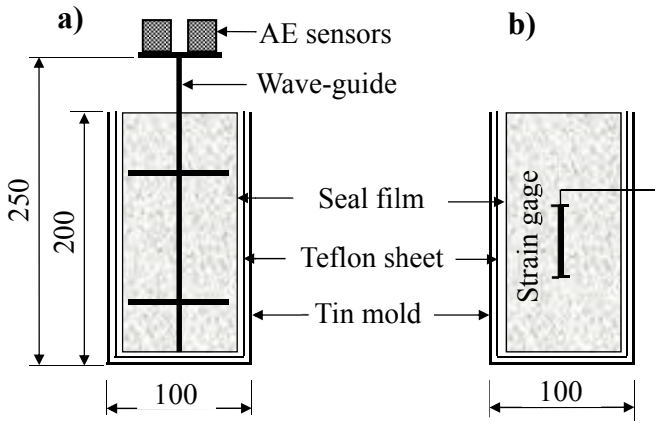

Fig. 3.5 Specimen preparation for **(a)** AE test, and **(b)** Net shrinkage measurement.

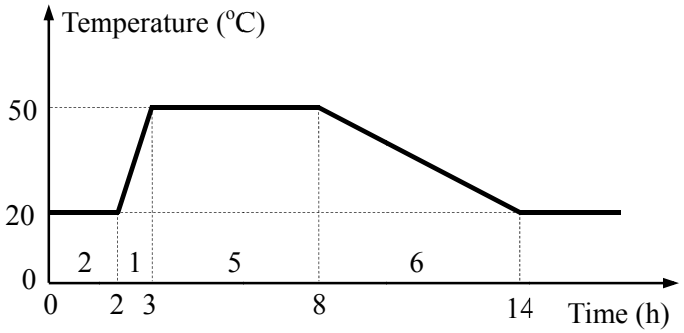

Fig. 3.6 Temperature regime simulated steam curing.

The time for preparing the specimen including installation of the waveguide and sensors was around 30 minutes. Right after the preparation was completed, concrete was sealed by polyethylene film inside the mold and placed in the temperature-controlled chamber, which had been maintained at 20°C. The heating began at 2 hours after the addition of water into the mix. The temperature regime applied for the specimens simulating steam curing (**Fig. 3.6**). Recording of AE signals started 1.5 hours after mixing.

3.2.3 Waveguide

To investigate microcracking inducing in concrete subjected to heat curing, the acoustic waves were measured after one hour and a half from mixing. Since concrete is in plastic form in early ages, AE sensors cannot be coupled directly on the surface of the specimens. To deal with this problem, AE waveguide (**Fig. 3.7**) was applied by Son and Hosoda. This waveguide was a stainless steel rod with 250 mm length and 4 mm diameter, with a sensor seat on the top [3.10]. Through this waveguide, acoustic waves from

microcracks inside specimens were collected to AE sensors and AE sensors could well detect microcracks in concrete with low water-to-binder ratio (W/B).

However, in the case of concrete with W/B of 0.5, there was very small number of microcracks. The reason for this may be the attenuation of acoustic wave in high moisture content ambient [3.11] due to energy absorption led to the less effectiveness of the waveguide in detecting AE signal in concrete with high W/B.

In order to solve the matter of attenuation, a new-shaped waveguide was employed in this research (**Fig. 3.8**). It was made from a 4-mm thick stainless steel plate. The section of the waveguide was a square measuring 4x4 mm. The main rod was 250 mm in length with two horizontal bars located at 50 mm and 150 mm, respectively, from the bottom. On the top, a 25x50 mm plate was bent perpendicularly to the vertical rod to make a sensor seat. Since two sensors could be coupled on the seat at a time, reliability of AE measurement could be confirmed for each specimen. The method for tightly coupling sensors to the sensor seat is described elsewhere [3.10]. The effectiveness of the new waveguide will be discussed in detail in section 3.8.

Fig. 3.7 Old AE waveguide.

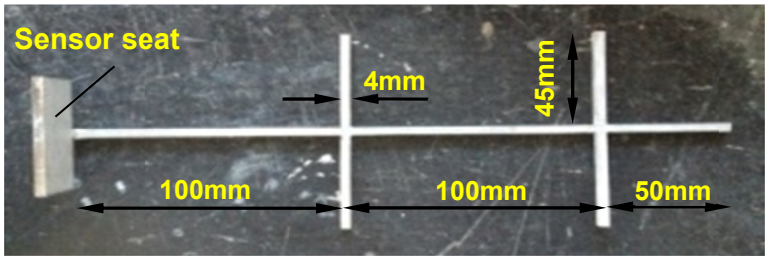

Fig. 3.8 New AE waveguide.

3.2.4 Net shrinkage measurement

Net shrinkage of mortar is defined as the total shrinkage from the peak expansion consisting of both autogenous and thermal shrinkages (Cusson, 2008) [3.12]. The net shrinkage of mortar was measured by using an embedded I-shaped strain gage, PMFL-60-2LT, 4 mm in diameter and 60 mm in length. **Figure 3.5b** describes the setup for measuring the net shrinkage of mortar. The preparation of specimens and temperature regime were the same as those in the AE test. Two specimens of one mix were tested at the same time and the mean value was calculated.

3.2.5 CTE testing

The experimental setup for measuring the CTE of mortar was similar to that of net shrinkage test. Two specimens of one mix were tested at the same time and the mean value was calculated. First, the specimens were subjected to a temperature history as shown in **Fig. 3**. Then, CTE testing was started at 24 hours after mixing. Specimens were heated from 20^{o}C to 50^{o}C over two hours, maintained at 50^{o}C for two hours, and then cooled down to 20^{o}C over two hours. The CTE of mortar was calculated separately for the heating and cooling stages and the average was taken.

For coarse aggregate, the CTEs were directly measured on the particles. FLG-1-11 flat-type strain gauges 1 mm in length were attached on the smooth surfaces of a particle in three orthogonal directions (**Fig. 3.9**). The temperature regime was the same as that applied for the mortar. The particles were sealed to prevent evaporation. Three particles of each type of coarse aggregate were used in a test and the mean value was taken.

Fig. 3.9 Measurement of CTE of coarse aggregate.

3.2.6 Direct tensile strength test

Direct tensile strength of concretes and mortars were investigated at the age of one day following heat curing. Specimens were cylinders 100mm in diameter and 100mm in height. The method for direct tensile strength test was the same as that proposed by Son and Hosoda (2010) [3.6] and was showed in **Fig. 3.10**. Three specimens were tested for each mix proportion and the average value was calculated.

3.3 Results and discussions

3.3.1 Effectiveness of new waveguide

Since the sensor seat of the redesigned waveguide is large enough to couple two sensors simultaneously, reliability of AE measurement could be confirmed in each specimen

In previous researches, there was almost no AE hit was recorded during the time from the beginning to 5 hour after mixing and the numbers of AE hits of concrete with W/B of 0.5 were significantly smaller than those of 0.3. One of the main reasons is the attenuation of acoustic waves in a high moist medium [3.13]. In this study; however, the result was reverse. Compared with concretes with W/B of 0.3, concretes with W/B of 0.5 presented much larger cumulative AE hits, particularly at the early ages (**Fig. 3.11**).

Fig. 3.10 Direct tensile strength test of concrete.

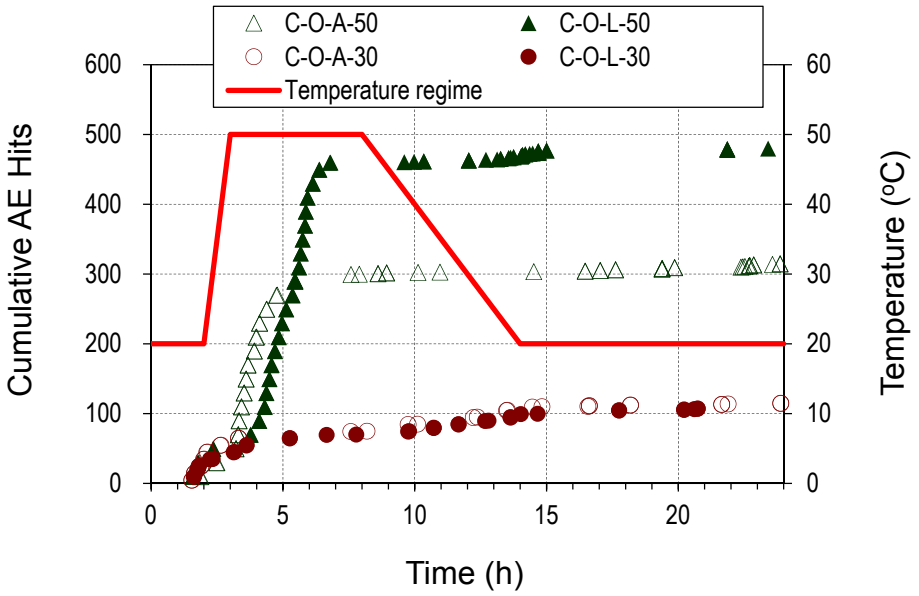

Fig. 3.11 Development of AE hits during heat curing.

Analysis of amplitude distribution of microcracks (**Fig. 3.12**) shows that microcracks in concrete with W/B of 0.5 occurred remarkably at low amplitude. Nearly 50% of them occurred in the range of 40dB to 42dB and 80% in the range of 40dB to 45dB, while in the case of W/B of 0.3, those percentages were just 25% and 50%, respectively. In very early ages, the amount of free water remaining in concrete with W/B of 0.5 is so large. When acoustic waves transmitted through out such a moist medium, attenuation caused drastic decreasing in amplitude. By using two additional horizontal bars, the distances from cracking points to the waveguide became shorter and hence the effect of attenuation must have been significantly reduced.

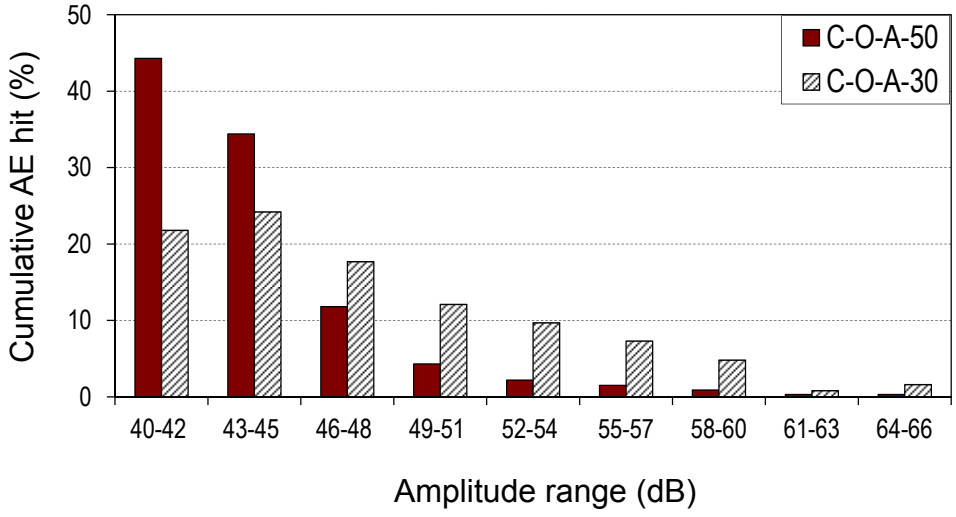

Fig. 3.12 Amplitude distribution of microcracks.

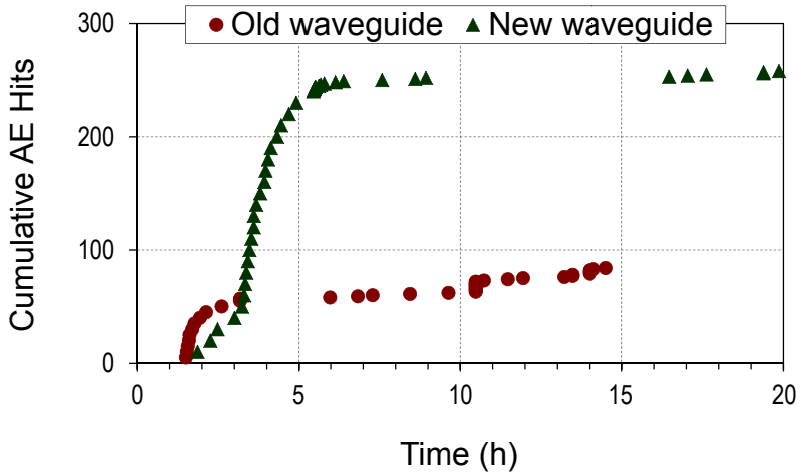

Fig. 3.13 Comparison of new and old waveguide in C-O-A-50.

The comparison of AE hits between the former waveguide and the new one in concrete with W/B of 0.5 is presented in **Fig. 3.13**. Number of hits detected by the new waveguide was considerably higher than that recorded by the old one, especially in very early ages (several hours after mixing). It can be clearly said that the new one is more effective.

3.3.2 Thermal characteristics of HAC mortars

Fig. 3.14 shows the CTEs of coarse aggregates and mortars. There was no difference between the CTEs of mortars with W/B of 0.3, while the CTE of M-H-50 was a bit smaller than that of M-O-50. The CTE of coarse aggregate was smaller than that of mortar, and the CTE of limestone was much smaller than that of andesite.

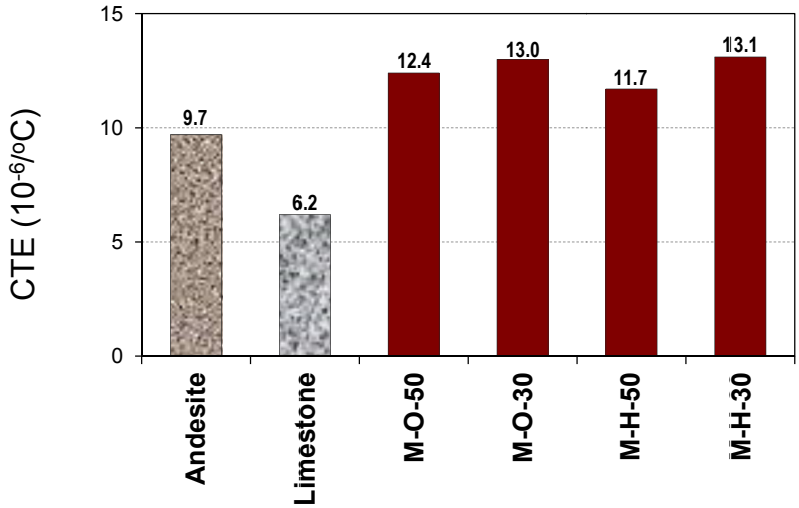

Fig. 3.14 CTE of aggregates and mortars.

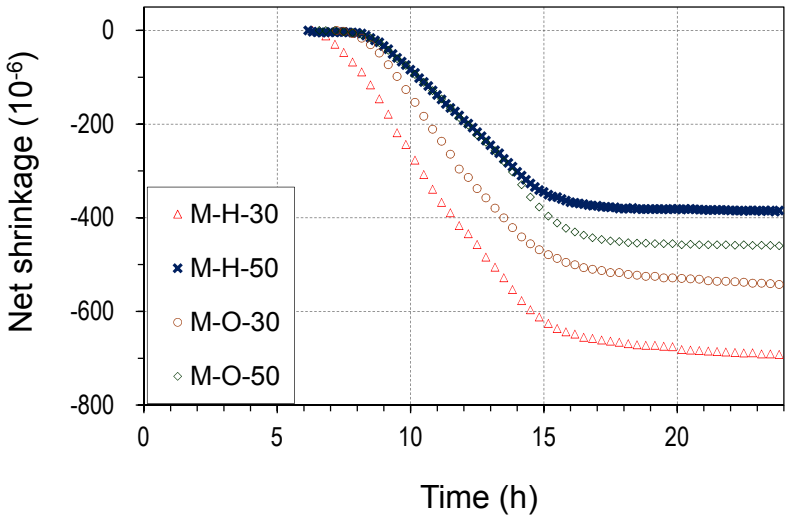

Fig. 3.15 Net shrinkage of mortars.

A clear distinct was observed in net shrinkage of mortars (**Fig. 3.15**). Because all the specimens were sealed, shrinkage of mortar means the summation of autogenous and thermal shrinkage. Autogenous shrinkage in a sealed condition is derived from chemical shrinkage and self-desiccation.

In the case of mortar with W/B of 0.3, HAC mortar shrank much larger than OPC mortar, especially in the age from 7 hours to 17 hours after mixing. Since the CTE of HAC mortar and OPC mortar were similar, this larger net shrinkage of HAC mortar must be attributed to larger autogenous shrinkage. According to the calculation of Tazawa [3.14], chemical shrinkage of alite and belite were 13.1% and 10.6%, respectively. Thus, HAC with high alite content could show larger chemical shrinkage than OPC. Moreover, HAC used more water during its hydration than OPC, and the hydration rate of HAC was faster than that of OPC. This information supports the larger autogenous shrinkage of HAC mortar. After around 17 hours from mixing, the net shrinkage of both mortars showed similar behaviors.

From the beginning of shrinkage (7 hours) to 14 hours after mixing, HAC mortar shrinkage was exactly equal to that of OPC mortar. Here, larger autogenous shrinkage of HAC mortar was compensated by smaller thermal shrinkage. From 14 hours after mixing, the temperature in the chamber was maintained at 20^{o}C. Therefore, shrinkage of the mortars just depended on autogenous shrinkage. Because hydration took place more slowly

for OPC than HAC, autogenous shrinkage of OPC mortar still continued up to 18 hours from mixing, resulting in the larger shrinkage of OPC mortar in this period. Past 18 hours, shrinkage of HAC and OPC hardly changed owing to the complete absence of thermal contraction and almost no autogenous shrinkage.

3.3.3 Capacity of HAC slag concretes to resist microcracking

Due to the heat curing and hydration heat of cement, the temperature inside specimens underwent two distinct temperature periods. The first period was a temperature increase period that led to the expansion of concrete (expansion period). Because the expansion of mortar is larger than that of coarse aggregate, radial microscopic tensile stress occurs. This driving force results in separation at the interface transition zone (ITZ) around aggregate particles. This type of deterioration is defined as separation cracks [3.15] (**Fig. 3.16a**).

The second period was a temperature decrease period; in this period the concrete shrank (shrinkage period). Based on the fact that the contraction of coarse aggregate is smaller than that of mortar, tangential microscopic tensile stress is generated in the mortar. The level of this tensile stress depends on the disparity in CTEs between the aggregate and mortar and the size of the coarse aggregate, as well as the distance from the center of the aggregate. The larger the size of the aggregate and the smaller the distance from the center of the aggregate, the larger this tensile stress becomes (Elices and Rocco, 2008) [3.16]. Moreover, the larger the difference in CTE between the mortar and the aggregate, the bigger the tensile stress that is produced. If the tensile stress exceeds the tensile strength of the mortar, microcracks will be generated in the mortar in the perpendicular direction to ITZ. Such cracks are called mortar cracks [3.15] (**Fig. 3.16b**).

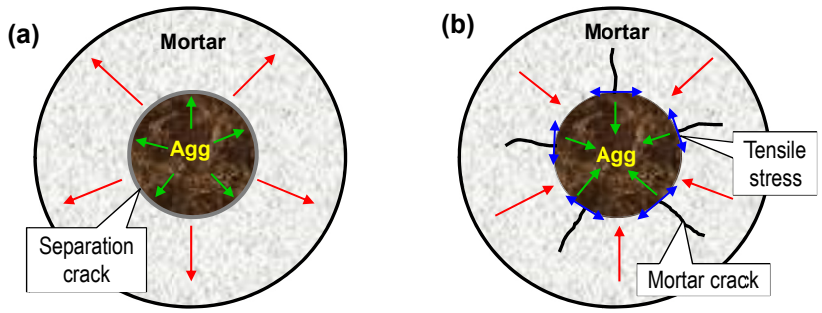

Fig. 3.16 Schemes of cracks in: **(a)** expansion period and **(b)** shrinkage period.

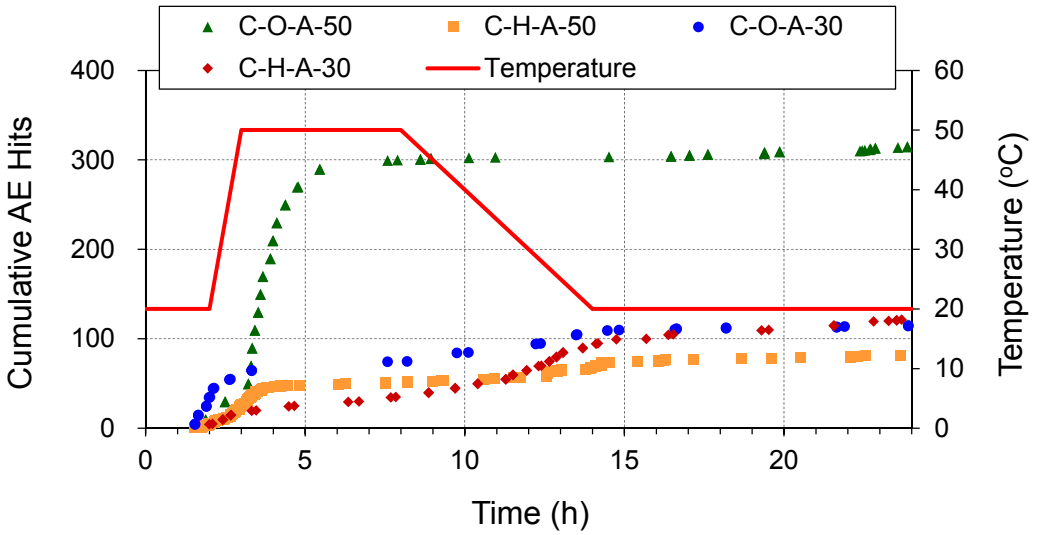

Fig. 3.17 Development of AE hits in concretes under heat curing.

Each event of cracking in concrete was detected by AE. The development of AE hits in slag concretes is depicted in **Fig. 3.17**. While in C-O-A-50, many microcracks occurred at a very early age (until 5 hours from mixing), a much smaller number of AE hits in that period were detected in C-H-A-50. The same trend can be observed in concretes with W/B of 0.3 although the difference was not as pronounced. Conversely, during the shrinkage period, more microcracks appeared in HAC concretes than in OPC concretes.

The comparison between the number of cracks and the energy rate per hit, which represents the degree of cracking, is presented in **Fig. 3.18**. It is clearly seen that, in the expansion period, the level of cracking was small in all cases. In the shrinkage period, however, the microcracks in OPC concretes were severer than those in HAC concretes, especially for concrete with W/B of 0.5. It can be inferred that HAC concretes can disperse tensile stress, leading to the formation of many small cracks rather than concentrating tensile stress to create a severe crack.

To interpret the degree of cracking in OPC and HAC slag concretes during temperature history, AE hits were classified into three categories due to their amplitude: class 1 consisted of hits with low amplitudes, i.e. from 40dB to 50dB. Those for class 2 and class 3 were medium (from 50dB to 60dB) and high amplitude (over 60dB), respectively. **Fig. 3.19a** reveals that the main difference between OPC and HAC slag concrete with W/B of 0.5 was the greater numbers of small and medium microcracks in OPC one, which mostly occurred in expansion period. There was no big difference in the number of severe microcracks.

Nevertheless, this trend in concretes with W/B of 0.3 was a bit distinct (**Fig. 3.19b**). The number of small micorcracks in increasing period was almost same while the amount of medium micorcracks in OPC concrete was higher than that in HAC concrete. In this stage, almost no severe micorcrack occurred in both of them. Conversely, in decreasing period the number of small micorcracks in HAC concrete was larger than that in OPC concrete while there was a somewhat increase in case of AE hits in the other categories. It can be seen that, larger shrinkage of M-H-30 than that of M-O-30 (**Fig. 3.15**) resulted only in the increase of smaller micorcracks, not in increasing severe micorcracks. It can be inferred that HAC concrete can disperse the tensile stress leading to the formation of many small micorcracks rather than concentrate them to create few severe cracks.

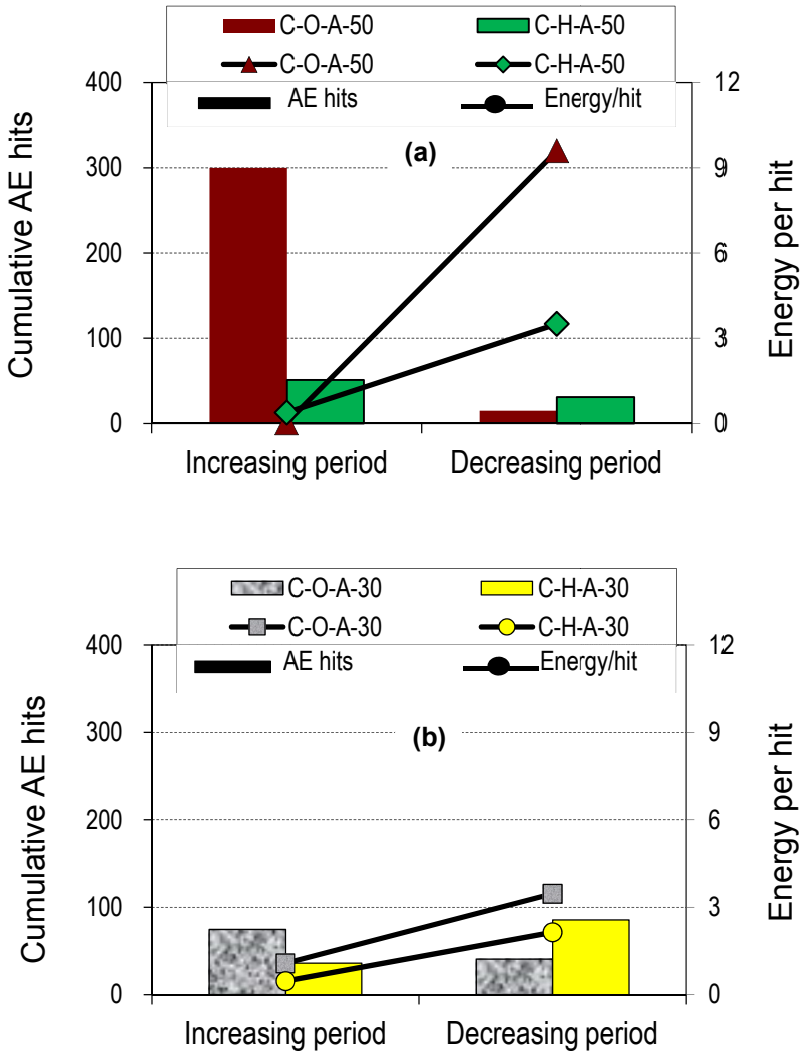

Fig. 3.18 Cumulative AE hits and energy rate per hit in concretes with (a) W/B = 0.5 and (b) W/B = 0.3.

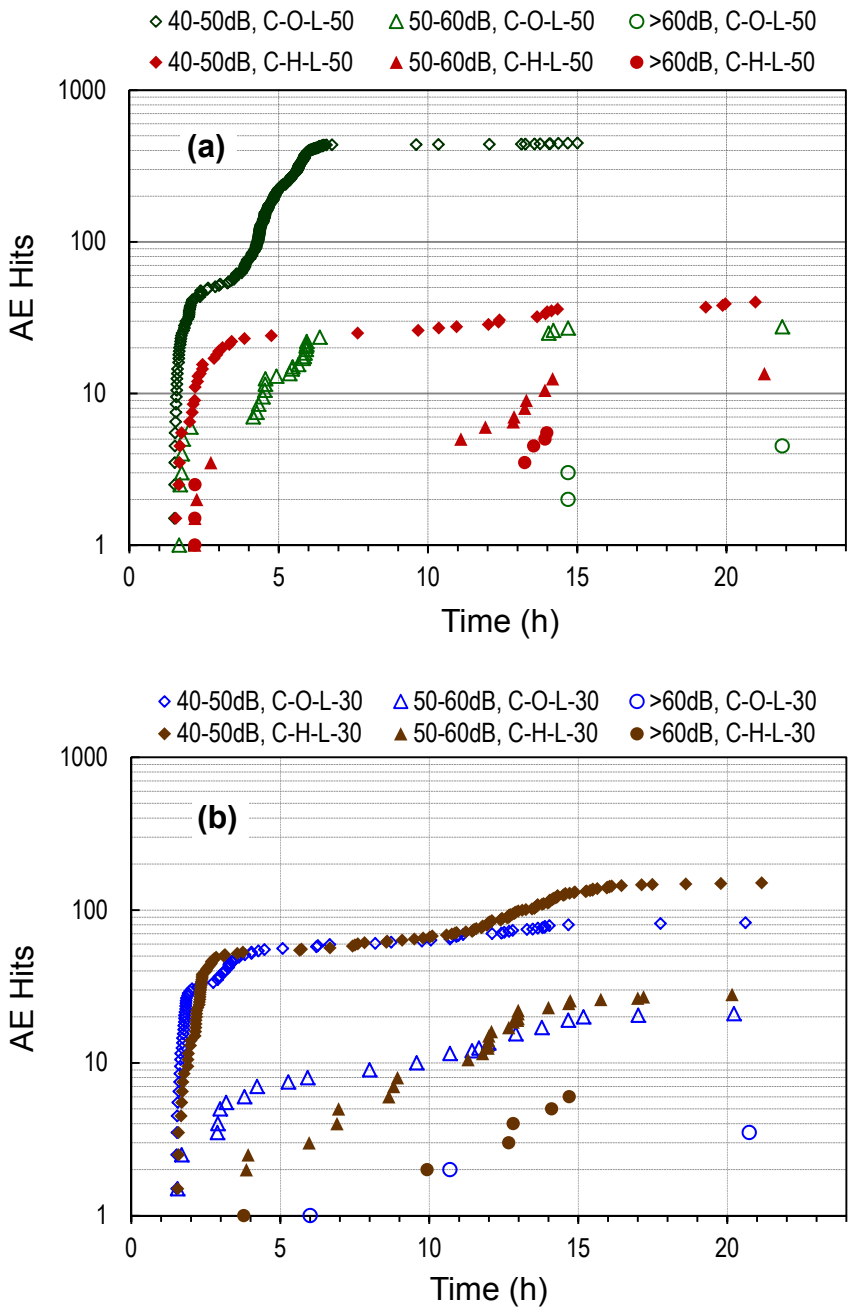

Fig. 3.19 Classified amplitude distribution of microcracks in OPC and HAC concretes with **(a)** W/B = 0.5 and **(b)** W/B = 0.3.

Ductility of concrete can be qualified by some parameters of AE events such as average frequency, rise time-to-amplitude ratio, and energy (Aggelis *et al.*, 2013) [3.17]. It was also found that AE events recorded in ductile materials were characterized by longer durations than those in brittle materials (Kuksenko *et al.*, 1987) [3.18]. Although the similar trend was found in concretes with limestone, to avoid the effects of chemical reaction between limestone and slag paste which was observed in the research by Kodama

et al. (2008) [3.9] and by Nam and Hosoda (2013) [3.19], only concretes with andesite were used in the discussion. In both cases of W/B of 0.5 and 0.3, AE events in HAC concretes showed the significant longer average duration than that in OPC ones (**Fig. 3.20**). This reveals that HAC concretes were more ductile than OPC concretes. As a result, HAC concretes presented higher tensile strengths than those of OPC concrete. Moreover, while the tensile strengths of OPC concretes were much smaller than those of the respective mortars, the tensile strength of HAC concrete was just a bit smaller (W/B = 0.5) or even larger (W/B = 0.3) than that of the respective mortars (**Fig. 3.21**). **Fig. 3.22** also shows good correlation between the loss of tensile strength and AE duration of concretes. The longer the average duration was, the smaller the loss of tensile strength.

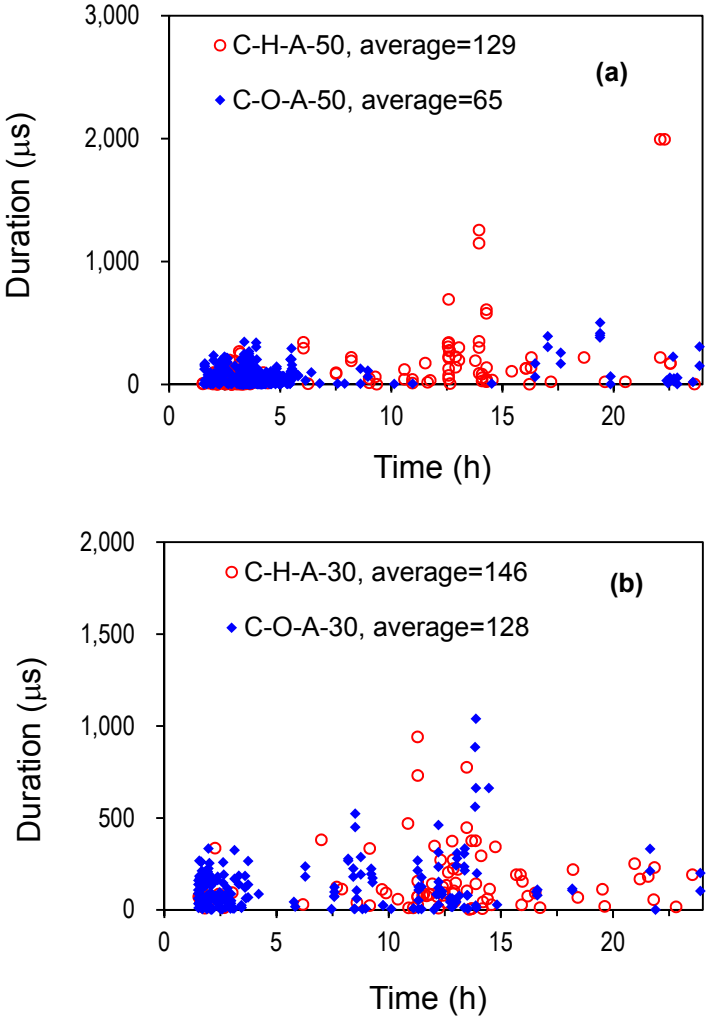

Fig. 3.20 Comparison of event durations between HAC and OPC slag concretes with **(a)** W/B = 0.5 and **(b)** W/B = 0.3.

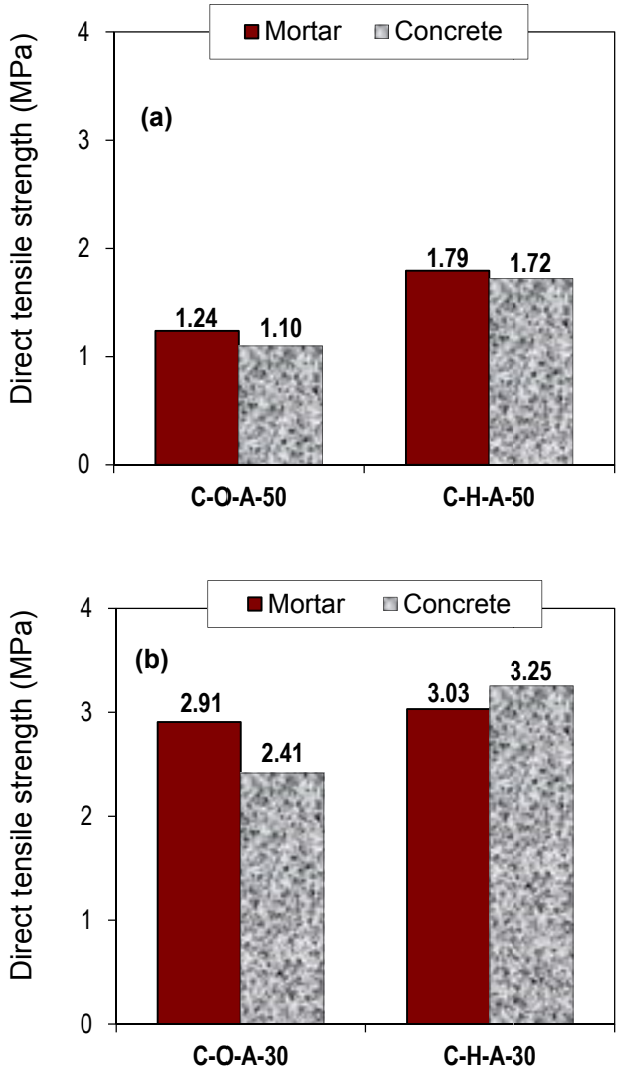

Fig. 3.21 Direct tensile strength of slag concretes and respective mortars with **(a)** W/B = 0.5 and **(b)** W/B = 0.3.

The effectiveness of HAC in improving resistance against microcracking may be partially explained by the role of calcium hydroxide (CH). In the hydration of cement, C_3S produces three times as much CH as formed by the hydration of C_2S. Therefore, HAC will create more CH than OPC in hydration. In contrast to CSH, CH is a well-crystallized material with a definite stoichiometry and it will only grow where free space is available (Mindess, 2003) [3.20]. Therefore, CH crystals can be distributed evenly in concrete and they might have become a kind of buffer to prevent the propagation of microcracks. The other reason of larger resistance is due to high bond strength between HAC mortar and coarse aggregate that is discussed in detail in section 3.3.4.

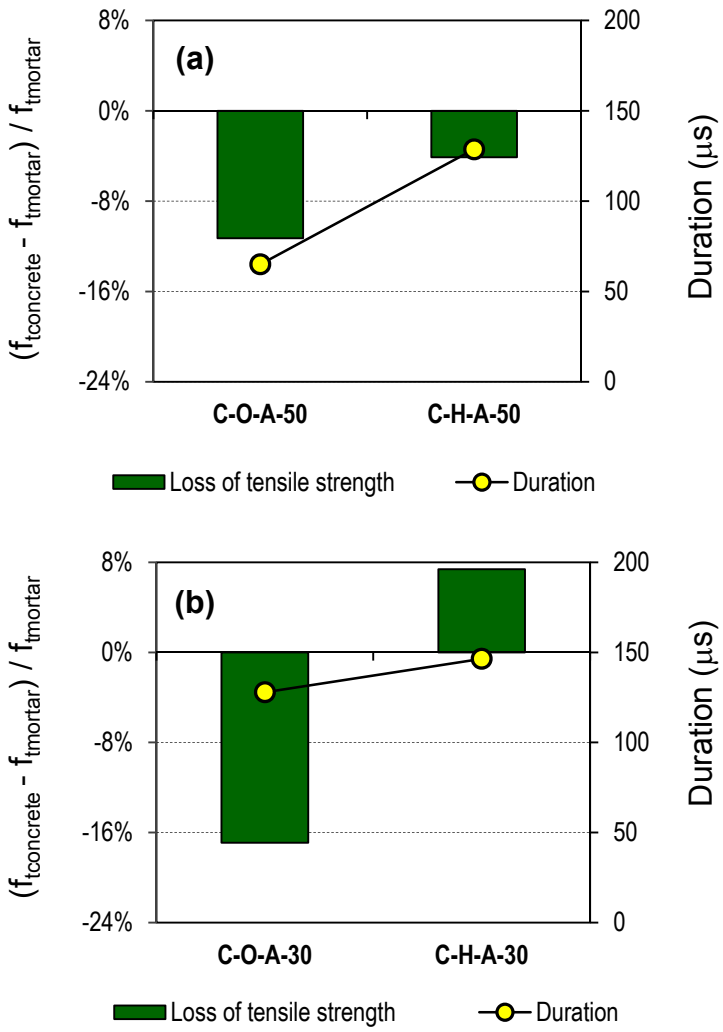

Fig. 3.22 Correlation between direct tensile strength rate and AE duration of concretes with **(a)** W/B = 0.5 and **(b)** W/B = 0.3.

3.3.4 High bond strength between aggregate and HAC slag mortar

Generally, the tensile strength of concrete depends on three factors: tensile strength of mortar, tensile strength of coarse aggregate, and bond strength between mortar and aggregate. Cracking will be initiated at the point that has the lowest strength.

Some evidence pointed to the existence of high bond strength in HAC concretes. The first evidence is the direct tensile strength of concretes and mortars with W/B of 0.3 subjected to steam curing, as shown in **Table 3.4**. In this experiment, mortar was made in two ways: in the first way, mortar was directly mixed from binders, sand, and water; while in the second way, mortar was taken from the respective concrete by removing coarse aggregate. However, the direct tensile strengths of two kinds of mortars showed almost no

Table 3.4 Direct tensile strength of concretes and respective mortars.

Mix proportion	Direct tensile strength (MPa)	Standard deviation (MPa)
M-O-30	2.91	0.15
M-H-30	3.03	0.19
C-O-L-30	2.74	0.01
C-O-A-30	2.41	0.17
C-H-L-30	3.37	0.04
C-H-A-30	3.25	0.07

difference. It can be seen in **Table 3.4** that while the tensile strengths of OPC mortar and HAC mortar were nearly similar, the tensile strength of OPC concrete was much smaller than that of HAC concrete. Furthermore, the tensile strength of HAC concretes was larger than that of the respective mortars. This improvement in tensile strength of HAC concrete must be due to the strong bond between HAC mortar and coarse aggregate. Higher concrete strength over respective mortar strength was not found in the case of W/B of 0.5 (**Fig. 3.21a**).

Concerning the effects of the type of aggregate, the direct tensile strength of OPC slag concretes with W/B of 0.3 showed a reverse tendency compared with the past research. In this study, the tensile strength of concrete with limestone was greater than that of concrete with andesite. Conversely, in the experiments by Son and Hosoda (2010) [3.6], the tensile strength of concrete with limestone was much smaller than that of concrete with andesite. This difference between the two experiments may be partly due to the smaller disparity between the CTEs of limestone and andesite in this research compared to past research. Another reason for the higher strength of concrete with limestone than that of concrete with andesite in this study might be the contribution to improved bond strength of the chemical reaction between OPC slag mortar and limestone. The effect of the chemical reaction in slag concrete with limestone was also noted in the research by Komada *et al*. (2008) [3.9].

In this research, however, the trend of direct tensile strength observed in HAC concretes with W/B of 0.3 was not similar to that in OPC concrete. The tensile strengths of both HAC concretes were larger than the strength of the respective mortars. Moreover, there was no remarkable difference between the direct tensile strengths of HAC concrete

with limestone and andesite (**Table 3.4**). This suggests that the chemical reaction did not play an important role with regard to the tensile strength of HAC concrete with limestone, because the bond strength was originally high enough.

The second evidence of high bond strength in HAC concrete was revealed from visual and SEM observation. The broken sections of OPC and HAC concrete under visual observation are shown in **Fig. 3.23**. Clearly, more numbers of debonding at ITZ were seen in C-O-A-30 than in C-H-A-30. Inversely, more broken coarse aggregate was noted in C-H-A-30 than in C-O-A-30. This means that the bond strength in HAC concrete was larger than that in OPC concrete. Besides, the SEM pictures of concretes in **Fig. 3.24** support this point of view. In OPC concrete with W/B of 0.3 (**Fig. 3.24a**) and of 0.5 (**Fig. 3.24c**), separation cracks were easily realized (particularly in C-O-L-50), while there was almost no debonding at the ITZ in HAC concretes (**Fig. 3.24b,d**).

High bond strength between HAC mortar and aggregate can also be observed in **Fig. 3.18**. In OPC concrete, many microcracks occurred in the expansion period, particularly in concrete with W/B of 0.5. They must be due to the debonding or the slippage between OPC mortar and aggregate. On the other hand, a much smaller number of microcracks were observed in HAC concrete in the same period, which must have resulted from higher bond strength.

It can be said that the tensile strength of concretes under temperature variation is affected by many factors. In the expansion period, separation cracks decrease the bond capacity between the aggregate and mortar. In the shrinkage period, mortar cracks reduce the tensile strength of mortar. The hydration rate, which affects the tensile strength of mortar and the bond strength, was also accelerated under heat curing. In order to grasp appropriately the effect of bond strength on tensile strength, some factors deriving from temperature variations should be eliminated. Therefore, an experiment with concretes subjected to constant temperature condition, i.e., 20^{o}C, was conducted. Under this curing condition, the tensile strength of concrete is mainly governed by mortar strength and the bond properties between the matrix and aggregate.

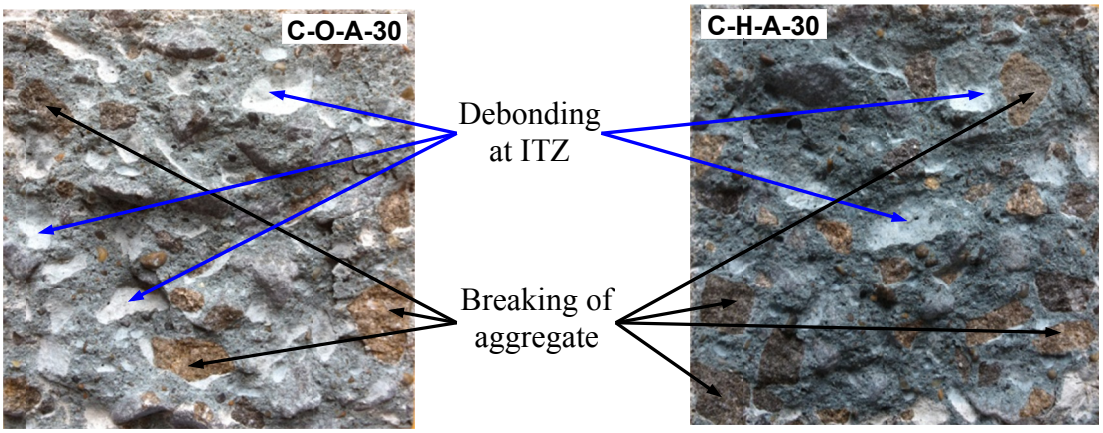

Fig. 3.23 Visual observation at broken section of HAC and OPC slag concrete.

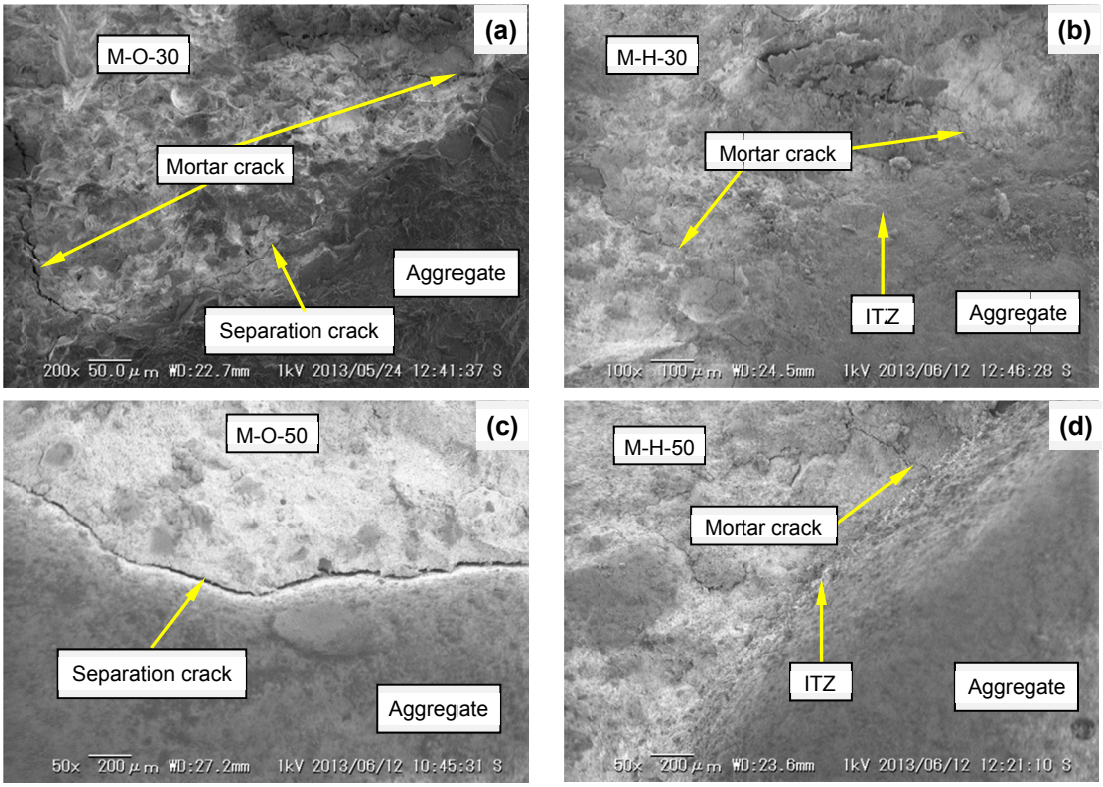

Fig. 3.24 SEM observation of HAC and OPC slag concretes
(a) C-O-L-30 **(b)** C-H-L-30 **(c)** C-O-L-50 **(d)** C-H-L-50

The time-dependent direct tensile strengths of OPC and HAC concretes with W/B of 0.3 cured at 20°C are presented in **Fig. 3.25**. Looking at this chart, while the tensile strengths of OPC concrete with limestone were larger than those of concrete with andesite (this could be mainly due to the chemical reaction between the limestone and slag mortar), the tensile strengths of HAC concrete with limestone and HAC concrete with andesite were almost equal. The rational explanation might be that the bond strengths in both HAC

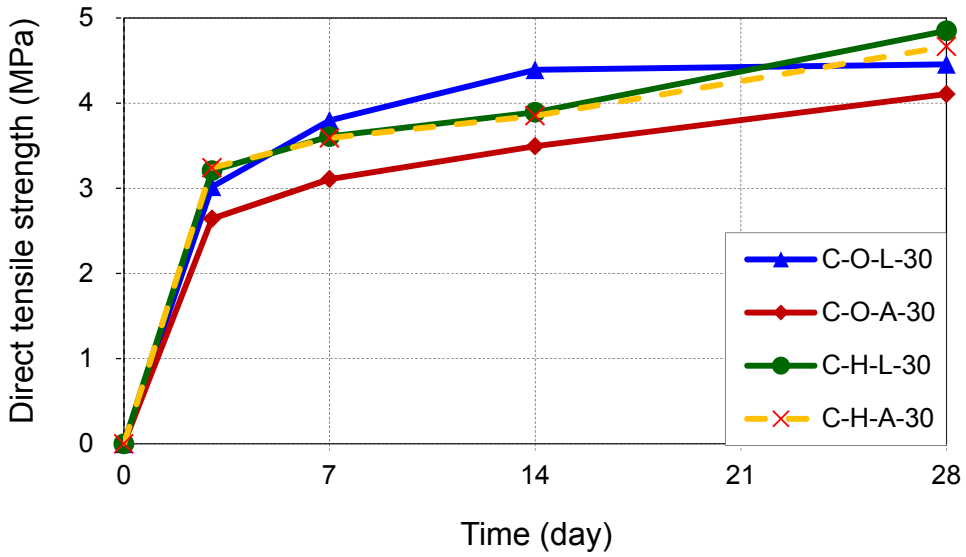

Fig. 3.25 Direct tensile strength of concretes cured at 20°C.

concrete with limestone and HAC concrete with andesite were larger than HAC mortar strength. In this case, chemical reaction did not affect the tensile strength of concrete. Because bond strength was larger than mortar strength, cracks did not occur at the ITZ but appeared in the mortar, and propagation of the cracks initiated in the mortar was perhaps prevented by the aggregate or strong ITZ. As a result, the tensile strength of HAC concrete with limestone was the same as that of HAC concrete with andesite.

The high bond strength in HAC concrete might be explained by the large amount of CH produced through the hydration of HAC. CH reacts with the active SiO_2 component in GGBFS and creates secondary CSH gel. The CSH gel located in pores near the ITZ and enhances the bonding capacity between the HAC mortar and coarse aggregate.

3.4 Conclusions of the chapter

In this chapter, by using the AE technique, physical and mechanical tests, and SEM, the effects of high alite cement (HAC) on improving tensile strength of slag concrete were investigated. The conclusions obtained from this research are as follows:

1. The redesigned waveguide with two additional wings showed the more effectiveness in detecting microcracks at very early ages, especially in concrete with high W/B ratio. The influence of attenuation of acoustic wave in high moisture content medium was significantly mitigated by reducing the distance from cracking points to waveguide.

2. Net shrinkage of HAC mortar with W/B of 0.3 was much larger than that of OPC mortar because of its larger autogenous shrinkage. Normally, larger shrinkage of mortar results in more extensive cracking in concrete. However, the number and the degree of microcracks in HAC slag concrete with W/B of 0.3 were smaller than those in OPC slag concrete. This means that HAC slag concrete with W/B of 0.3 obviously achieved larger resistance against microcrack than OPC slag concrete. On the other hand, net shrinkage of HAC mortar with W/B of 0.5 was a bit smaller than that of OPC mortar due to its smaller thermal contraction. Therefore, microcracking in HAC slag concrete with W/B of 0.5 was also smaller than that in OPC slag concrete.

3. HAC can improve resistance against microcracking of slag concrete with W/B of 0.5 and 0.3. Evenly distributed CH crystals acting as a kind of buffer that prevents the propagation of microcracks in HAC slag concrete might be one of the reasons.

4. Another reason for the high cracking resistance of HAC slag concrete was the strong bond between mortar and coarse aggregate. This high bond strength was more clearly observed in concrete with low W/B than in concrete with high W/B. The high bond strength of HAC slag concrete was verified through mechanical tests, AE test, and visual and SEM observation. The strong bond in HAC slag concretes might be due to the formation of secondary CSH gel from the reaction of CH and active SiO_2 in slag at pores near the ITZ.

References

[3.1] Ohtsu, M., and Watanabe, H., "Quantitative damage estimation of concrete by acoustic emission", *Construction and Building Materials*, Vol. 15, pp. 217–224, 2001.

[3.2] Verstrynge, E., *et al*., "Monitoring and predicting masonry's creep failure with the acoustic emission technique", *NDT & E International*, Vol. 42, No. 6, pp. 518–523, 2009.

[3.3] Sagar, R. V., "An experimental study on acoustic emission energy and fracture energy of concrete", *National Seminar & Exhibition on Non-Destructive Evaluation*, pp. 225–228, 2009.

[3.4] Aggelis, D. G., *et al*., "Acoustic emission characterization of the fracture process in fibre reinforced concrete", *Construction and Building Materials*, Vol. 25, No. 11, pp. 4126–4131, 2011.

[3.5] ACI committee 233, “Ground Granulated Blast-Furnace Slag as a Cementitious Constituent in Concrete”, *American Concrete Institute (ACI)*, 1995.

[3.6] Son, H. N. and Hosoda, A., “Detection of microcracking in concrete subjected to elevated temperature at very early age by acoustic emission”, *Journal of Advanced Concrete Technology*, Vol. 8, No. 2, pp. 201–211, 2010.

[3.7] Hashimoto, A., *et al*., “Properties of high alite cement”, *Proceeding of the JCA*, Vol. 66, pp. 32-33, 2012. (in Japanese)

[3.8] Siribudhaiwan, N., *et al*., “Influence of alite content on the hydration of blended cement”, *The 1st International Conference on Concrete Sustainability (ICCS13)*, pp. 447-452, 2013.

[3.9] Kodama, A., *et al*., “Properties in compression and tension of concrete with GGBFS subjected to high temperature history”, *Proceedings of the JCI*, Vol. 30, No. 1, pp. 363-368, 2008. (in Japanese)

[3.10] Son, H. N., Hosoda, A. and Watanabe, T., “Characterization of microcracking in very early age concrete subjected to elevated temperature by AE”, *Proceedings of the JCI*, Vol. 32, No. 1, pp. 323–328, 2010.

[3.12] Aggelis, D. G., Polyzos, D. and Philippidis, T. P., “Wave dispersion and attenuation in fresh mortar: Theoretical predictions vs. experimental results”, *Journal of the Mechanics and Physics of Solids*, Vol. 53, No. 4, pp. 857–883, 2005.

[3.12] Cusson, D., “Effect of blended cements on effectiveness of internal curing of HPC”, *ACI Special Publication - Internal Curing of High-Performance Concrete: Lab and Field Experiences*, Vol. 256, pp. 105-120, 2008.

[3.13] Landis, E. N. and Shah, S. P. , “The influence of microcracking on the mechanical behavior of cement based materials”, *Advanced Cement-Based Materials*, Vol. 2, No. 3, pp. 105–118, 1995.

[3.14] Tazawa, E., “Influence of curing time on shrinkage and weight loss of hydrating Portland cement”, *Proceedings of the JSCE*, Vol. 156, pp. 39-52, 1969.

[3.15] Tazawa, E., *et al*., “Influences of aggregate types on mechanical properties of concrete subjected to high temperature”, *Proceedings of the JCI*, Vol. 9, No. 1, pp. 13-18, 1987. (in Japanese)

[3.16] Elices, M. and Rocco, C. G., “Effect of aggregate size on the fracture and mechanical properties of a simple concrete”, *Engineering Fracture Mechanics*, Vol. 75, No. 13, pp. 3839–3851, 2008.

[3.17] Kuksenko, V. S., *et al*., "Investigation of fast processes during stable growth of a wedge-shaped crack in steel by the method of acoustic emission", *Strength of Materials*, Vol. 19, No. 7, pp. 901–905, 1987.

[3.18] Aggelis, D. G., *et al*., "Monitoring of the mechanical behavior of concrete with chemically treated steel fibers by acoustic emission", *Construction and Building Materials,* Vol. 48, pp. 1255–1260, 2013.

[3.19] Nam, H. P. and Hosoda, A., "Resistance against microcracking of slag concrete with Hight Alite Cement analyzed by AE with new wave-guide", *Proceedings of the JCI*, Vol. 35, No. 1, pp. 241–246, 2013.

[3.20] Mindess, S., Young, J. F. and Darwin, D., *Concrete*, 2nd ed. Prentice Hall, 2003.

Chapter 4 Effects of fly ash on the resistance against microcracking of concrete subjected to elevated temperature in early ages

4.1 Introduction

Fly ash (FA) is a by-product of coal power generation and mainly consists of SiO_2, Al_2O_3, Fe_2O_3 and CaO. Because fly ash owns pozzolanic characteristic, it can be used as an additive in concrete. Fly ash can improve long-term compressive strength and chloride resistance of concrete. In this chapter, the effects of class F fly ash in concrete subjected to temperature variation in very young ages in term of microcracking resistance was investigated by AE and physical and mechanical tests. Fly ash was used as a cementitious material as well as fine aggregate. In addition, a combination of fly ash and HAC, which was effective in improving resistance against microcracking in slag concrete, was studied.

4.2 Experimental program

OPC, HAC and slag using in this section were the same those in **Table 3.1**. Pit sand was fine aggregate and andesite was coarse aggregate. Fly ash was supplied by DC company with chemical and physical properties are shown in **Table 4.1**.

In all mixes, W/B was 0.45 and sand to aggregate ratio (s/a) was 0.45. To evaluate the effect of fly ash on properties of concrete, fly ash was used as cementitious material with the replacement contents were 15% and 30% by mass. In additional, fly ash also utilized as a part of fine aggregate with the replacement content was 10% by volume. The controlled mix was OPC concrete without fly ash. Slag and HAC were utilized as well for comparison with OPC fly ash concrete. Because concretes in cold region in Japan are subjected to frog damage, air content was controlled at 6 ± 0.5% to prevent concrete from

Table 4.1 Properties of fly ash.

Binder	SiO_2 (%)	Loss in ignition (%)	Density (g/cm^3)	Specific area (cm^2/g)
Fly ash	60.2	1.5	2.23	3940

scaling under freeze/thaw cycles. Slump of fresh concretes was around 10 cm. In order to meet those requirements, air entraining and water reduction admixture were used for all mixes. Mix proportions and properties of fresh concretes are given in detail in **Table 4.2**.

Mix proportion of respective mortar for each kind of concrete was decided by just removing coarse aggregate from concrete while keeping the other proportion and are shown in **Table 4.3**.

The temperature history applied for specimens was simulated as steam curing as described in **Fig. 3.6**.

Table 4.2 Mix proportion of concretes.

Mix proportion	W/C (%)	W/B (%)	s/a (%)	Mix composition (kg/m^3)									Air (%)	Slump (cm)
				W	Binder				Fine aggregate		Andesite	Admixture		
					OPC	HAC	FA	Slag	Sand	FA		101	AE	
C-O-45	45	45	45	165	367	-	-	-	767	-	948	0.92	4.4	5.8	10.6
C-O-45-F15	53				312	-	55	-	758	-	938	1.83	3.7	6.0	14.0
C-O-45-F30	64				257	-	110	-	750	-	927	5.13	2.2	6.2	14.0
C-H-45-F30	64				-	257	110	-	749	-	926	5.13	2.2	6.1	13.7
C-O-45-S15	53				312	-	-	55	765	-	946	0.92	3.7	6.1	10.4
C-O-45-S30	64				257	-	-	110	763	-	944	0.92	2.9	6.0	11.2
C-O-45-FA10	45	38			367	-	-	-	690	66	948	2.57	3.1	5.9	11.2

101: air entraining admixture, AE: water reduction admixture

C-O-45-FA10: FA as fine aggregate, replacement was 10% by volume

Table 4.3 Mix proportion of respective mortars.

Mix proportion	Mix composition (kg/m^3)								
	W	Binder				Fine aggregate		Admixture	
		OPC	HAC	FA	Slag	Sand	FA	101	AE
M-O-45	285	634	-	-	-	1326	-	1.6	7.6
M-O-45-F15	284	536	-	95	-	1303	-	3.2	6.3
M-O-45-F30	282	438	-	188	-	1280	-	8.8	3.8
M-H-45-F30	282	-	438	188	-	1278	-	8.8	3.8
M-O-45-S15	285	538	-	-	95	1321	-	1.6	6.3
M-O-45-S30	285	443	-	-	190	1317	-	1.6	5.1
M-O-45-FA10	285	634	-	-	-	1193	114	5.2	6.4

4.3 Results and discussions

4.3.1 Effects of fly ash on fresh concrete

From the usage of 101 admixture shown in **Table 4.2**, it can be seen that to fix air content at around 6%, 101 agent content increased with the increase of fly ash content, e.g. fly ash reduced air content of concrete. High amount of air-entraining admixture in fly ash concrete was also reported in the research of Geble and Klieger [4.1]. The reason for that was high carbon content, loss on ignition and alkali content of fly ash. However, fly ash increased slump of fresh concrete [4.1]. When fly ash content increased, slump increased regardless the decrease of AE admixture. This finding is in agreement with the result of Berndt (2009) [4.2].

In the other hand, slag seemed not affect air content of concrete due to the similar density between slag and cement. Nonetheless, slag also increased slump of concrete with a slighter effectiveness compared with fly ash.

4.3.2 OPC concretes containing different fly ash replacement ratios

Under the variation of temperature, microcracks occurred in concretes containing fly ash. The development of AE hits and cumulative AE hits and energy in concrete with and without fly ash are shown in **Fig. 4.1** and **Fig. 4.2**, respectively.

It can be pointed out that in both expansion and shrinkage periods, the number of microcracks reduced with the increase of fly ash content, but the difference was clearer in the expansion period. In this stage, concrete with 30% fly ash replacement ratio showed a much smaller number of microcracks while concrete with 15% fly ash replacement ratio presented a bit smaller number of microcracks compared with OPC concrete. In shrinkage period, the amount of microcracks of all concretes was not so much different (**Fig. 4.2**). Most microcracks appeared in this stage at the same time, i.e. from 12 hours to 15 hours after mixing (**Fig. 4.1**). This time corresponded to the largest shrinkage of respective mortars (**Fig. 4.3**).

Considering level of cracking, the cracking was more severe in the concrete without fly ash. Cumulative AE energy was smaller in the concretes containing fly ash, particularly in shrinkage period (**Fig. 4.2**). This can be explained by the smaller net shrinkage of fly ash mortars in this stage (**Fig. 4.3**).

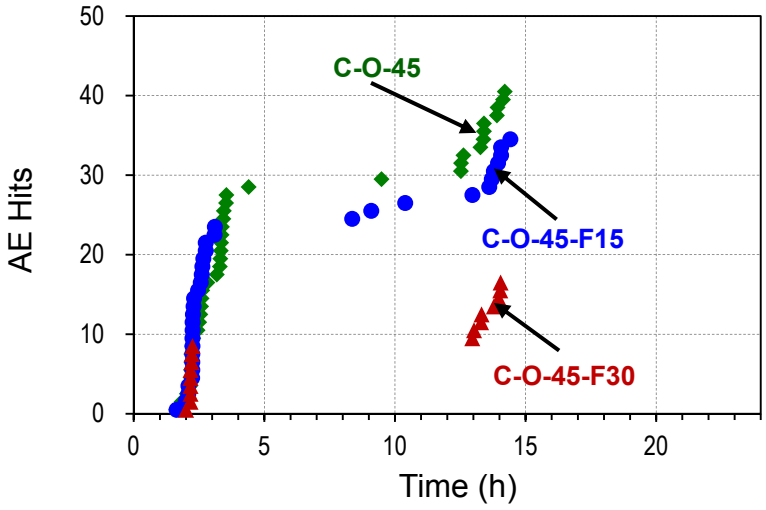

Fig. 4.1 Development of cracking in normal and fly ash concretes.

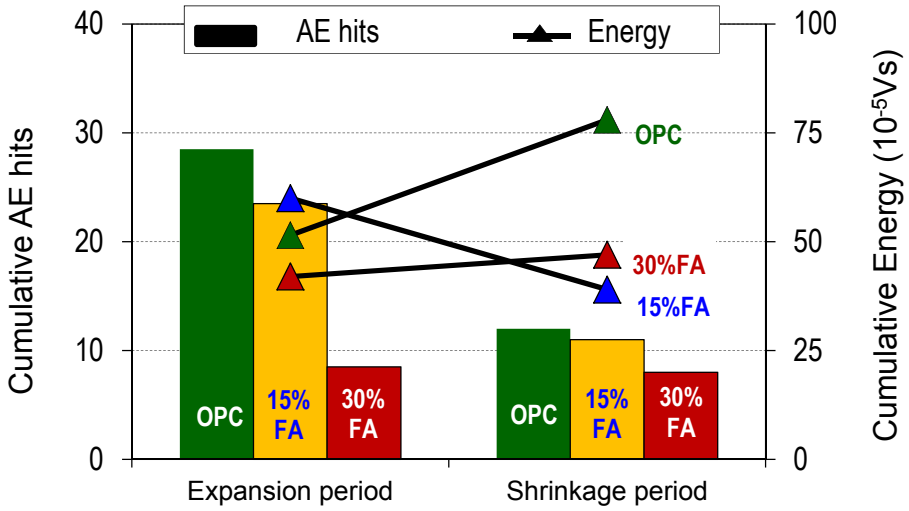

Fig. 4.2 Cumulative AE hits and AE energy of normal and fly ash concretes.

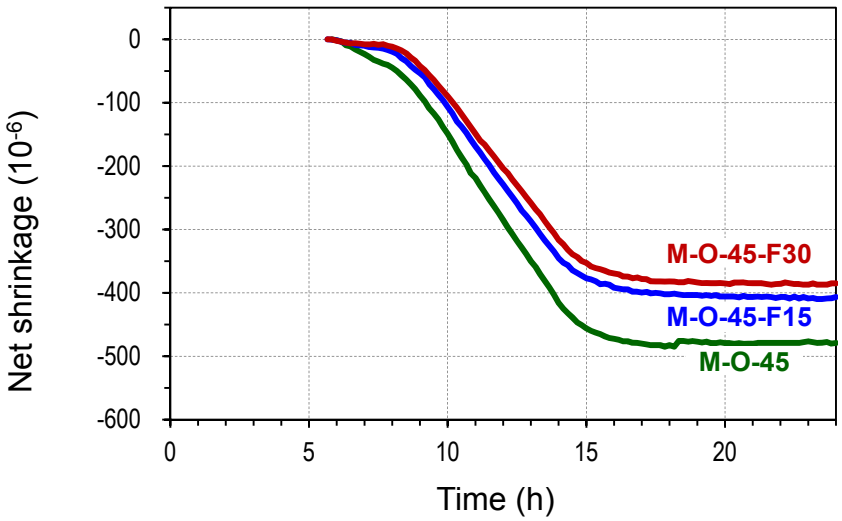

Fig. 4.3 Net shrinkage of normal and fly ash mortars.

Direct tensile strength in early ages of normal and fly ash concretes and respective mortars are expressed in **Fig. 4.4**. Direct tensile strengths of concretes as well as mortars containing fly ash were smaller than those without fly ash. The reason was the reduction of amount of OPC in fly ash concrete. Naik and Hossain [4.3] also reported that splitting tensile strength of fly ash concrete was also smaller than that of OPC concrete in the later ages. Although direct tensile strength of fly ash concretes were smaller than those of corresponding mortars, the loss of tensile strength in fly ash concretes were not so large, just around 10% (**Fig. 4.5**). It means that microcracking a bit adversely affected tensile strength of fly ash concrete.

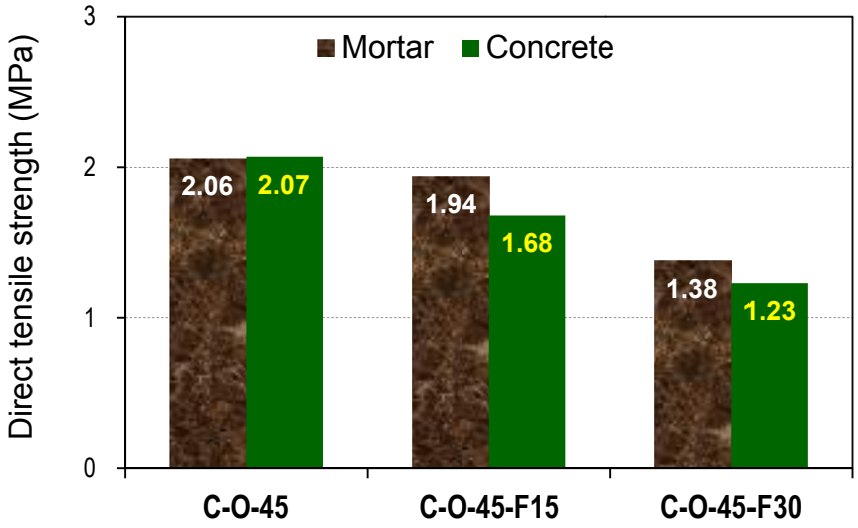

Fig. 4.4 Direct tensile strength of normal and fly ash concretes and respective mortars.

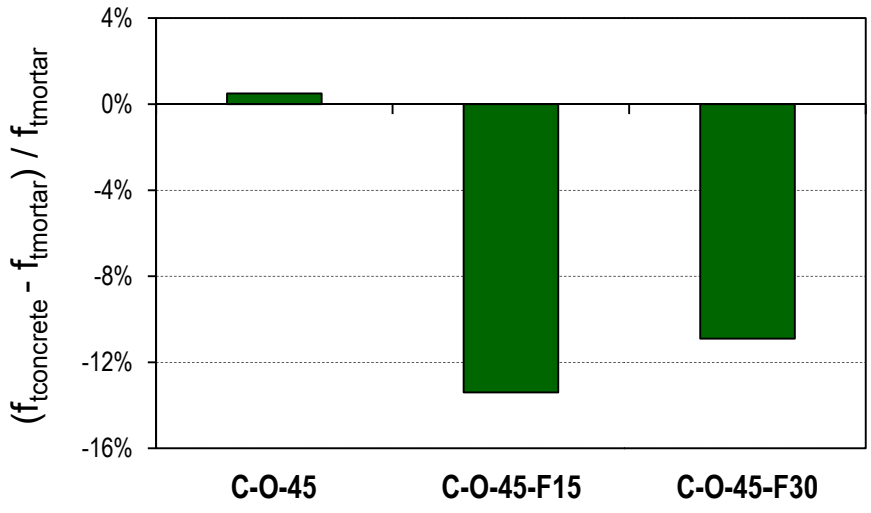

Fig. 4.5 The loss of direct tensile strength of normal and fly ash concretes.

Generally, it can be said that fly ash concrete was not so weak against elevated temperature in early ages. This supports the fact that so far there has been no report about severe cracking in real structures using fly ash.

4.3.3 Comparison of effects of fly ash and slag in OPC concrete

The CTEs and net shrinkage of OPC mortars containing slag and fly ash are presented in **Fig 4.6** and **Fig 4.7**, respectively. CTEs of fly ash mortars were a bit smaller than those of slag mortars. In both fly ash and slag mortars, their CTEs reduced with the decrease of additive content.

Fly ash reduced net shrinkage of mortar rather largely. When fly ash content increased, net shrinkage of fly ash mortars decreased. However, there was not so much difference in net shrinkage of mortars with 15% and 30% fly ash. The decrease of net shrinkage of fly ash mortars was contributed by the decrease of both thermal and chemical shrinkage. Thermal shrinkage of fly ash mortars reduced due to their smaller CTEs. Chemical shrinkage of mortars containing fly ash reduces due to the smaller amount of OPC. In addition, the hydration of fly ash in early ages was very slow [4.4, 4.5] that also led to small chemical shrinkage of fly ash mortars. Slag (with 15% and 30% replacement ratio) also decreased shrinkage of mortars but the reduction was unremarkable. The similar results were found in the research of Li and Guo [4.6].

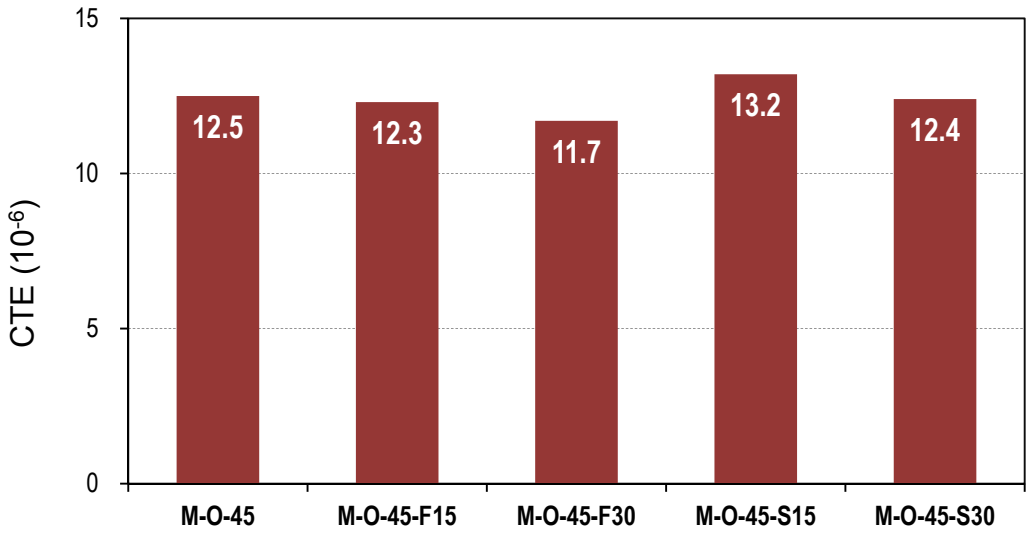

Fig. 4.6 CTEs of OPC mortars containing fly ash and slag.

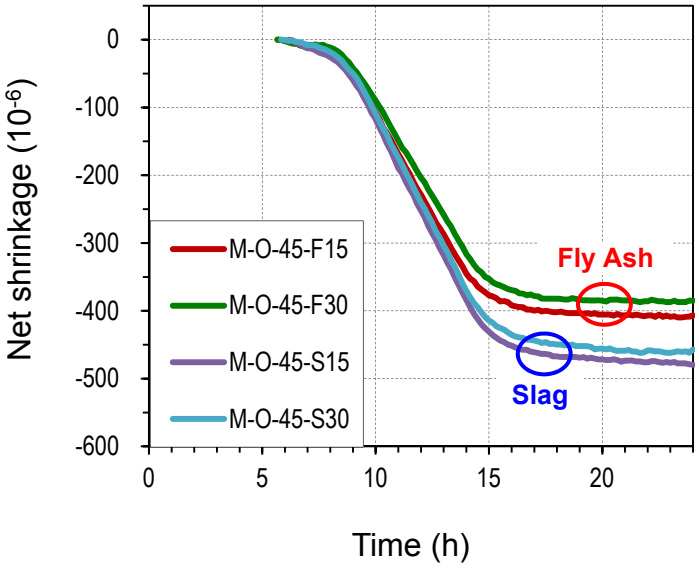

Fig. 4.7 Net shrinkage of OPC mortars containing FA and slag.

Due to the difference in deformation of mortar and aggregates during temperature history, microcracking raised in concretes. The development of microcraking in OPC concrete containing fly ash and slag are shown in **Fig. 4.8**. It can be seen that the number of AE hits in concrete containing 15% fly ash was a bit larger than that in concrete containing 15% slag, whereas the number of AE hits in concrete containing 30% fly ash was much smaller than that in concrete containing 30% slag (although in expansion period they were similar).

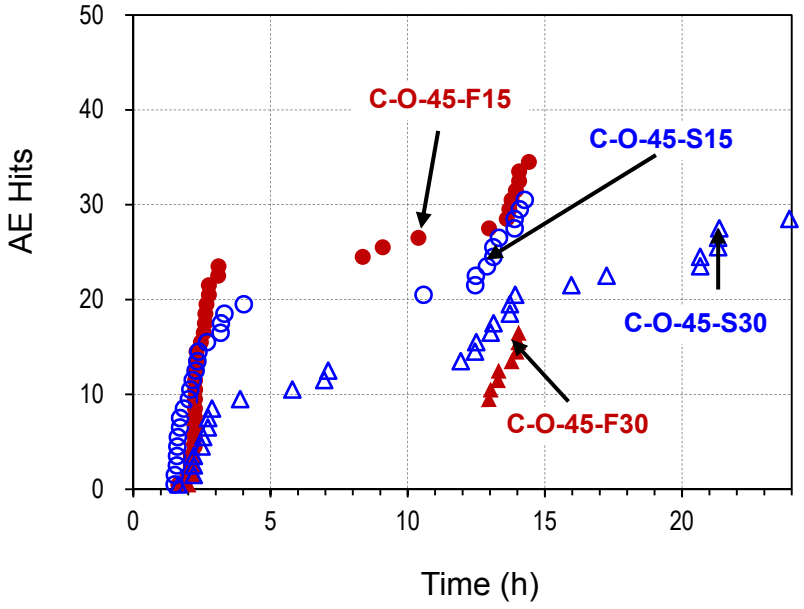

Fig. 4.8 Development of cracking in concretes containing fly ash and slag.

The low hydration rate in early ages even under accelerated temperature of fly ash resulted in the smaller direct tensile strength of both mortar and concrete containing fly ash compared with those containing slag as presented in **Fig. 4.9**. However, the loss of tensile strength in fly ash concretes was a bit smaller than that in slag concretes (**Fig. 4.10**). It can be inferred that microcracking in fly ash concretes was not as severe as that in slag concretes.

4.3.4 Effects of HAC in fly ash concrete

As mentioned in chapter 3, HAC was very effective in resistance against microcracking of slag concrete in early ages under temperature variation due to high bond strength between HAC slag mortar and coarse aggregate. Therefore, an investigation about the effectiveness of HAC in fly ash concrete was conducted with the fly ash replacement ratio of 30%. The development and level of microcraking in OPC and HAC concrete containing fly ash are presented in **Fig. 4.11** and **Fig. 4.12**, respectively.

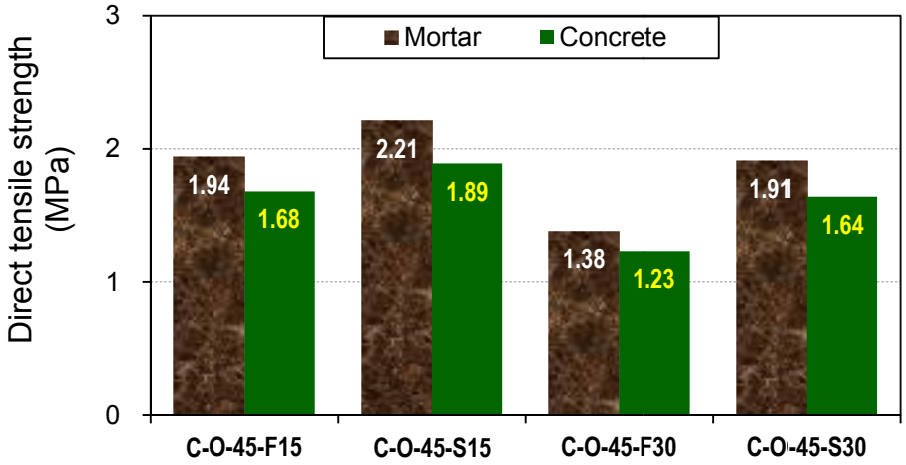

Fig. 4.9 Direct tensile strength of fly ash and slag concretes and respective mortars.

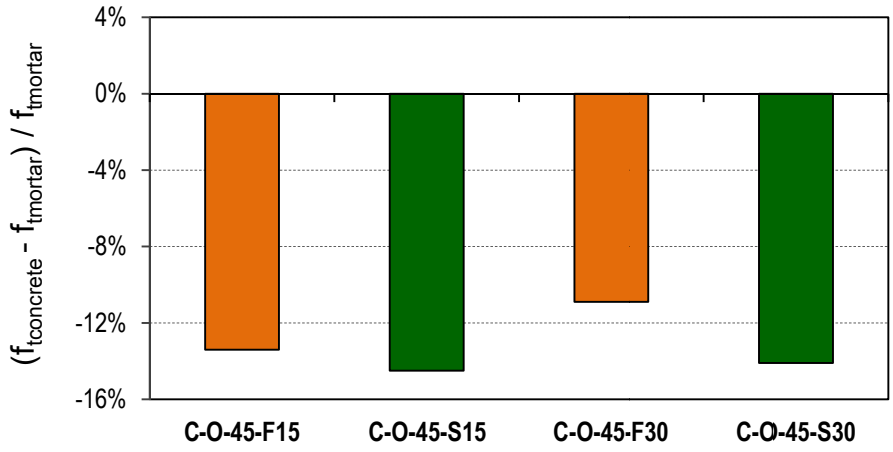

Fig. 4.10 The loss of direct tensile strength of fly ash and slag concretes.

In can be seen that HAC fly ash concrete under elevated temperature was more susceptible to microcracking than OPC fly ash concrete. HAC fly ash concrete showed a larger number of microcracks and a bit higher microcracking level. This was different in slag concrete: HAC slag concrete had larger number of microcracks but lower microcracking level than OPC slag concrete (as analyzed in section 3.3.3). One of the reasons for more microcracking in HAC fly ash concrete compared with OPC fly ash concrete in shrinkage period is that HAC fly ash mortar shrank more largely than OPC fly ash mortar (**Fig. 4.13**). Net shrinkage of M-H-45-F30 was larger than that of M-O-45-F30 because of its larger thermal shrinkage (CTEs of HAC fly ash mortar and OPC fly ash mortar were 11.7×10^{-6} and 12.1×10^{-6}, respectively) and its larger chemical shrinkage due to high hydration rate of HAC.

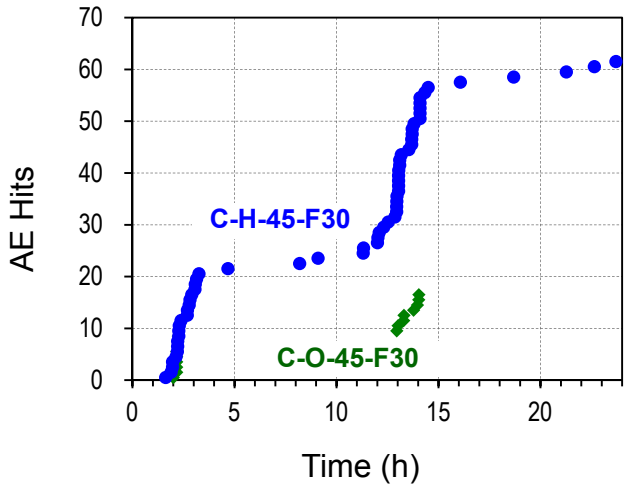

Fig. 4.11 Development of cracking in OPC and HAC FA concretes.

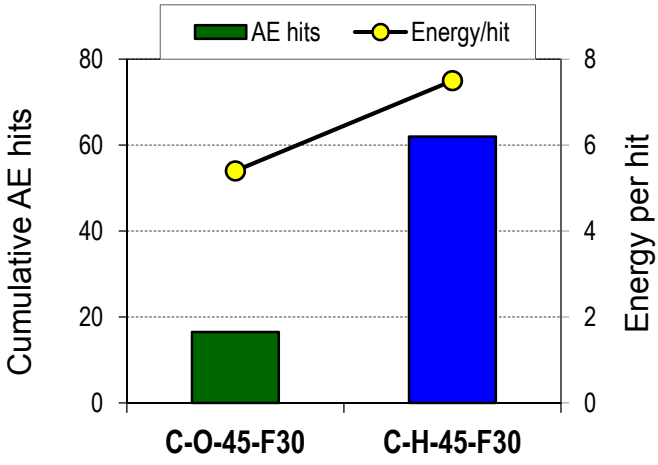

Fig. 4.12 Cumulative AE hits and AE energy per hit of OPC and HAC FA concretes.

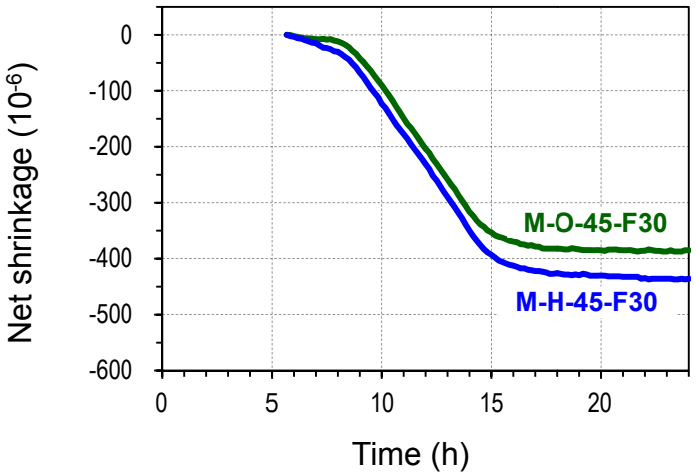

Fig. 4.13 Net shrinkage of OPC and HAC mortars containing 30% fly ash.

Direct tensile strengths of OPC and HAC concretes containing fly ash and respective mortars are expressed in **Fig. 4.14**. Direct tensile strengths of HAC fly ash concrete and respective mortar were much larger than those of OPC fly ash concrete. It means that HAC was also affective in fly ash concrete. However, the larger direct tensile strength of HAC fly ash concrete in young ages was mainly due to the higher hydration rate of HAC rather than the reaction between CH (hydration product of HAC) and fly ash. If the reaction between CH and fly ash occurred in early ages, secondary CSH might increase bond strength leading to the higher tensile strength of HAC fly ash concrete compared with HAC fly ash mortar. However, the result indicated that tensile strength of HAC fly ash concrete was smaller than that of HAC fly ash mortar (this trend was similar in OPC fly ash concrete). It can be said that large bond strength did not appear in HAC fly

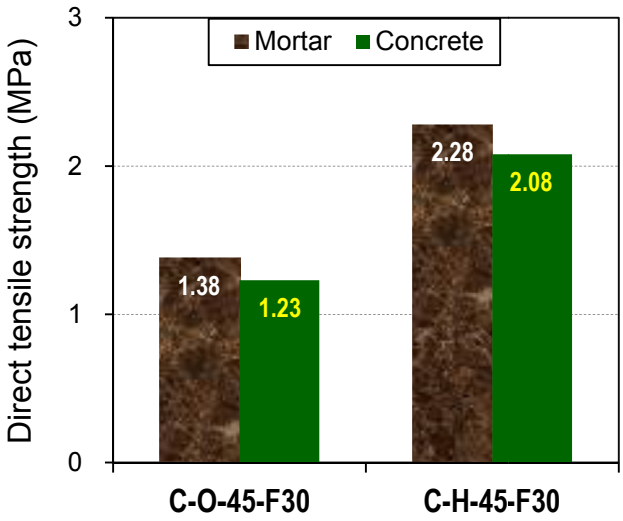

Fig. 4.14 Direct tensile strength of OPC and HAC fly ash concretes and respective mortars.

ash concrete like in HAC slag concrete. The reason for small bond strength in HAC fly ash concrete is that although fly ash has pozzolanic characteristic it is not active in early ages even under high temperature. Sakai *et al*. also reported that fly ash did not react for the first 7 days in OPC concrete sealed at 20°C, independent of the glass content and replacement ratio [4.7].

4.3.5 Effectiveness of fly ash used as a part of fine aggregate

In literature, some researchers also utilized fly ash as a part of fine aggregate [4.8-4.11] but there has not had any report in case of resistance against microcracking in early ages. Thus, in this section effect of fly ash as a part of fine aggregate on microcracking resistance was investigated. The acummulative AE hits and degree of microcraking in normal concrete (C-O-45) and OPC concrete containing fly ash as a part of fine aggregate with replacement content of 10% by volume (C-O-45-FA10) under temperature variation are presented in **Fig. 4.15** and **Fig. 4.16**, respectively.

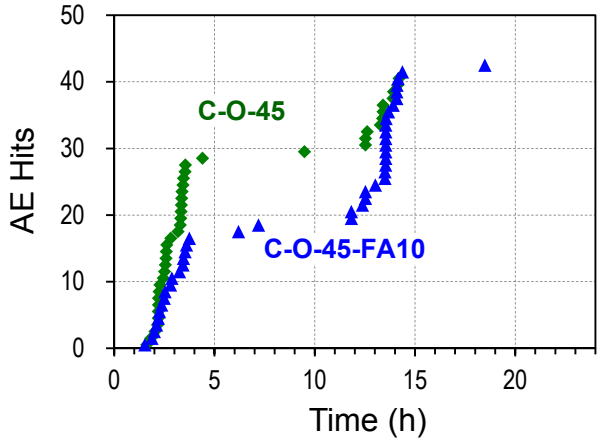

Fig. 4.15 Development of cracking in C-O-45 and C-O-45-FA10.

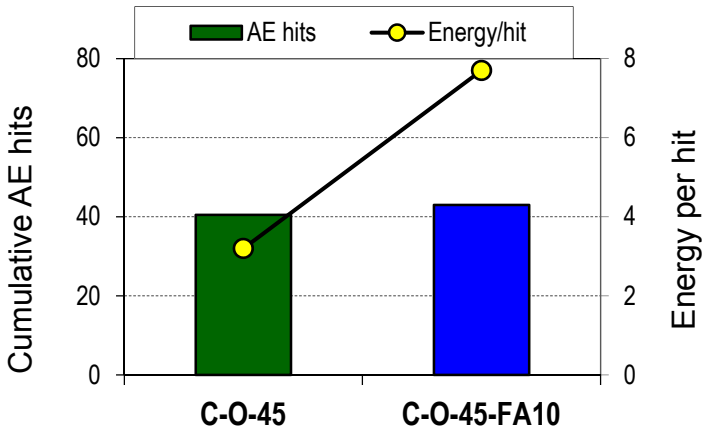

Fig. 4.16 Cumulative AE hits and AE energy per hit of C-O-45 and C-O-45-FA10.

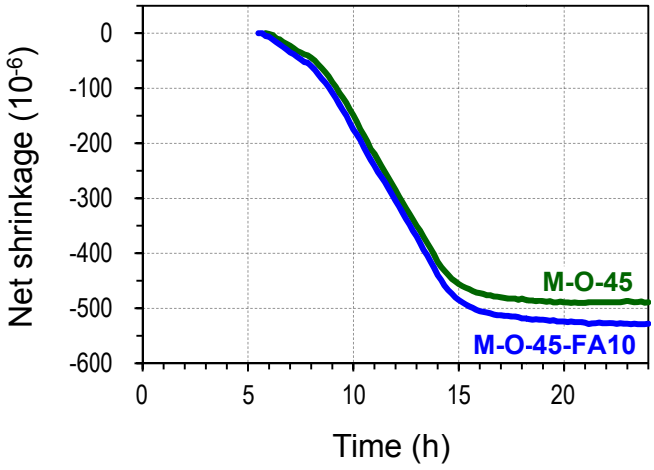

Fig. 4.17 Net shrinkage of M-O-45 and M-O-45-FA10.

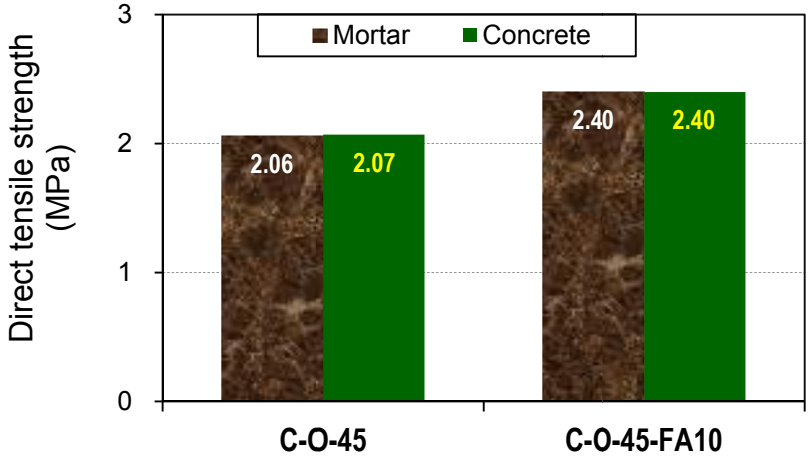

Fig. 4.18 Direct tensile strength of C-O-45 and C-O-45-FA10 and respective mortars.

It is clearly seen that C-O-45-FA10 had smaller number of microcracks in expansion period but larger number of microcracks in shrinkage period compared with C-O-45 but total number of microcracks in two concretes were similar. The larger number of microcracks of C-O-45-FA10 in shrinkage stage might be attributed to the larger net shrinkage of its respective mortar (**Fig. 4.17**). Although total number of microcracks was similar, the level of microcracking in C-O-45-FA10 was much larger than that in normal concrete (**Fig. 4.16**).

From the comparison of direct tensile strength of C-O-45, C-O-45-FA10 and respective mortar as expressed in **Fig 4.18**, it can be seen that direct tensile strength of concretes and respective mortars were similar. It implies that fly ash as a part of fine aggregate did not play any role in improving bond strength between aggregate and the matrix. However, it is apparent that direct tensile strengths of both concrete and mortar

containing fly ash were much larger than those of normal concrete and mortar. When fly ash used as a part of fine aggregate, it could increase the denseness of the matrix. This improved direct tensile strength of both concrete and mortar.

4.4 Conclusions of the chapter

Some conclusions can be drawn in this chapter as follows.

1. Concrete containing fly ash was not so weak against elevated temperature. Nevertheless, fly ash reduced tensile strength of concrete remarkably. The reason is that fly ash is not so active in early ages even under steam curing.

2. In early age, slag is more active than fly ash leading to the higher tensile strength of slag concrete compared with fly ash concrete. However, microcracking in slag concrete was severe than that in fly ash concrete due to larger shrinkage of slag mortar compared with fly ash mortar.

3. HAC can significantly improve tensile strength of concrete containing fly ash due to high hydration rate of HAC. However, high bond strength in HAC fly ash concrete was not observed from the direct tensile test.

4. When fly ash is used as a part of fine aggregate, it can improve tensile strength of concrete remarkably.

References

[4.1] Geble, S. and Klieger, P., “Effect of fly ash on the air void stability of concrete”, *Proceeding of the 1st International Conference of the Use of Fly Ash, Silica Fume, Slag and Other Mineral by Products in Concrete, ACI SP-79*, pp. 103-142, 1983.

[4.2] Berndt, M. L., “Properties of sustainable concrete containing fly ash, slag and recycled concrete aggregate”, *Construction and Building Materials*, Vol. 23, No. 7, pp. 2606-2613, 2009.

[4.3] Naik, T. R., Singh, S. S., and Hossain, M. M., “Enhancement in mechanical properties of concrete due to blended ash,” *Cement and Concrete Research*, Vol. 26, No. 1, pp. 49-54, 1996.

[4.4] He, J. Y., Barry, E. S., and Della, M. R., “Hydration of fly ash - Portland cement”, *Cement and Concrete Research*, Vol. 14, No. 4, pp. 505-512, 1984.

[4.5] Zhang, Y., Sun, W., and Yan, H., “Hydration of high-volume fly ash cement paste”, *Cement and Concrete Composites*, Vol. 22, No. 6, pp. 445-452, 2000.

[4.6] Li, Y., Bao, J., and Guo, Y., “The relationship between autogenous shrinkage and pore structure of cement paste with mineral admixtures”, *Construction and Building Materials*, Vol. 24, pp. 1855-1860, 2010.

[4.7] Sakai, E. *et al*, “Hydration of fly ash cement”, *Cement and Concrete Research*, Vol. 35, pp. 1135-1140, 2005.

[4.8] Siddique, R., “Effect of fine aggregate replacement with Class F fly ash on the mechanical properties of concrete”, *Cement and Concrete Research*, Vol. 33, No. 4, pp. 539-547, 2003.

[4.9] Siddique, R., “Effect of fine aggregate replacement with Class F fly ash on the abrasion resistance of concrete”, *Cement and Concrete Research*, Vol. 33, No. 11, pp. 1877-1881, 2003.

[4.10] Varughese, K. T., and Chaturvedi, B. K., “Fly ash as fine aggregate in polyester based polymer concrete”, Cement & Concrete Composites, Vol. 18, No. 2, pp. 105-108, 1996.

[4.11] Singha Roy, D. K., “Performance of blast furnace slag concrete with partial replacement of sand by fly ash”, *International Journal of Earth Sciences and Engineering*, Vol. 4, No. 6, pp. 949-952, 2011.

Chapter 5 Improvement of chloride penetration resistance of concrete containing mineral admixtures by HAC

5.1 Introduction

Great Earthquake happened on March 11, 2011 which completely destroyed wide area in Tohoku region. Thus, the reconstruction in this region has been rapidly executed. There has been hundreds kilometer of the "revival road" and "reconstruction assistant road" under construction now (**Fig. 5.1**). The revival road is along the east coastal line of Japan. Many concrete structures will be constructed in the roads.

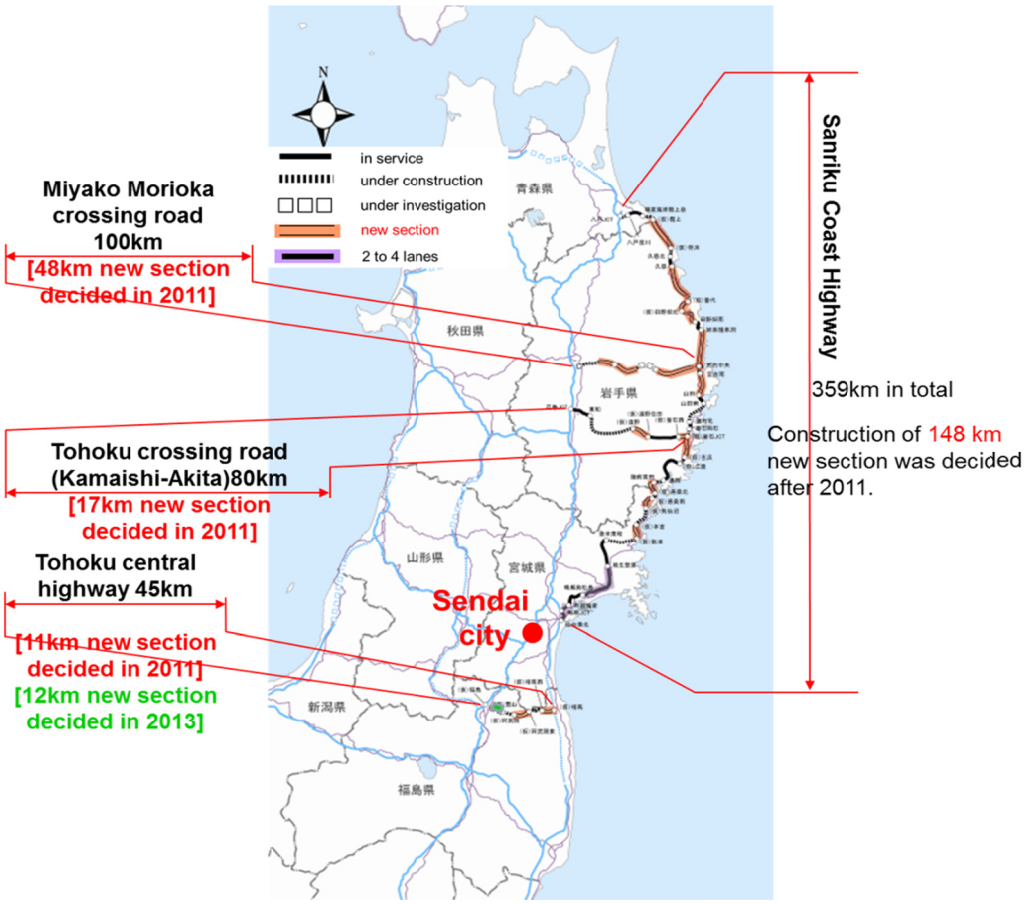

Fig. 5.1 Revival roads and reconstruction assistance roads in Tohoku region [5.1].

Because Tohoku region is located at the north of Japan, temperature is very low in winter. In consequence, concrete structures in Tohoku will suffer from severe condition such as freezing and thawing or sea weather. Moreover, the excessive use of deicing agent in winter may lead to severe scaling and chloride induced corrosion. ASR may be activated due to the supply of alkali from the deicing agent. These many concrete structures will be constructed in very short term with limited human power and materials, so it is not easy to construct durable structures.

Especially, the deterioration of concrete slabs due to fatigue under the effects of deicing agent is severe. The upper slabs of PC box girders are important targets to be made more durable, because it is almost impossible to replace them. To improve the resistance against chloride penetration, utilizing mineral additives such as slag and fly ash is effective. It is also well known that concrete with slag or fly ash needs appropriate curing to show its full performance. It has been pointed out by many researchers that slag or fly ash concrete is more susceptible to poor curing condition than OPC concrete.

In this chapter, Surface Water Absorption Test (SWAT), a method developed by Hayashi and Hosoda [5.2], and penetration depth test will be applied to clarify the effectiveness of HAC in improving the resistance against water and chloride ions penetration depth. SWAT is employed because it is very sensitive to concreting works, which is the most important factor affecting the quality of covercrete of concrete structures. Fundamental researches on SWAT [1.3-1.5] have shown that several indices from SWAT measurement have good correlation with concrete properties related to durability. Moreover, it is a simple, nondestructive, and rapid method in actual site.

5.2 Backgrounds

Soon after the hydration of cement has begun, the protective passivity layer on the surface of reinforcing bar, which consists of γ-Fe_2O_3 tightly adhering to the steel, is self-generated. This oxide film keeps the steel bar intact. Nonetheless, when touching reinforcing bar, chloride ions destroy the layer and corrosion will occur with the presence of water and oxygen [5.3]. In this case, therefore, the ultimate penetration depth of chloride ions is the key factor for the corrosion of reinforcement and needs to be investigated. If the ultimate penetration depth of chloride ions is smaller than convercrete, the structures will be safe in term of chloride attack.

One important thing needs to be noted here that the ultimate water penetration depth in this research is obtained when the absorption becomes stable after a certain period. Several researchers have pointed out that the penetration depth of chloride ions is governed by the penetration depth of liquid water especially in good quality concrete [5.4]. In this research, the penetration depth of chloride ions is also investigated, but it is not the ultimate penetration depth of chloride ion. Chloride ions can continue moving inward due to diffusion even after the absorption becomes stable especially when the quality of concrete is not good.

The ultimate depth of water penetration is also very important because it is related not only with chloride-induced corrosion but also with other deterioration problems such as carbonation-induced corrosion.

Chloride penetration can be evaluated by several methods from long-term tests such as AASHTO T295 [5.5] (salt ponding test), bulk diffusion test (Nordtest NTBuild 443) [5.6] to short-term tests such as AASHTO T277 [5.7] (rapid chloride permeability test – RCPT) or rapid migration test [5.8]. Indirect measurement of chloride penetration has also been developed but it has not been successful [5.9, 5.10].

In this study, the resistance against water absorption of concrete is tested by SWAT firstly, and the ultimate penetration depth of liquid water due to absorption is examined later. Iwamoto [5.11] found that there was a good correlation between the water absorption rate at 2 minutes and ultimate penetration depths in OPC concrete (**Fig. 5.2**).

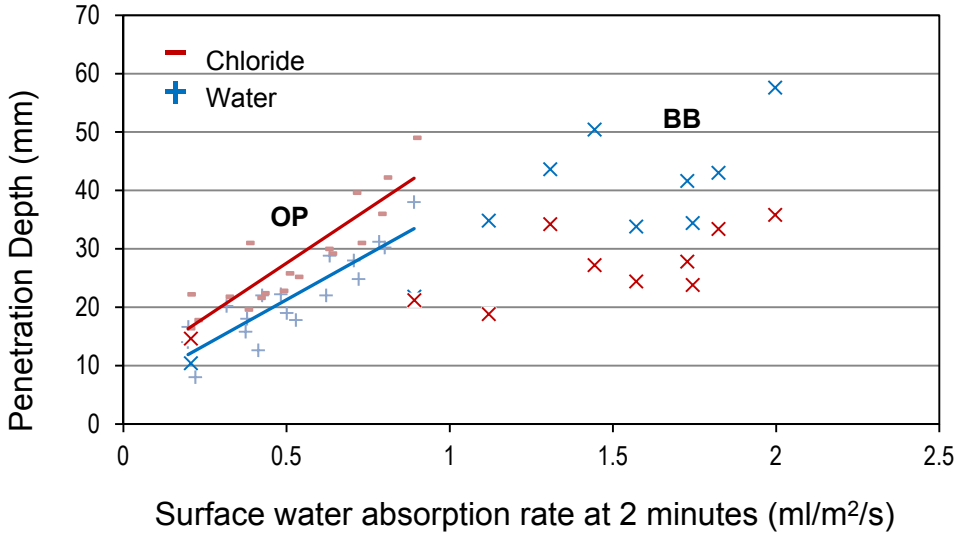

Fig. 5.2 Correlation between penetration depth and SWAT index [5.10].

In **Fig. 2**, the horizontal axis presents the surface absorption rate at 2 minutes (p_{120}) obtained from SWAT and the vertical axis shows the penetration depths of water and chloride ions. The p_{120} and the penetration depths of water and chloride ions were measured on the same specimen. Iwamoto investigated OPC concretes with different W/B ratios subjected to 6 curing conditions covering from very good curing to very poor curing. Concrete containing slag was also studied in his research with only 9 specimens. All data was plotted on the chart and the correlation between p_{120} and water and chloride ions penetration depths was analyzed.

It can be seen from **Fig. 5.2** that in OPC concrete penetration of chloride ions (identified by $AgNO_3$) was deeper than that of water (identified by colored change agent). One of the reasons for this difference is that the ingress of chloride ions is not only due to absorption but also due to diffusion. Concrete with slag cement type B showed the opposite trend, which may be due to the capacity of slag in binding chloride ions as Friedel's salt [5.12]. The covercrete quality of concrete with slag seems to be much affected by curing conditions but the potential of slag concrete with larger resistance against chloride ingress can be also recognized.

As confirmed in section 3.3.4, HAC can improve bond strength between aggregates and the matrix in slag concrete due to formation of secondary CSH from reaction of CH and active SiO_2 component in slag. Better ITZ may increase tortuosity of penetration path that results in high resistance against liquid ingress. Although inactive in very early ages as slag as explained in chapter 4, fly ash is expected to be effective in long-term period in HAC concrete. Therefore, the use of HAC may improve the mass transfer resistance of concrete containing slag or fly ash.

5.3 Objectives

It can be stated that normal concrete (with OPC only) is undurable when concrete structures are subjected to severe environmental conditions. Thus, the objective of this chapter is to clarify the effectiveness of HAC in improving the resistance of covercrete containing mineral additives against water and chloride penetration. The effectiveness of HAC will be clarified by SWAT and water/chloride penetration depth test. Based on the investigation results in this research, a method to utilize SWAT to evaluate the durability of actual structures will be proposed.

5.4 Experimental program

5.4.1. Mix proportions

In this research, four types of binder were used: OPC, HAC, slag, and fly ash. Concrete with OPC only was the control mix. In other mixes, the cements were replaced by slag or fly ash with the replacement ratios of 40% or 15% by mass, respectively. W/B ratios were 0.4, 0.5, and 0.6 to cover from good concrete to poor concrete. Coarse aggregate of andesite with maximum particle size of 19 mm was used. Air content of concrete was controlled at 6 ± 0.5% to prevent concrete from scaling under freeze/thaw cycles. Three-binder concretes containing slag and fly ash with W/B of 0.4 were also prepared. Ten cylindrical specimens of 100 mm diameter and 200 mm height for each type of concrete were placed.

As discussed in chapter 3, chemical reaction between limestone and OPC slag mortar increased bond strength at ITZ. A denser ITZ might improve liquid resistance of concrete. To investigate the effect of bond on mass transfer, some concretes made with limestone were added in the cases of concrete with W/B of 0.4 and 0.5.

Mix proportions of concrete are given in **Table 5.1**.

5.4.2 Curing conditions and experimental program

(1) Curing conditions

Ten specimens of each type of concrete were cured in 5 different conditions covering from very good to very poor curing condition as shown in **Fig. 5.3**. Two specimens were prepared for each condition.

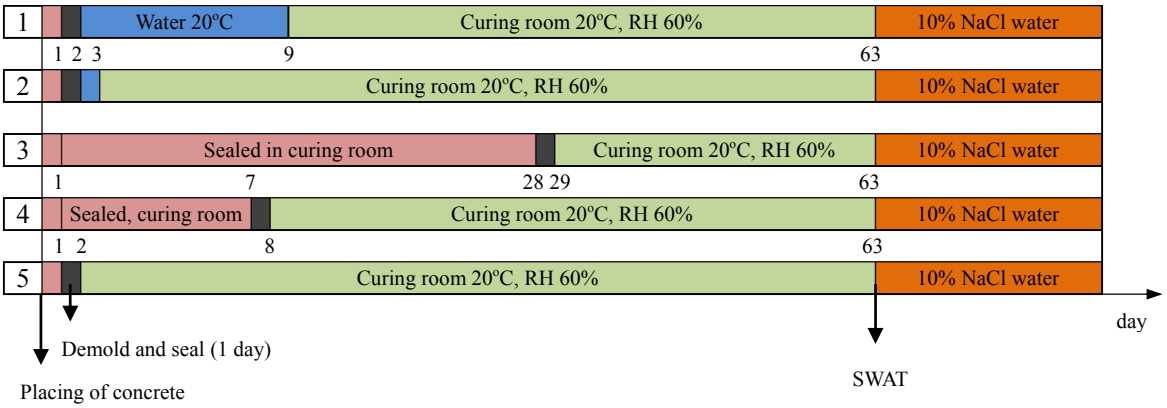

Fig. 5.3 Curing conditions and experimental process.

Table 5.1 Mix proportions of concretes.

Mix proportion	W/B (%)	s/a (%)	Mix compositions (kg/m^3)								
			W	Binder				Sand	Coarse aggregate		Admixture	
				OPC	HAC	Slag	FA		Andesite	Limestone	101	AE
O-40-A	40	45	165	413	-	-	-	750	927	-	1.24	5.0
O-40-S-A				248	-	165	-	745	921	-	1.24	2.1
O-40-F-A				351	-	-	62	740	915	-	2.27	3.7
H-40-S-A				-	248	165	-	744	920	-	1.44	2.5
H-40-F-A				-	351	-	62	739	914	-	2.27	3.7
O-40-S-F-A				210	-	140	62	736	910	-	2.89	1.2
H-40-S-F-A				-	210	140	62	736	910	-	2.89	1.2
O-40-S-L				248	-	165	-	745	-	945	1.24	2.1
O-40-F-L				351	-	-	62	740	-	940	2.68	1.2
H-40-S-L				-	248	165	-	744	-	945	1.24	2.5
H-40-F-L				351	-	-	62	739	-	938	2.68	1.4
O-50-A	50			330	-	-	-	780	965	-	0.99	2.1
O-50-S-A				198	-	132	-	776	960	-	0.99	0.7
O-50-F-A				281	-	-	50	773	955	-	2.15	0.3
H-50-S-A				-	198	132	-	776	959	-	0.99	-
H-50-F-A				-	281	-	50	772	954	-	2.15	-
O-50-S-L				198	-	132	-	776	-	986	0.99	-
O-50-F-L				281	-	-	50	773	-	981	2.15	-
H-50-S-L				-	198	132	-	776	-	985	0.99	-
H-50-F-L				-	281	-	50	772	-	980	2.15	-
O-60-A	60			275	-	-	-	801	990	-	0.83	0.6
O-60-S-A				165	-	111	-	798	986	-	0.83	-
O-60-F-A				234	-	-	41	794	982	-	2.48	-
H-60-S-A				-	165	111	-	797	986	-	1.38	-
H-60-F-A				-	234	-	41	794	982	-	2.75	-

(2) Sealing method

Right after demolding, the surface and side of the specimens were sealed (the bottom was opened) to ensure that evaporation or permeation of water just occurred in one direction, i.e. moisture was evenly distributed in the specimen. Iwamoto [5.11] explored that only epoxy resin coating could not perfectly prevent moisture transportation from inside the concrete to the ambient. Thus, the specimen was wrapped by alumina tape firstly and then coated by epoxy resin (**Fig. 5.4**). It took 1 day for hardening of epoxy resin. After that, the curing process was continued.

(3) Surface water absorption test (SWAT)

After the curing process, all the specimens were dried in a room with the temperature of 20°C and RH of 60% (**Fig. 5.5**). Because the moisture content of concrete is the most influential factor on water absorption of concrete [5.13], all the specimen were dried until the water contents inside the specimens reached stable situations. According to the ASTM C140-11a [5.14], the stable situation can be determined when two successive weighings at intervals of 2h show an increment of water loss not larger than 0.2% of the last previously detected weight of the specimen. Before conducting SWAT measurement, the moisture content of concrete was measured at the surface by moisture tester HI-520 and the results are shown in **Table 5.3**. Initial weight of the specimens had been measured, and then SWAT using pure water was applied to obtain SWAT indices. For cylindrical specimens, a frame was employed to fix the water cup to the surface of the specimen (**Fig. 5.6**).

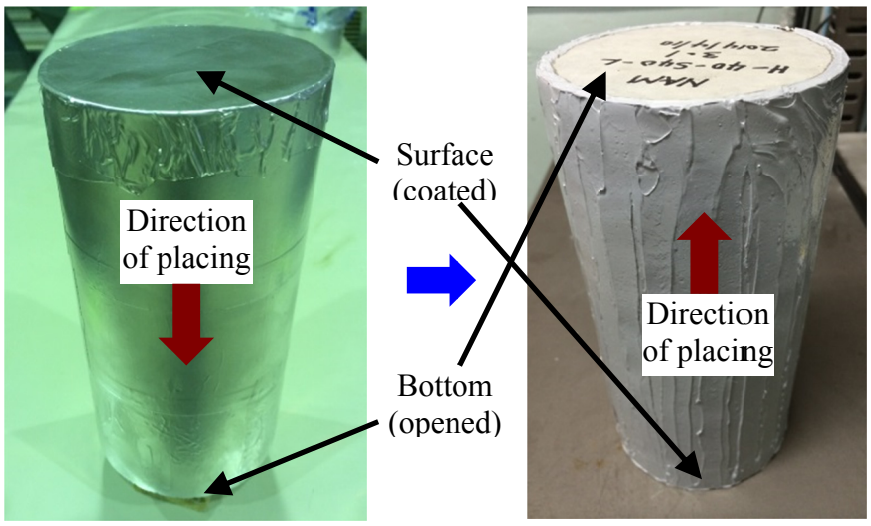

Fig. 5.4 Specimen was wrapped by alumina tape (left) and then coated by epoxy resin (right).

Table 5.2 Moisture content of the surface of specimens.

	Moisture content (%)									
Curing condition	**1 (7d in water)**		**2 (1d in water)**		**3 (28d in mold)**		**4 (7d in mold)**		**5 (1d in mold)**	
Specimen No.	**1.1**	**1.2**	**2.1**	**2.2**	**3.1**	**3.2**	**4.1**	**4.2**	**5.1**	**5.2**
O-40-A	4.7	4.8	4.6	4.7	5.2	5.1	4.8	4.8	4.7	4.6
O-40-S-A	4.9	4.9	4.7	4.6	5.2	5.1	4.8	4.7	4.7	4.5
O-40-F-A	4.8	4.8	4.6	4.5	4.9	4.9	5.0	4.9	4.6	4.6
H-40-S-A	5.0	5.0	4.8	4.8	5.2	5.2	5.0	4.9	4.6	4.7
H-40-F-A	4.9	4.6	4.7	4.9	5.1	5.1	4.8	4.9	4.5	4.6
O-40-S-F-A	4.9	4.8	4.7	4.7	5.2	5.0	5.0	5.0	4.7	4.6
H-40-S-F-A	5.1	5.1	4.8	4.7	5.1	5.2	5.1	5.0	4.8	4.7
O-50-A	4.5	4.5	4.3	4.1	4.7	4.8	4.9	4.5	4.3	4.3
O-50-S-A	4.7	4.9	4.6	4.8	5.1	5.1	4.7	4.8	4.6	4.5
O-50-F-A	4.8	4.9	4.8	4.7	4.9	5.0	4.9	4.8	4.6	4.6
H-50-S-A	5.0	4.9	4.8	4.8	5.1	5.1	5.0	4.9	4.7	4.6
H-50-F-A	5.1	4.9	4.8	4.8	5.2	5.1	4.9	5.0	4.7	4.5
O-60-A	4.8	4.5	4.6	4.7	5.0	4.8	4.7	4.7	4.6	4.6
O-60-S-A	4.8	4.6	4.6	4.4	5.0	4.8	4.7	4.7	4.4	4.4
O-60-F-A	4.6	4.7	4.5	4.6	4.8	4.7	4.5	4.6	4.4	4.3
H-60-S-A	4.7	4.8	4.7	4.7	4.9	4.9	4.7	4.8	4.5	4.5
H-60-F-A	4.9	4.8	4.8	4.7	5.0	4.9	4.7	4.6	4.5	4.2

Fig. 5.5 Specimens dried in curing room.

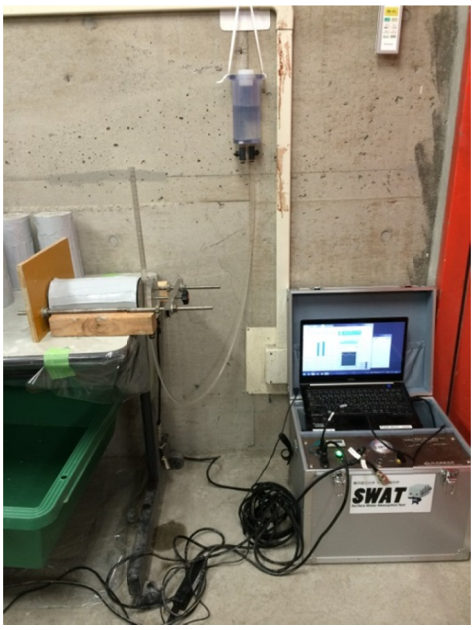

Fig. 5.6 SWAT testing.

(4) Penetration test

(i) Immersion of the specimens in salt water

Right after conducting SWAT, the specimens were immersed in 10% NaCl water following JSCE G572-2010 [5.15] (**Fig. 5.7**) and were continuously weighed specified in ASTM C1585-04 [5.16] until their weights became stable. Finally, the specimens were split to measure penetration depth of liquid water.

(ii) Splitting of specimen

In order to compare penetration depth of water and chloride in short-term period, only one specimen of each parameter was split at the time of 42 days after immersing into

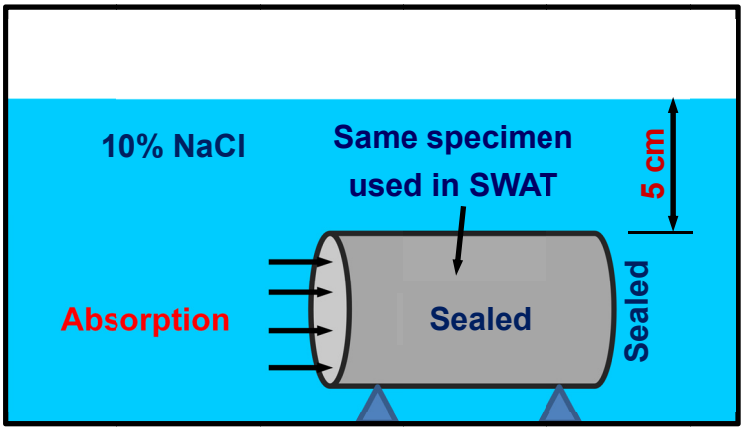

Fig. 5.7 Specimens were immersed in 10% NaCl water.

salt water. The other specimen of each parameter was remained for measurement in long-term period, e.g. 90 days.

Normally, when a usual concrete specimen is subjected to splitting load it is easily to be split at the cross section traversing to the center under a small pressure. It this case, the surface of section is rather flat. Thus, it is easy to obtain the water front or the chloride front. In this study, however, because of epoxy resin coating, a larger load was needed to split the specimen. Therefore, concrete close to the surface of the specimen was easily destroyed, which caused more difficulty in detecting the penetration front due to the rough surface of the split section. To avoid this inconvenience, when the epoxy resin coating was broken due to loading, the coating was removed by hand before applying loading again.

(iii) Detection of water front

After splitting, penetration depth of water was measured immediately before the evaporation of water. Firstly, water front was observed in two halves of split specimen by naked eyes to detect the difference of color between the wet part and the dry part. The wet part showed a bit darker color than the dry part. With this visual detecting method, the water front was clearer in the specimen whose inside part was drier, e.g. concrete with low W/B subjected to poor curing. **Figure 5.8** shows the water front detected by naked eyes (black line).

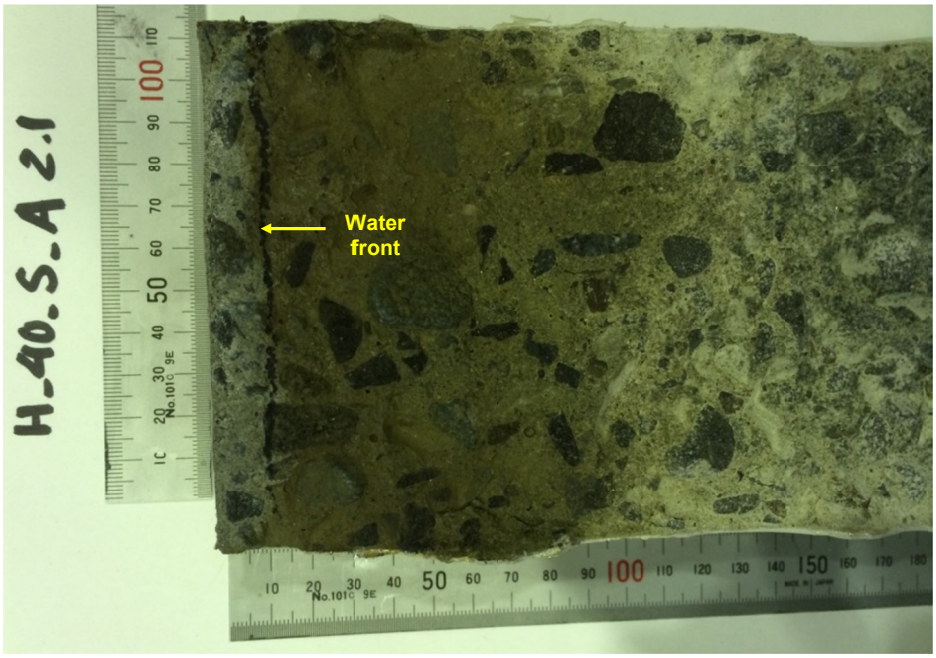

Fig. 5.8 Water front detected by naked eyes (black line).

After that, water front was investigated by applying colored-change agent to one half of the specimen (the other half was remained for chloride depth measurement). The agent was sprayed evenly onto the surface of the section. The water front was recorded by a zigzag line at the interface between wet part and dry part, as shown in **Fig. 5.9**. In this case, the depth was measured at 5 points on the front, and then the average value was taken. Considering point number 5, water might have intruded around a coarse aggregate particle. Compared with the water front recorded by naked eyes (**Fig. 5.8**), the water front detected by colored-change agent was almost the same.

When the line of the water front was not zigzag, the number of measuring points could be reduced (**Fig. 5.10**). Because the water fronts were not always identical in two methods, it is necessary to select only one value of the water penetration depth for each specimen. The way to select the data will be discussed in detail in section 5.4.4.

One important thing should be noticed here that if the colored-change agent was sprayed too much or too less, the water front would be too unclear to detect (**Fig. 5.11**).

(iv) Detection of chloride front

The penetration depth of chloride ions was measured on the second half of the specimen by spraying 0.1mol/lit $AgNO_3$ solution onto the surface. The color change from dark to light indicates the presence of chloride ions (**Fig. 5.12**). The silver nitrate solution can record the existence of chloride ions down to a concentration of 60 ppm [5.17].

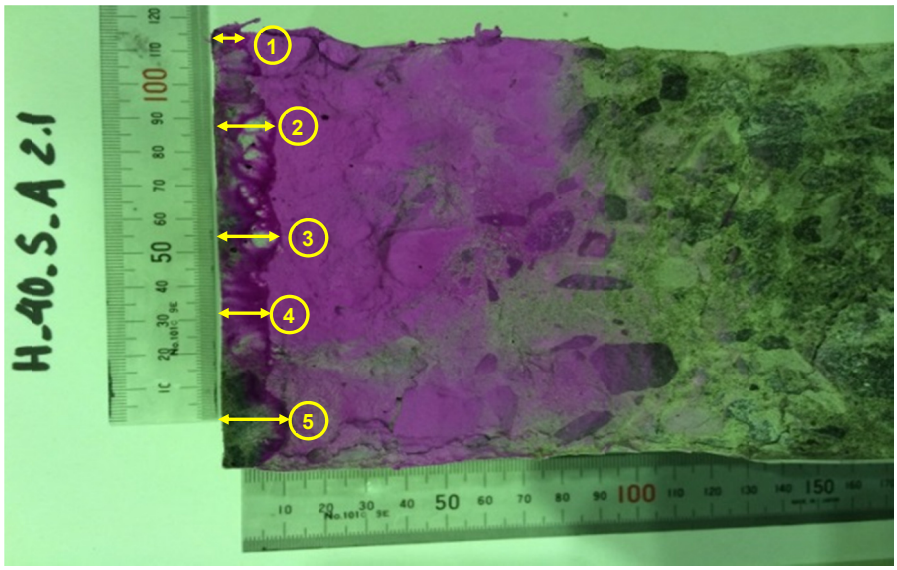

Fig. 5.9 Measurement of penetration depth of water (zigzag front).

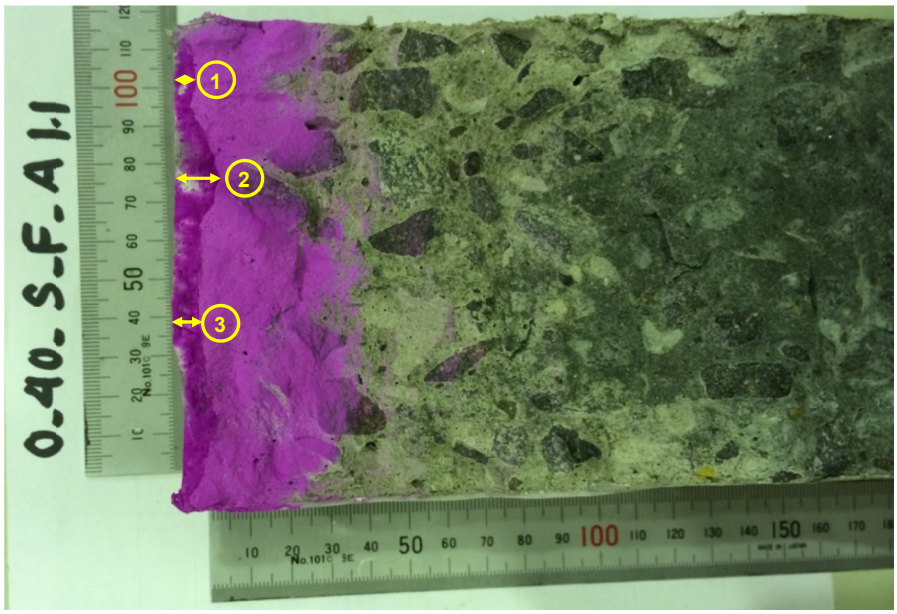

Fig. 5.10 Measurement of penetration depth of water (not so zigzag front).

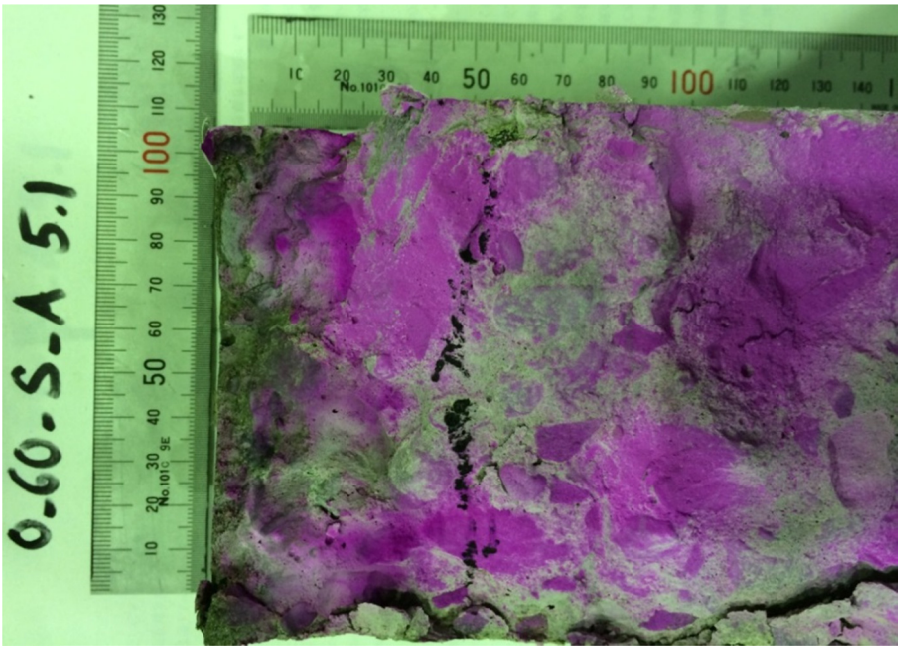

Fig. 5.11 Unclear water front.

It can be seen in **Fig. 5.12** that the chloride front was almost a straight line but it had an abnormal point. In this case, the abnormal point was neglected in the measurement. As explained in the water penetration depth measurement, the chloride penetration depth was measured at several points when the chloride front was zigzag **(Fig. 5.13)** and the mean value was taken.

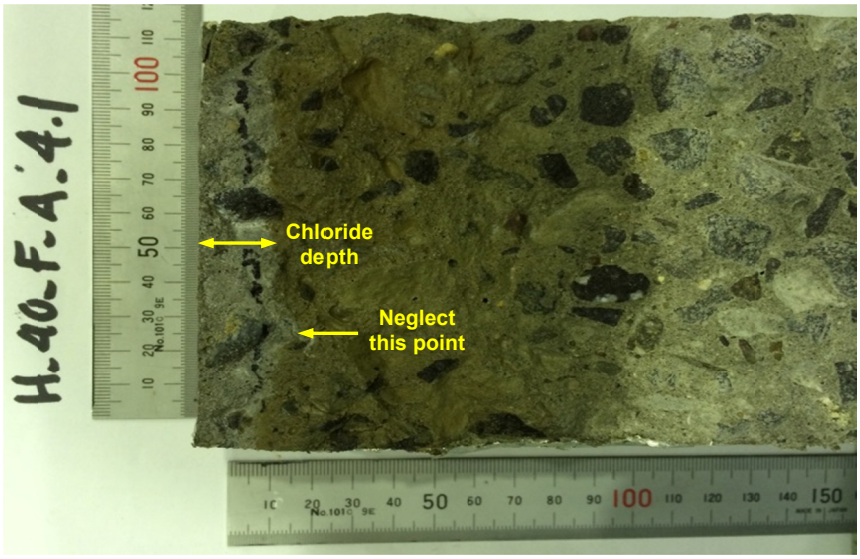

Fig. 5.12 Measurement of penetration depth of chloride ions (straight front).

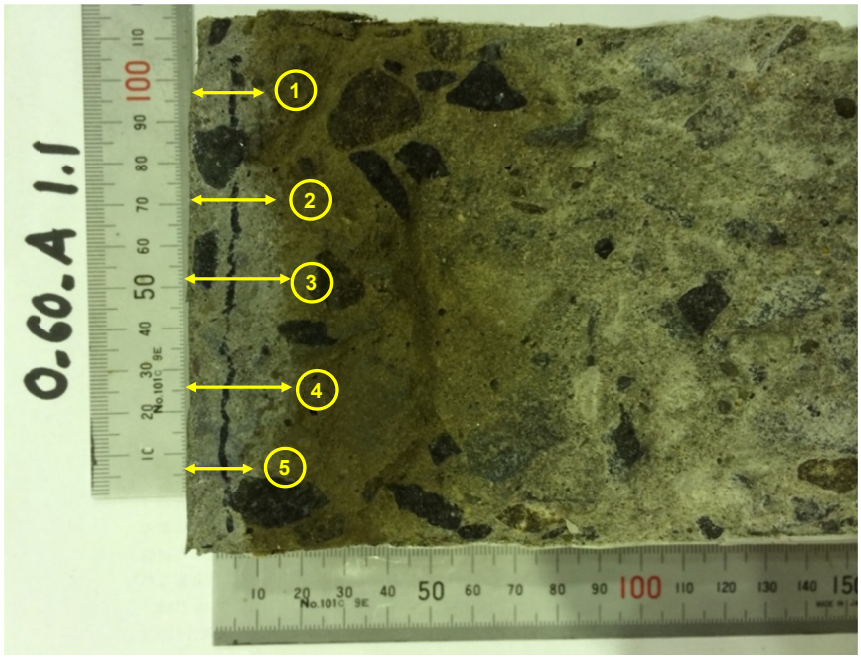

Fig. 5.13 Measurement of penetration depth of chloride ions (zigzag front).

5.5 Results and discussion

5.5.1 Penetration depth of water and chloride

The water penetration depths of the specimens detected by two methods, i.e. naked eyes and colored-change agent, and chloride immigration depths are shown in **Table 5.3**. Because chloride front was very clear to detect, the discussion in this section only focuses on the water penetration depth measurement.

Table 5.3 Penetration depth of water and chloride.

Mixtures	Specimens														
	1.1			2.1			3.1			4.1			5.1		
	Water		Cl^-	Water		Cl^-	Water		Cl^-	Water		Cl^-	Water		Cl^-
	Eye	Agent		Eye	Agent		Eye	Agent		Eye	Agent		Eye	Agent	
O-40-A	8	8	14	6	5.5?	13.5	4?	7	15	9	3.5?	14	9.5	-	18
O-40-S-A	8	14?	10	11?	11	10.5	7.5	15?	9	12	6?	10	17	-	15
O-40-F-A	6	12?	13	13	11?	13	8	17?	17	9.5	x	11	14.5	-	14.5
H-40-S-A	4.5	10?	9	11	11	11	6	12?	10	8?	12	10	17.5	-	15.5
H-40-F-A	5?	13	11	6.5	7.5	12	11	16?	19	9	12?	13.5	13	-	13.5
O-40-S-F-A	5?	5	9	9	7?	10.5	6	11?	9	7	6	9.5	14	x	14
H-40-S-F-A	4	5	8	7	5?	8	5	9?	10	8	14?	10	18?	12	10
O-50-A	14	15	20	16?	10	19	14?	9	18	13	x	18	14	-	21.5
O-50-S-A	9?	8	9	14	12?	13	8?	8	10	19	12?	12	37	-	20
O-50-F-A	8?	8	10.5	13.5	x	12	7.5	x	14	18?	11.5	12	30	-	22.5
H-50-S-A	6	6.5	11	10	x	10	8?	6	10	9?	12	12	20	-	15.5
H-50-F-A	5	5	14	9	x	13	8?	9	18	9	17?	15	18	-	19
O-60-A	8	8	15	18	9?	18	10?	10	18	14	x	18	41?	20	25
O-60-S-A	10	10	11	21	x	14	11	5?	11	15	15	12	46	x	28
O-60-F-A	9?	9	15	25	x	24	13	10?	18	21?	14	14	50	20?	33
H-60-S-A	9.5?	12	11	18	x	14	12.5	15?	13	12?	15	13.5	30	x	22
H-60-F-A	10	12?	18.5	12	x	21	11	x	19	12?	14	20	31	x	29

- : agent not used, ? : unclear observation, x : data can not obtained, number in the red: chosen value

Due to some difficulties in detecting water front as aforementioned, the water front was unclear in some cases (in both cases of observation by naked eyes and by agent) or it was impossible to detect the water front in some cases (in the case of using agent), as shown in **Table 5.3**. All the specimens were categorized into two groups: the first group includes the specimens whose water front was clear in both observation methods, and the second group consists of the specimens whose water front was clear only in one method of observation. For the first group specimens (the numbers in the cells with yellow background), the water penetration depth was determined by taking the mean value. In this group, the average water penetration depths recorded by naked eyes and by agent were 8.6 mm and 8.8 mm, respectively. The similar average water penetration depths recorded by the two methods in the first group indicate that the water penetration depth can be measured by each of them. In consequence, in the second group specimens, the water

penetration depth was chosen from the clearer value among two values, represented by the red number.

5.5.2 Effectiveness of HAC in concrete containing slag

(1) SWAT index

The comparisons of water absorption rate at 10 minutes (p_{600}) of slag concretes with OPC and HAC is presented in **Fig. 5.14**. In the graph, values of HAC slag concretes are connected by solid lines while those of OPC slag concretes are linked by dash lines.

Clearly, HAC slag concretes showed the smaller p_{600} than OPC slag concretes, especially in the cases of low W/B. The same trend was observed in concrete with limestone. It can be said that HAC can improve resistance against water absorption of concrete. Denser matrix and better bond between aggregate and mortar might be the reasons for this advantage of HAC concrete.

(2) Effectiveness of HAC in improving resistance against water and chloride penetration of concrete containing slag

Figure 5.15 exhibits the correlation between p_{600} and penetration depth of water and chloride ions in OPC concrete, OPC slag concrete and HAC slag concrete.

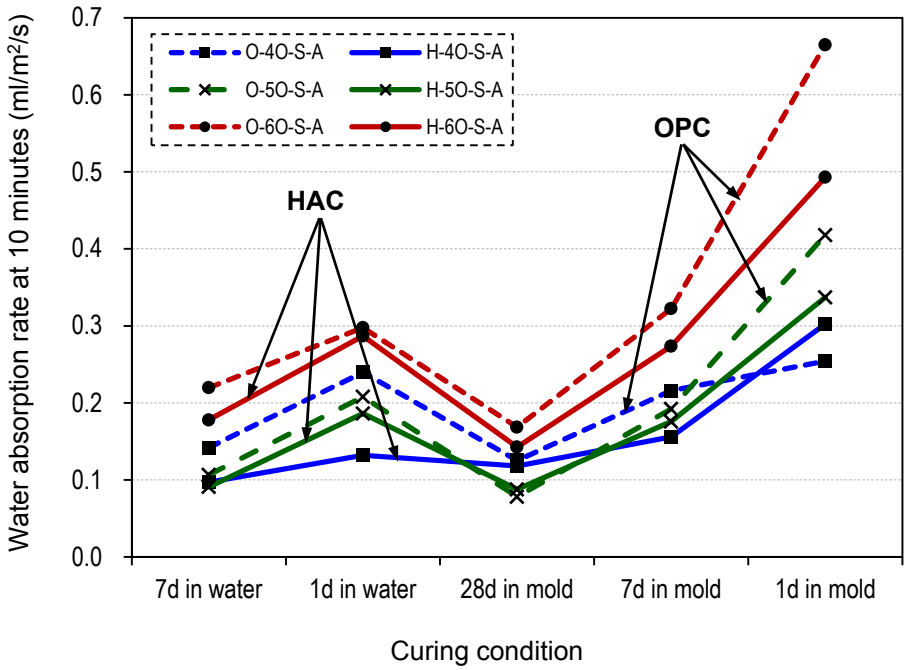

Fig. 5.14 Water absorption rate at 10 minutes of slag concretes with OPC and HAC.

It can be seen that p_{600} covered a wide range from very good quality to very poor quality of covercrete. Because quality of covercrete is much affected by concreting works, it can be said that SWAT could differentiate curing condition of concrete.

In three concretes, p_{600} had a good correlation with penetration depth of water as well as chloride ions. The linear relationship implies that water absorption rate and penetration depth of liquid water of concrete were mainly controlled by the same factor, i.e. microstructure of concrete.

The tendencies of water penetration in the all concretes were almost similar. The only difference here was the range of value. Apparently, the quality of concrete containing slag (both OPC and HAC) was more sensitive with curing condition than OPC concrete. As a result, water absorption rate at 10 minutes as well as water penetration depth in slag concretes subjected to poor curing were much larger than those in OPC concrete. It implies that appropriate curing condition must be supplied for concrete containing slag to achieve the durability of concrete structures. Fortunately, HAC slag concrete presented a less sensitivity to curing condition than OPC slag concrete. It may be due to the high hydration rate of HAC. Even in a poor curing condition, due to rapid hydration of C_3S, higher resistance against water absorption of HAC slag concrete was observed. Less sensitivity to poor curing is one of the advantages of HAC slag concrete.

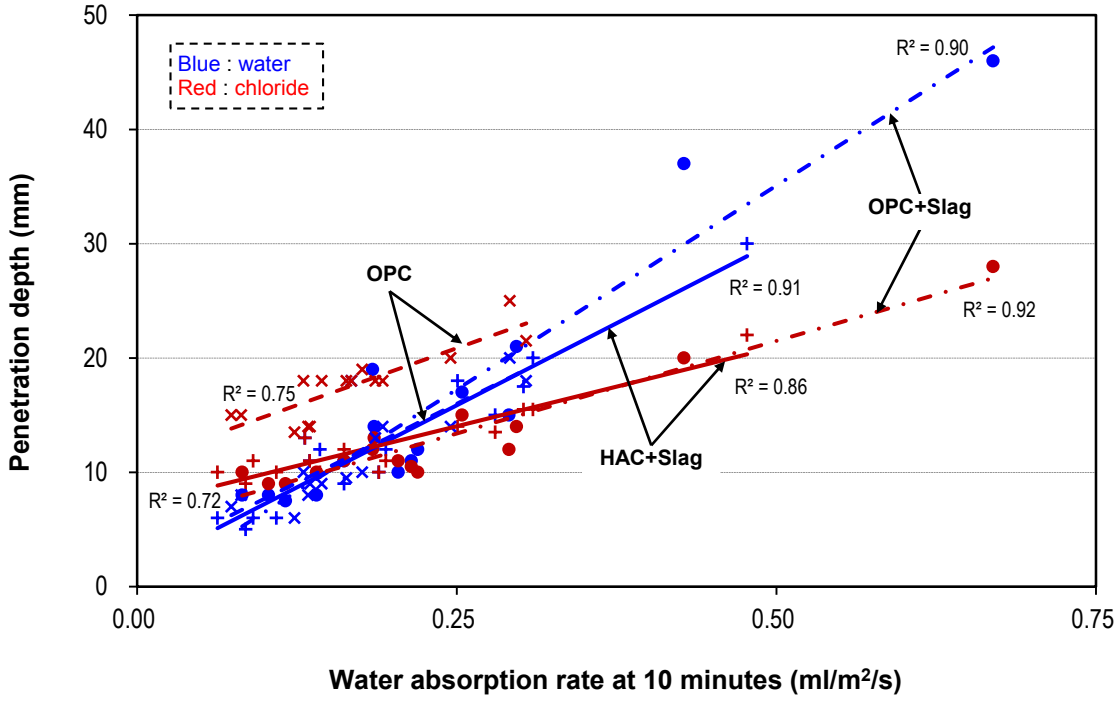

Fig. 5.15 Comparison between OPC, OPC slag, and HAC slag concretes.

The same trends of water penetration in concretes regardless of the type of binder indicates that p_{600} is related to a kind of governing characteristics of microstructure of concrete. Sakai *et al.* [5.18] reported that there was a good correlation between threshold pore size and water permeability of concrete. Here, threshold pore size is the minimum pore size which mass should pass to penetrate the objective. Water absorption resistance and threshold pore size also had a good correlation [5.19]. It can be said that SWAT can be utilized as an effective technique to examine microstructure of concrete. This is very significant because SWAT is a simple, rapid, and nondestructive method and it is easy to be applied in actual sites.

Considering about chloride penetration, there were two clearly distinct tendencies between concrete with and without slag. In OPC concrete, chloride ions penetrated much more deeply than water, i.e. OPC concrete was very weak to resist chloride ingress. The same trend was observed in the research of Iwamoto [5.10]. The reason for that is the difference in transportation mechanisms of liquid and ion. The main mechanism of water movement is absorption due to capillary suction force, absorption stops when concrete reaches to saturated situation [5.20]. Whereas, the main mechanism of chloride ion transfer is not only absorption (together with water) but also diffusion. In OPC concrete, firstly, chlorides moves into concrete together water owing to absorption. When absorption stops, due to the concentration differential, chloride ions continue to diffuse inward specimen.

On the other hand, in both concretes containing slag, chloride ions penetrated much shallower than water, especially in very poor quality concrete. It means that chloride movement was restricted in these concretes. It is well known that the rate of chloride ingress into concrete is influenced by the chloride binding ability of the concrete. The chloride binding capacity is controlled by the cementitious materials. Chemically, chloride ions can be bound by C_3A to form calcium chloroaluminate, $3CaO.Al_2O_3.CaCl_2.10H_2O$, sometimes related as Friedel's salt [5.21]. Because of rich C_3A content, slag can improve chloride binding ability of concrete. In the consequence, during the movement of salt water into concrete, chloride ions were bound by slag leading to the shallower penetration of chlorides compared with pure water. In terms of resistance against chloride ion, HAC slag concrete did not show a better performance than OPC slag concrete.

5.5.3 Comparison between slag concrete and fly ash concrete with OPC and HAC

The comparison between slag concrete and fly ash concrete with OPC and HAC in terms of resistance against water and chloride ions are shown in **Fig. 5.15** and **Fig. 5.16**, respectively.

As slag concretes, close relationships between p_{600} and penetration depth of water and chlorides were also obtained in OPC fly ash concrete (**Fig. 5.16**) and in HAC fly ash concrete (**Fig. 5.17**). OPC fly ash concrete was a bit less sensitive to curing condition than HAC fly ash concrete.

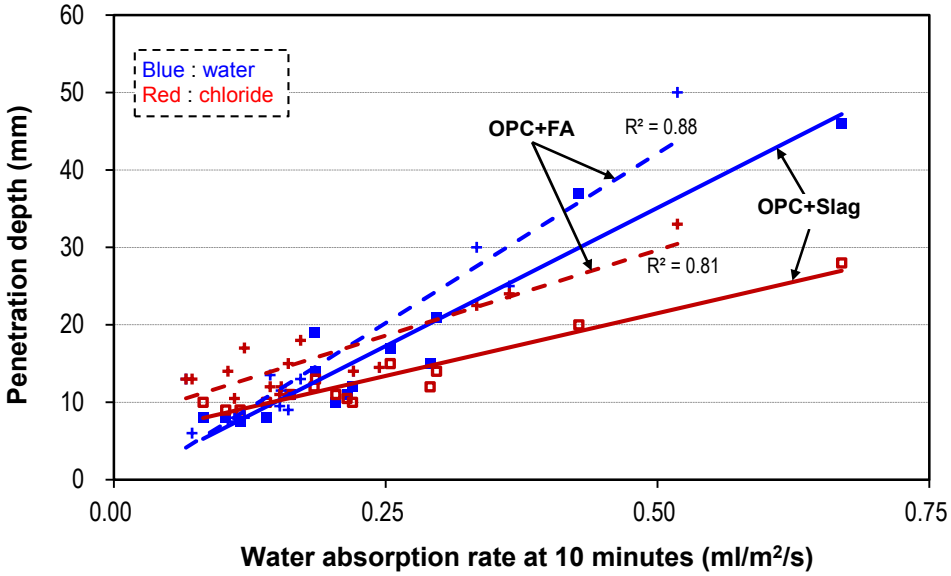

Fig. 5.16 Comparison of the effectiveness of slag and fly ash in OPC concrete.

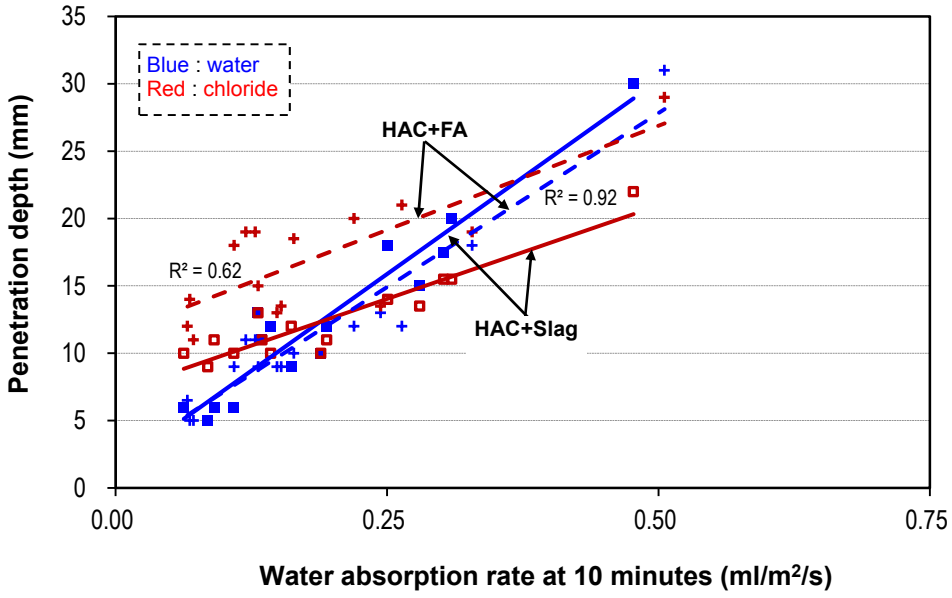

Fig. 5.17 Comparison of the effectiveness of slag and fly ash in HAC concrete.

Concerning water penetration, there was similar trend between slag concrete and fly ash concrete. This supports the results obtained in section 5.4.2 that the tendencies of water penetration evaluated by SWAT in the all concretes were similar regardless of the type of binder. It must be due to the same factor governing SWAT index and penetration depth, i.e. microstructure of concrete, as above explained.

In terms of the resistance against chloride attack, fly ash concrete also showed a good performance. However, slag was more effective than fly ash in both OPC and HAC concrete. It might be due to higher Al_2O_3 content in slag compared with that in fly ash.

5.5.4 Three-binder concrete with W/B of 0.4

Penetration depth of water and chloride ions also presented a close relationship with p_{600}. The comparisons between three-binder concrete and slag concrete in the case of W/B of 0.4 are exhibited in **Fig. 5.18** (OPC) and **Fig. 5.19** (HAC). Both types of three-binder concretes had a bit higher resistance against mass transportation. Better chloride restriction ability of three-binder concretes might be due to high C_3A content.

Among all kinds of concrete with W/B of 0.4, HAC three-binder concrete showed the best performance. However, the effectiveness of three-binder concrete needs to be confirmed in the other W/B ratios.

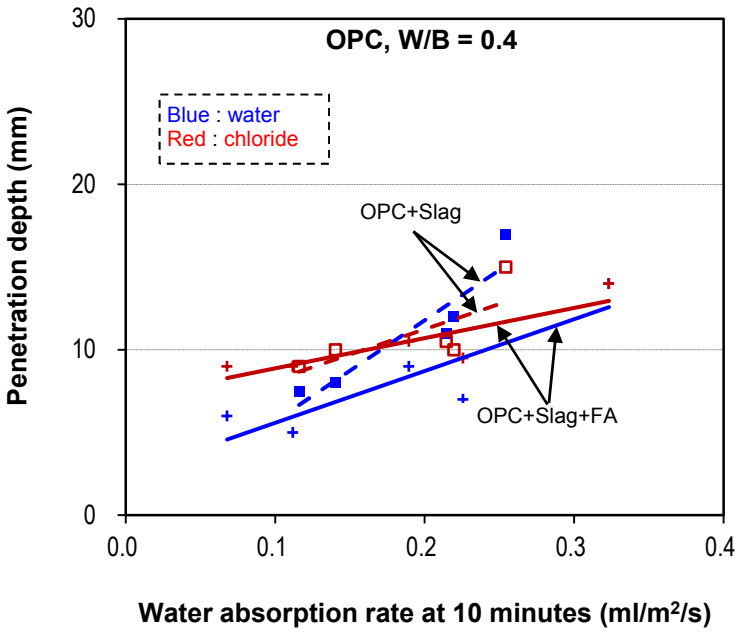

Fig. 5.18 Comparison of three-binder concretes and slag concretes used OPC.

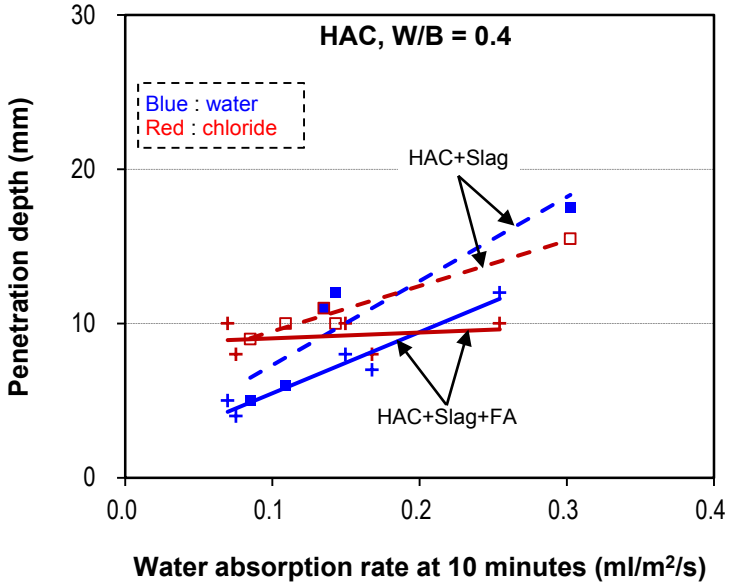

Fig. 5.19 Comparison of three-binder concretes and slag concretes used HAC.

5.5.5 Correlation between p_{600} and initial rate of absorption S_i

According to ASTM C1585-04, the absorption, I, is the change in mass divided by the product of the cross-sectional area of the test specimen and the density of water. For the purpose of this test, the temperature dependence of the density of water is neglected and a value of 0.001 g/mm^3 is used. The units of I are mm.

$$I = \frac{m_t}{a/d} \tag{5.1}$$

where;

I – the absorption

m_t – the change in specimen mass in grams, at the time t,

a – the exposed area of the specimen, in mm^2, and

d – the density of the water in g/mm^3.

The initial rate of water absorption (mm/s$^{1/2}$), S_i, is defined as the slope of the line that is the best fit to I plotted against the square root of time (s$^{1/2}$). Obtain this slope by using least squares, linear regression analysis of the plot of I versus time$^{1/2}$. For the regression analysis, use all the points from 1 min. to 6 hrs., excluding points for times after the plot shows a clear change of slope. If the data between 1 min. and 6 hrs. do not follow a linear relationship (a correlation coefficient of less than 0.98) and show a systematic curvature, the initial rate of absorption cannot be determined. If the data follows a linear relationship, I and S_i relation can be expressed by the **Eq. 5.2**.

$$I = S_i\sqrt{t} + b \tag{5.2}$$

In this study, the initial rate of absorption S_i of all specimens could be detected. For each concrete with different type of binders, there were a good correlation between p_{600} and the initial rate of absorption S_i as shown in **Fig. 5.20**.

It can be seen from **Fig. 5.20** that the tendencies in the all concretes were almost similar regardless of the type of binder. This is because initial absorption rate is also controlled by microstructure of concrete. Nonetheless, compared with OPC concrete, concretes with additives subjected to poor curing showed the very lower quality of covercrete with very high initial absorption rate, it means that concretes containing slag and fly ash were more sensitive to curing condition than OPC concrete.

5.5.6 Effectiveness of curing conditions

Figure 5.21 presents p_{600} of the concretes with andesite in all curing conditions. It can be seen that the curing condition of 7 days in water and of 28 days in mold show the similar effectiveness on covercrete quality. The same p_{600} values are observed in the concretes cured in the conditions of 1 day in water and of 7 days in mold. The same tendency also occurred in the concretes with limestone.

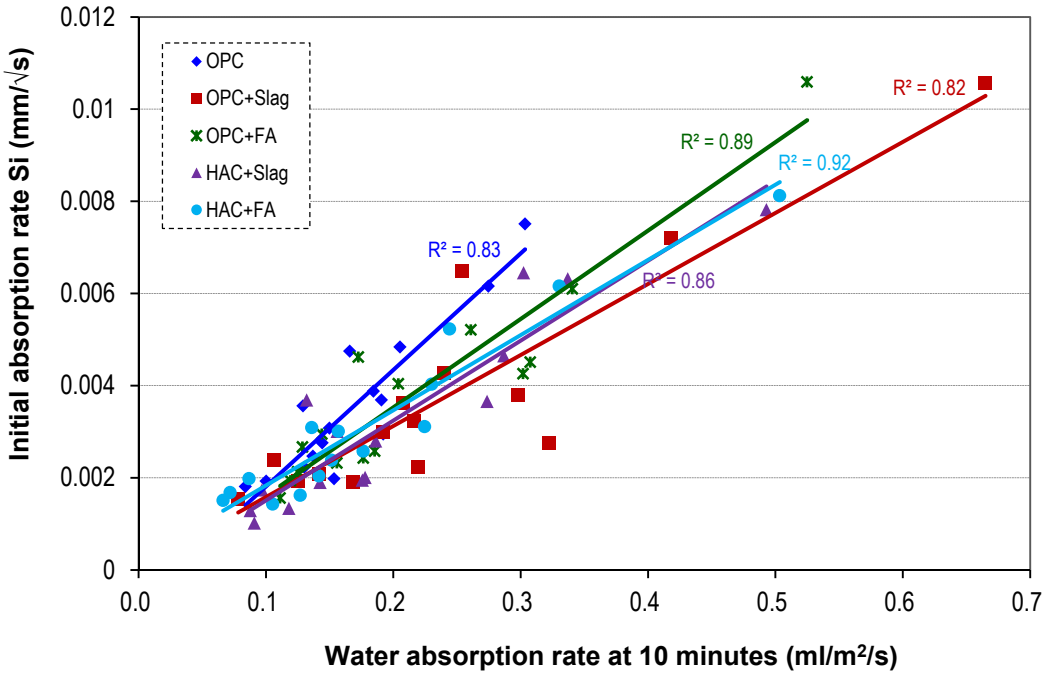

Fig. 5.20 Correlation between p_{600} and S_i in concretes with andesite.

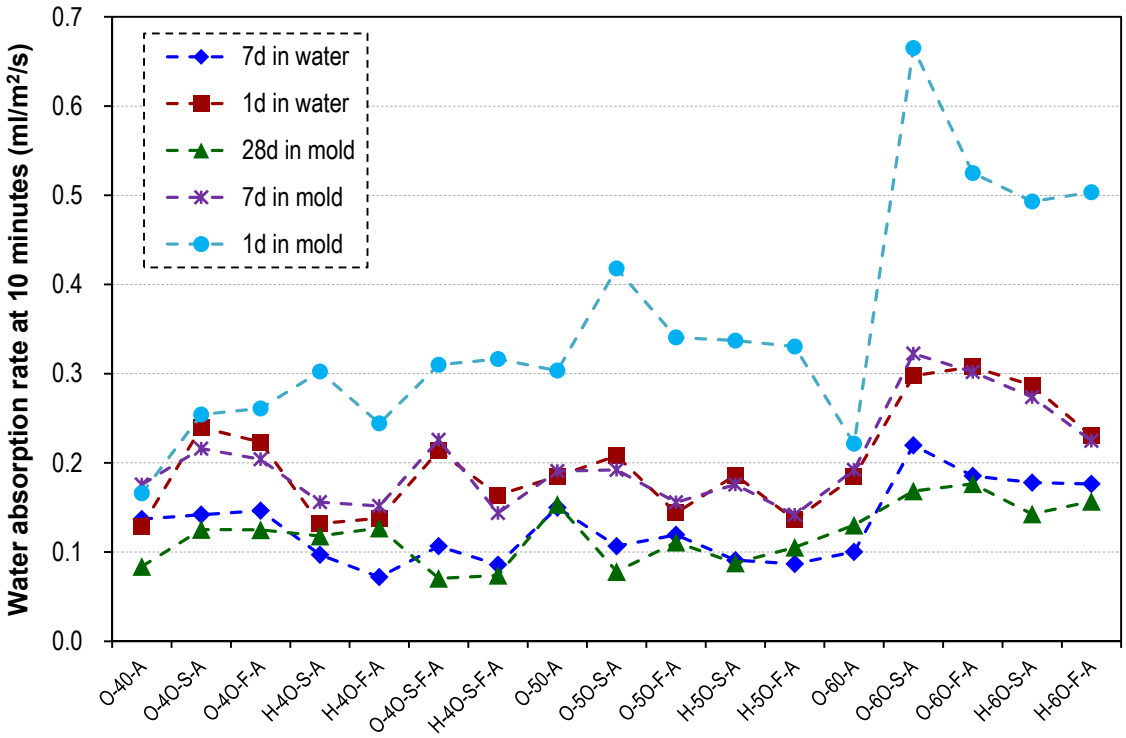

Fig. 5.21 Water absorption rate at 10 minutes of concretes with andesite.

5.5.7 Comparison of Iwamoto's research and this research

Comparison of OPC concrete between Iwamoto's results [5.11] and this research is shown in **Fig. 5.22**. In two studies, water front was deeper than chloride front. Nonetheless, the depths of water and chlorides ions in this study were much shallower than those in the previous research.

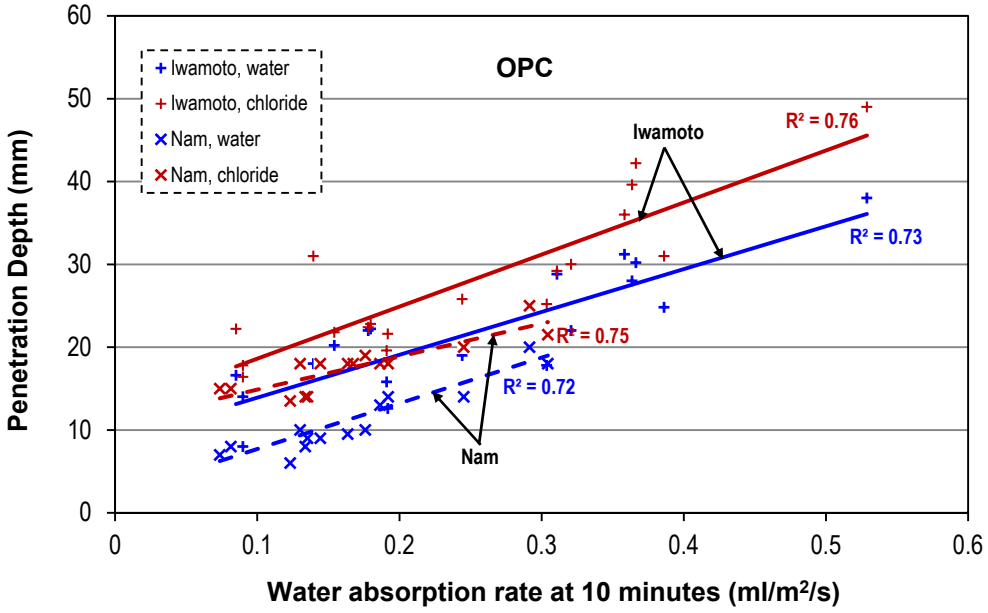

Fig. 5.22 Comparison between Iwamoto's research and this research in OPC concrete.

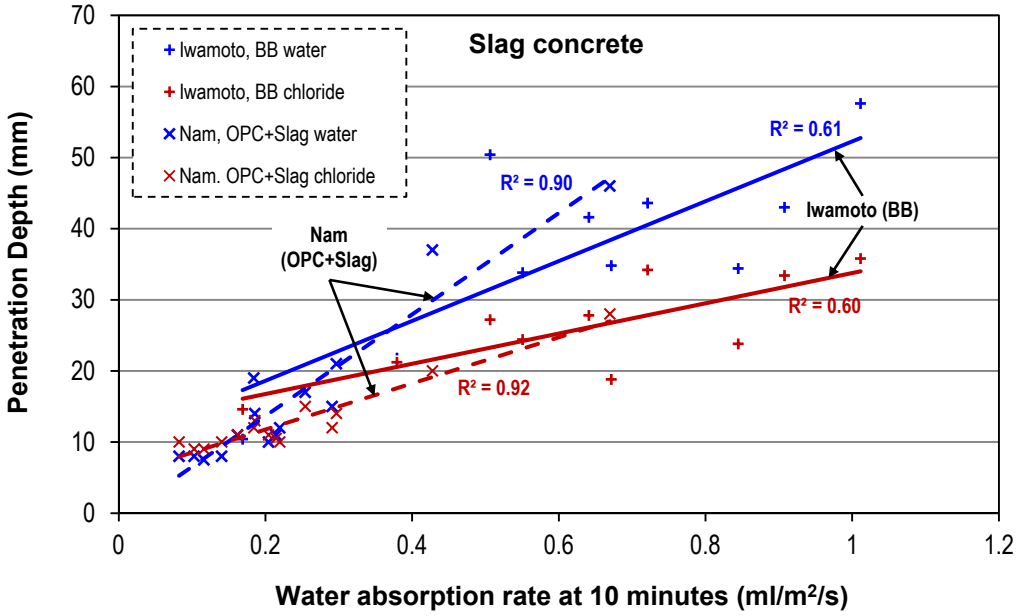

Fig. 5.23 Comparison between Iwamoto's research and this research in slag concrete.

One of the reasons might be the different types of coarse and fine aggregate used in two researches. Water absorption of aggregate itself, bond between aggregate and the matrix might cause this difference. Iwamoto utilized limestone from Chichibu, Saitama. The author's results using in this comparison were obtained from concretes with andesite from Tohoku region. Further investigation to clarify the influence of aggregate on the SWAT indices as well as on the penetration depth of water/chloride should be done.

Some concretes with slag cement type B investigated in Iwamoto's study presented a less correlation between p_{600} and penetration depth compared with those in this research (**Fig. 5.23**). However, the trend was similar, i.e. chlorides ingress was shallower than water movement. The scatter of data in Iwamoto's study must be due to the different types of slag concrete in his research [5.11].

5.6 Conclusions of the chapter

In this chapter, OPC and HAC concrete containing slag, fly ash, or both with W/B of 0.4, 0.5, and 0.6 subjected to five curing conditions were investigated by SWAT (water absorption rate at 10 minutes: p_{600}) and water/chloride penetration depth test. The conclusions can be drawn as follows.

1. There were good correlations between p_{600} and penetration depth of water and chloride ions in all kind of concretes. It means that SWAT can be applied to

evaluate the resistance against mass transfer into concrete.

2. The same linear relationship was observed between the water penetration depth and p_{600} regardless of the type of binder. It means that p_{600} is related to a kind of governing characteristic regarding the microstructure of concrete, which should be studied further. The effects of curing conditions were fully reflected in SWAT results. If linear lines expressing the correlations between SWAT index and parameters related to durability of concrete such as penetration depth of water or chloride ion, carbonation depth, etc. are established, SWAT index can be used as an indicator of durability of concrete structures.

3. Slag or fly ash could improve the resistance against chloride ingress of concrete remarkably due to the chloride binding ability of C_3A component existing in slag and fly ash. However, OPC concretes containing additives were much more sensitive to curing condition than concretes with OPC only.

4. Owing to the high hydration rate of C_3S, HAC slag/fly ash concrete was less sensitive to curing conditions than OPC slag/fly ash concrete. Therefore, HAC should be utilized with slag or fly ash in concrete structures subjected to severe conditions.

5. Three-binder concrete showed a better performance in resisting chloride penetration, which might be due to higher C_3A content. Among all the kinds of concrete with W/B of 0.4 in this research, HAC three-binder concrete showed the best performance. However, the effectiveness of three-binder concrete needs to be confirmed in other W/B ratios.

References

[5.1] Hosoda, A., *et al*., "Quality assurance management of revival road in Tohoku region after the Great East Japan Earthquake", *Proceedings of the Concrete Innovation Conference (CIC)*, 2014.

[5.2] Hayshi, K. and Hosoda, A., "Developement of Water Absorption Test Method Applicable to Actual Concrete Structures", *Proceedings of the JCI*, Vol. 33, No.1, pp. 1769-1774, 2011. (in Japanese)

[5.3] Neville, A. M., "Properties of Concrete," John Wiley & Sons, pp.563-571, 1996.
[5.4] Okazaki, S., Yagi, T., Kishi, T. and Yajima, T., “Study on the effectiveness of curing on the strength and permeability of concrete”, *Proceedings of Cement and Concrete*, No. 60, pp. 227-234, Cement Concrete Association, 2006. (n Japanese)
[5.5] “Standard Method of Test for Resistance of Concrete to Chloride Ion Penetration”, (T259-80), American Association of State Highway and Transportation Officials, Washington, D.C., U.S.A., 1980.
[5.6] *Nordtest Method: Accelerated Chloride Penetration into Hardened Concrete*, Nordtest, Espoo, Finland, Proj. 1154-94, 1995.
[5.7] “Electrical Indication of Concrete’s Ability to Resist Chloride”, (T277-93), American Association of State Highway and Transportation Officials, Washington, D.C., U.S.A., 1983
[5.8] Tang, L. and Nilsson, L.-O., “Chloride Diffusivity in High Strength Concrete”, *Nordic Concrete Research*, Vol. 11, pp. 162-170, 1992.
[5.9] Armaghani, J. M., and Bloomquist, D. G., “Durability Specification and Rating For Concrete”, *Concrete 2000*: *Economic and Durable Construction Through Excellence*, (eds. R.K. Dhir and M.R. Jones), Vol. 2, E & FN Spon, Cambridge, pp. 1639-1652, 1993.
[5.10] Meletiou, C. A., Tia, M., and Bloomquist, D. G., “Development of a Field Permeability Test Apparatus and Method for Concrete”, *ACI Materials Journal*, Vol. 89, No. 1, pp. 83-89, 1992.
[5.11] Iwamoto, Y., Master thesis submitted to Yokohama National University (Concrete Laboratory), 2014. (in Japanese)
[5.12] Hansson, C. M., and Sorenson, B., “The Threshold Concentration of Chloride in Concrete for the Initiation of Corrosion”, *Corrosion Rates of Steel in Concrete,* ASTM SP 1065(99), pp. 3-16, 1990.
[5.13] Dirh, R. K., Hewlett, P. C., and Chan, Y. N., “Near-surface characteristics of concrete: assessment and development of in situ test methods”, *Magazine of Concrete Research*, Vol. 39, No. 141, pp. 183-195, 1987.
[5.14] ASTM International, ASTM C140-11a, Standard test method for sampling and testing concrete masonry units and related units, 2011.
[5.15] JSCE, JSCE-G 572-2010, Test method for apparent diffusion coefficient of chloride ion in concrete by submergence in salt water, 2010.
[5.16] ASTM International, ASTM C1585-04, Standard test method for measurement of rate of absorption of water by hydraulic-cement concretes, 2004.
[5.17] McCarter, W. J., Ezirim, H., and Emerson, M., “Absorption of water and chloride

into concrete", *Magazine of Concrete Research*, Vol. 44, No. 158, pp. 31-37, 1992.
[5.18] Sakai, Y., Nakamura, C., and Kishi, T., "Correlation between permeability of concrete and threshold pore size obtained with epoxy-coated sample", *Journal of Advanced Concrete Technology*, Vol. 11, pp. 189-195, 2013.
[5.19] Sakai, Y. and Kishi, T., "Evaluation of the resistance of concrete based on threshold pore radius", *Proceedings of the JCI*, Vol. 36, No.1, pp. 688-693, 2014. (in Japanese)
[5.20] Neville, A. M., "Properties of Concrete," John Wiley & Sons, pp.484-485, 1996.
[5.21] Neville, A. M., "Chloride attack of reinforced concrete: an overview", *Materials and Structures*, Vol. 28, pp. 63-70, 1995.

Chapter 6 Conclusions and Recommendations

6.1 General

Important findings about the resistance against microcracking and water and chloride penetration of HAC concrete containing slag and fly ash are summarized in this chapter. Besides, recommendations for future research are proposed.

6.2 Main conclusions of the study

1. The redesigned waveguide with two additional wings showed the more effectiveness in detecting microcracks at very early ages, especially in concrete with high W/B ratio. The influence of attenuation of acoustic wave in high moisture content medium was significantly mitigated by reducing the distance from cracking points to waveguide.

2. Net shrinkage of HAC mortar with W/B of 0.3 was much larger than that of OPC mortar because of its larger autogenous shrinkage. Normally, larger shrinkage of mortar results in more extensive cracking in concrete. However, the number and the degree of microcracks in HAC slag concrete with W/B of 0.3 were smaller than those in OPC slag concrete. This means that HAC slag concrete with W/B of 0.3 obviously achieved larger resistance against microcrack than OPC slag concrete. On the other hand, net shrinkage of HAC mortar with W/B of 0.5 was a bit smaller than that of OPC mortar due to its smaller thermal contraction. Therefore, microcracking in HAC slag concrete with W/B of 0.5 was also smaller than that in OPC slag concrete.

3. HAC can improve resistance against microcracking of slag concrete with W/B of 0.5 and 0.3. Evenly distributed CH crystals acting as a kind of buffer that prevents the propagation of microcracks in HAC slag concrete might be one of the reasons.

4. Another reason for the high cracking resistance of HAC slag concrete was the

strong bond between mortar and coarse aggregate. This high bond strength was more clearly observed in concrete with low W/B than in concrete with high W/B. The high bond strength of HAC slag concrete was verified through mechanical tests, AE test, and visual and SEM observation. The strong bond in HAC slag concretes might be due to the formation of secondary CSH gel from the reaction of CH and active SiO_2 in slag at pores near the ITZ.

5. Concrete containing fly ash was not so weak against elevated temperature. Nevertheless, fly ash reduced tensile strength of concrete remarkably. The reason is that fly ash is not so active in early ages even under steam curing. Although HAC can improve tensile strength of fly ash concrete significantly, high bond strength between HAC mortar and aggregate was not observed in fly ash concrete as in slag concrete.

6. There were good correlations between p_{600} (water absorption rate at 10 minutes obtained by SWAT) and penetration depth of water and chloride ions in all kind of concretes. It means that SWAT can be applied to evaluate the resistance against mass transfer into concrete.

7. There were good correlations between p_{600} and penetration depth of water and chloride ions in all kind of concretes. The same linear relationship was observed between the water penetration depth and p_{600} regardless of the type of binder. It means that p_{600} is related to a kind of governing characteristic regarding the microstructure of concrete, which should be studied further. The effects of curing conditions were fully reflected in SWAT results. If linear lines expressing the correlations between SWAT index and parameters related to durability of concrete such as penetration depth of water or chloride ion, carbonation depth, etc. are established, SWAT index can be used as an indicator of durability of concrete structures.

8. Slag or fly ash could improve the resistance against chloride ingress of concrete remarkably due to the chloride binding ability of C_3A component existing in slag and fly ash. However, OPC concretes containing additives were much more sensitive to curing condition than concretes with OPC only.

9. Owing to the high hydration rate of C_3S, HAC slag/fly ash concrete was less sensitive to curing condition than OPC slag/fly ash. Thus, HAC should be utilized with slag or fly ash in concrete structures subjected to severe conditions.

10. Three-binder concrete showed a better performance in resisting chloride penetration, might be due to higher C_3A content. Among all the kinds of concrete with W/B of 0.4 in this research, HAC three-binder concrete showed the best performance. However, the effectiveness of three-binder concrete needs to be confirmed in other W/B ratios.

6.3 Recommendations for future works

The effectiveness of HAC in improving microcracking resistance of slag concrete in mesoscopic level was confirmed. However, the resistance against macroscopic cracking of concrete with external restraint is not governed only by the resistance against microcracking, but affected by many concrete characteristic. The author believes HAC concrete with external restrained will show higher crack resistance than OPC concrete, which should be verified in cracking test with external restraint.

In mesoscopic level, new waveguide was highly effective in detecting microcracking. Nevertheless, the waveguide for AE in macroscopic degree is distinct from that in mesoscopic level due to the different shape of the specimens. Hence, a modification of the shape of wave-guide to mitigate the influence of attenuation in macroscopic level should be done.

At very early ages, AE results showed that fly ash concrete was also susceptible to microcracking, even in HAC concrete. Severe cracking problems of fly ash concrete structures have not been reported. The crack resistance of fly ash concrete with external restraint has not been fully investigated. The resistance against microcracking and against macroscopic cracking of concrete with the combination of three binders, e.g. cement, slag, and fly ash, should also be investigated.

The most important factor affecting SWAT results is moisture content of the surface of concrete at the testing time. If the surface of concrete is too wet, water

absorption rate will be small, and vice versa. An investigation to determine the threshold of moisture content for applying SWAT is highly recommended.

The type of aggregate may be a factor influencing SWAT indices and absorption properties of concrete. Further investigation to clarify the influence of aggregates on the SWAT indices as well as on the penetration depth of water/chloride should be done.

To detect the front of water absorption was much more difficult than that of chloride front. Although naked-eye observation and colored-change agent were combined in this research, the water front was still not as clear as chloride front, which recorded by $AgNO_3$ solution. The more effective method to determine the water front should be continuously investigated.

Three-binder concrete with W/B of 0.4 showed a bit higher resistance against water and chloride ion than slag or fly ash concrete, especially in the case of HAC. The effectiveness of three-binder concrete with high W/B should be studied.

PUBLICATIONS RELATING TO THE RESEARCH

Reviewed conference papers:

1. Nam, H. P. and Hosoda, A., "Improvement of Crack Resistance of Slag Concrete by Utilizing High Alite Cement", *Proceedings of the Ninth International Conference of Creep, Shrinkage, and Durability Mechanics*, MIT, September 22-25, 2013, pp.356-365.

2. Nam, H. P. and Hosoda, A., "Resistance against microcracking of slag concrete with Hight Alite Cement analyzed by AE with new wave-guide", *Proceedings of the JCI*, Vol. 35, No. 1, pp. 241–246, 2013.

Journal paper under review:

1. Nam, H. P. and Hosoda, A., "Mechanism for Improving Crack Resistance of Slag Concrete with High Alite Cement", submitted to the Journal of JSCE on November, 2013; accepted on August 14, 2014.

Award: Excellent paper prize, the 35th JCI Annual Convention, 2013.